FLOTATION CHARACTERISTICS OF ARSENOPYRITE

by

Morris John Aloysius Vreugde

B.A.Sc. The University of British Columbia, 1971
M.A.Sc. The University of British Columbia, 1973

A THESIS SUBMITTED IN PARTIAL FULFILMENT OF
THE REQUIREMENTS FOR THE DEGREE OF
DOCTOR OF PHILOSOPHY

in

THE FACULTY OF GRADUATE STUDIES

Department of Mining and Mineral
Process Engineering

We accept this thesis as conforming

to the required standard

The University of British Columbia
October 1982

In presenting this thesis in partial fulfilment of the requirements for an advanced degree at the University of British Columbia, I agree that the Library shall make it freely available for reference and study. I further agree that permission for extensive copying of this thesis for scholarly purposes may be granted by the head of my department or by his or her representatives. It is understood that copying or publication of this thesis for financial gain shall not be allowed without my written permission.

Department of Mining and Mineral Process Engineering

The University of British Columbia
1956 Main Mall
Vancouver, Canada
V6T 1Y3

Date March 3, 1983

ABSTRACT

Electrochemical methods, surface spectroscopy and flotation tests have been used to study the influence of the oxidation of arsenopyrite on its floatability with xanthate.

Cyclic voltammetric studies indicated that the oxidation of arsenopyrite at pH greater than 7 results in the formation of ferric hydroxide deposits on the surface of the mineral. Arsenic is oxidized to arsenate and sulphur is oxidized to sulphate. The arsenate is incorporated in the ferric hydroxide deposits while sulphate diffuses into solution. Below pH=7, soluble iron species are formed and the surface becomes increasingly covered with elemental sulphur with decreasing pH. Increasing temperature has no influence on the quantity of hydroxide formed over the range 30° to 45°C but results in thick, porous films at temperature greater than 45°C. The oxidation of arsenopyrite was demonstrated to occur at lower oxidation potentials than for pyrite although this effect decreased with increasing temperature.

Mixed potential studies indicated that the potentials required for arsenopyrite oxidation could be achieved with common oxidizing agents. Selective oxidation of arsenopyrite in a bulk pyrite-arsenopyrite concentrate was indicated to be possible.

The formation of iron hydroxide deposits on the surface of arsenopyrite resulted in the inhibition of subsequent oxidation of xanthate to dixanthogen at the mineral's surface.

ESCA studies confirmed the formation of oxidized iron

layers at the surface of arsenopyrite and revealed that essentially all the arsenate which was formed was incorporated in these layers. Sulphur became oxidized at the pH studied and to a large extent went into solution.

Flotation studies demonstrated the use of oxidation for arsenopyrite depression. In the presence of oxidation, increasing pH above pH = 7 resulted in increased arsenopyrite depression while increasing temperature had little effect until a temperature of 40°C was exceeded. Previously activated arsenopyrite could be depressed through the use of oxidizing agents. Arsenopyrite could be selectively depressed from a bulk pyrite-arsenopyrite concentrate through the use of oxidizing agents.

ACKNOWLEDGEMENT

The author wishes to express sincere thanks to Dr. G.W. Poling for his support and guidance during the course of this work.

Particular appreciation is expressed to Dr. W.G. Bacon without whose help this project could not have been initiated and who ensured the continued support of Bacon, Donaldson and Associates Ltd.

The incentive to initiate this project and the endurance to carry it through to completion results from an unending desire to carry my education to the highest attainable level. My most heartfelt appreciation is expressed to my parents for instilling in me the desire to learn and to my wife, Kate, whose total support and often essential encouragement enabled me to fulfill my desire.

Appreciation is also expressed to Morny without whose unselfish efforts this manuscript could not have been completed.

Mr. Stephen Pickett of the Department of Chemistry is appreciated for his time in performing the ESCA analyses.

Financial assistance in the form of a B.C. Science Council Grant is gratefully acknowledged.

Table of Contents

Table of Figures

List of Tables

Chapter 1

INTRODUCTION

Arsenic occurs in nature with numerous other elements. A number of primary and secondary arsenic minerals are listed in Table 1. Those arsenic minerals which lie in the Fe-As-S system are shown in Figure 1. Arsenopyrite is the most common mineral containing arsenic. It is found with silver and copper ores, galena, spalerite and pyrite.

In certain ores arsenopyrite has considerable economic significance since it carries the major portion of gold in the ore. Such gold may occur as discrete grains between individual crystals of arsenopyrite and as such be recoverable from an arsenopyrite concentrate by direct cyanidation (1).

Gold may also occur in solid solution or as minute inclusions in arsenopyrite (2) and may require more exotic recovery procedures (3). An example of such an occurrence from the Hedley area of British Columbia is shown in Figure 2. The most successful treatment of ores of this type to date has been achieved by flotation of an arsenopyrite bearing concentrate which is subsequently roasted and then cyanided. Such a process is in operation at Giant Yellowknife Mines Ltd. (4,5). A flowsheet for this operation is shown in Figure 3.

While this process for the recovery of gold from arsenopyrite is very successful from a metallurgical point of view, there are serious pollution consequences (6). The data

Table 1
Arsenic Minerals

Arsenic	As
Loellingite	$FeAs_2$
Realgar	AsS
Orpiment	As_2S_3
Arsenopyrite	FeAsS
Glaucodot	(Co,Fe)AsS
Cobaltite	CoAsS
Gersdorffite	NiAsS
Skutterudite	$(Co,Ni,Fe)As_3$
Niccolite	NiAs
Enargite	Cu_3AsS_4
Proustite	Ag_3AsS_3
Pearcite	$(Ag,Cu)_{16}As_2S_{11}$
Tennantite	$(Cu,Fe,Zn,Ag)_{12}As_4S_{13}$
Sperrylite	$PtAs_2$
Allemontite	AsSb
Geocronite	$Pb_5(Sb,As)_2S_8$
Scorodite	$FeAsO_4 \cdot 2H_2O$
Pitticite	$Fe_2(AsO_2)(SO_4)OH \cdot 2H_2O$
Pharmacosiderite	$6FeAsO_4 \cdot 2Fe(OH)_3 \cdot 12H_2O$
Symplesite	$Fe_3As_2O_3 \cdot 8H_2O$
Erythrite	$CO_3(AsO_4)_2 \cdot 8H_2O$
Annabergite	$Ni_3(AsO_4)_2 \cdot 8H_2O$

shown in Table 2 indicate that 47.5% of arsenic emissions in Canada result from the metallurgical processing of gold ores. The predominant source of aqueous contamination by arsenic is also industrial smelting operations (6).

As a commodity, arsenopyrite is of minor consequence. While in the 1920's the mineral was viewed as a valuable potential source of arsenic for the control of pests such as the boll weavil (7), at present it is viewed as a troublesome impurity in base metal concentrates (8,59). While the arsenic present in such concentrates is recovered to some extent, the total yearly demand for arsenic in the U.S. is only 15,000 tons (13,600 tonnes) (9) and the recovery of arsenic from waste streams is costly. Smelters at present prefer to receive concentrates which are essentially free of arsenic.

The presence of arsenopyrite in sulphide concentrate can

Table 2
Arsenic emissions in Canada,1972 (6)

SOURCE	EMISSIONS TONS	PERCENT
INDUSTRY		
Primary copper and nickel	661	16.2
Primary lead production	18	0.4
Primary zinc production	359	8.8
Primary iron and steel	1041	25.6
Metallurgical processing of gold	1934	47.5
Miscellaneous sources	15	0.4
Subtotal	4028	98.9
FUEL COMBUSTION/STATIONARY SOURCES		
Power Generation	25	0.6
Industrial and commercial	13	0.3
Domestic	<1	<0.1
Subtotal	38	0.9
Transportation	<1	<0.1
Solid waste incineration	1	<0.1
Pesticide application	6	0.2
Total	4073	100.0

lead to serious health hazards apart from the contamination of smelter gases with arsenic. The presence of arsenopyrite in such concentrate has on occasion resulted in arsine generation during gold precipitation in cyanide circuits (10) or hydrometallurgical processing and refining (11).

The association of arsenopyrite with pyrite is of particular interest. This association is wide spread and can result in significant economic consequences. If pyrite is to be recovered for the production of sulphuric acid the presence of arsenopyrite is highly undesirable due to contamination of the

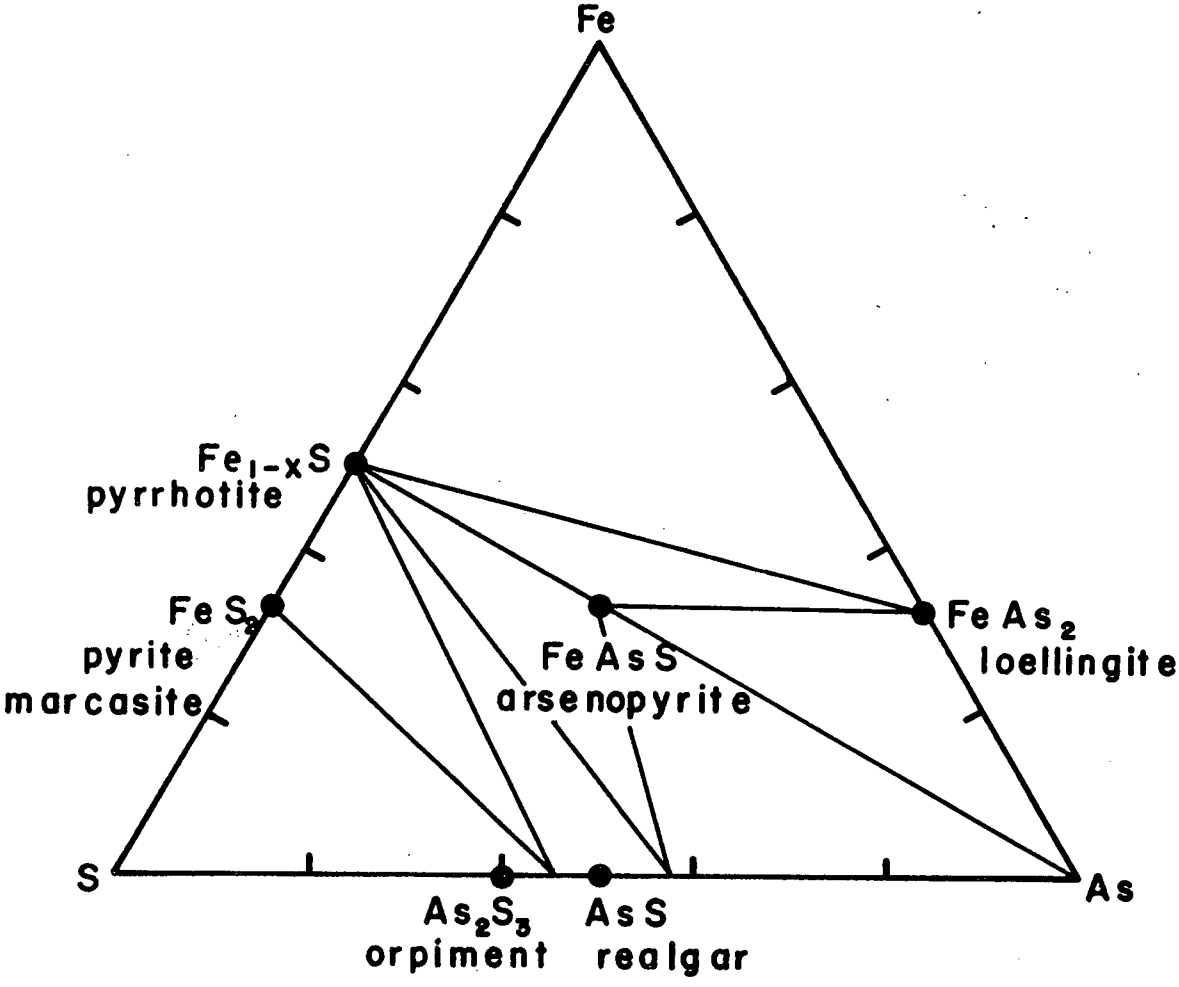

Figure 1

Minerals in the Fe-As-S System (600°C)

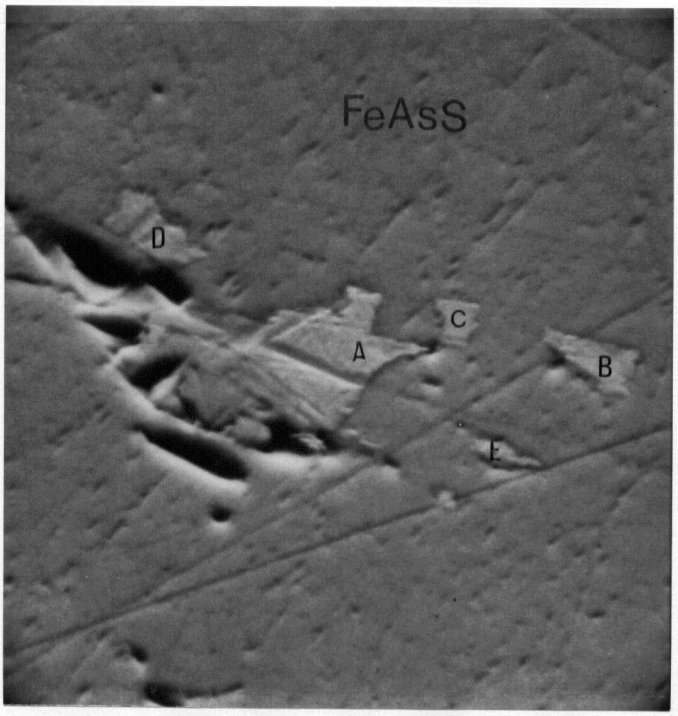

Area A - Gold with minor silver
Area B - Bismuth and tellurium
Area C - Gold and antimony
Area D, E - Bismuth

Figure 2

Arsenopyrite from Hedley, B.C. (3600x)

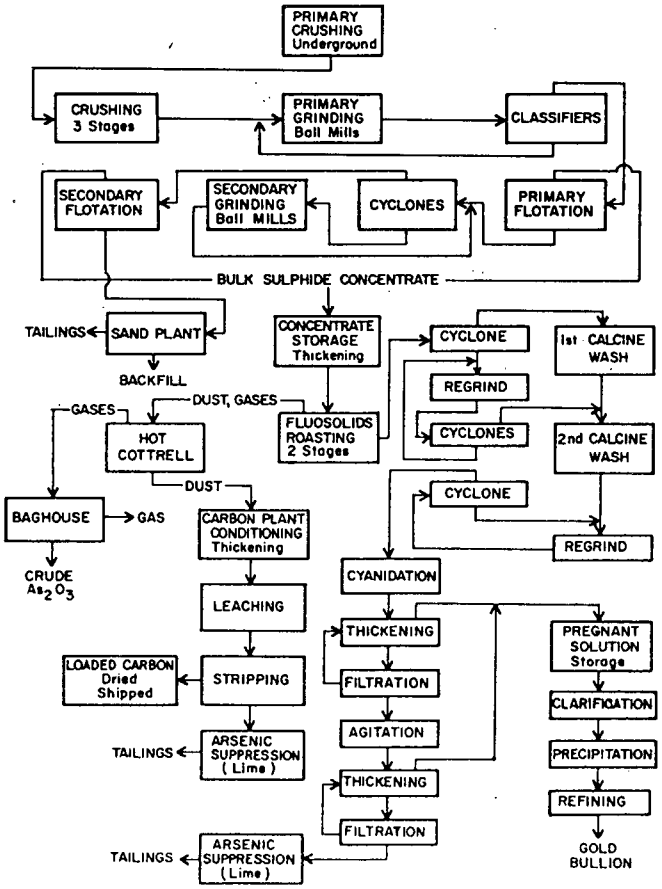

Figure 3

Giant Yellowknife Mines flowsheet

acid by arsenic (11). In gold ores the gold values may be entirely associated with either mineral.

The recovery or depression of arsenopyrite during sulphide flotation is of apparent interest. In the case of gold ores, the maximum recovery of arsenopyrite may be desirable to maximize the recovery of associated gold values. On the other hand, the maximum depression of arsenopyrite is desirable during base metal production.

Since fundamental investigations of the aqueous surface chemistry of arsenopyrite have previously not been undertaken, a comprehensive literature survey relating to this mineral was carried out. While certain aspects of this review may not have apparent significance to the flotation response of arsenopyrite they are believed to contribute to the overall understanding of its occurence and behaviour.

Chapter 2

LITERATURE REVIEW

2.1 State of the Art of Arsenopyrite Flotation

In reviewing the literature relating to the flotation of arsenopyrite it is apparent that the separation of arsenopyrite from pyrite is among the most significant separations to be considered. Whether it is for analytical purposes to determine whether associated gold is with pyrite or arsenopyrite or for the production of a pure pyrite product, free of arsenic, the separation of these two minerals receives frequent mention.

In discussing the characteristics of arsenopyrite under flotation conditions, frequent reference will be made to the behaviour of pyrite under the same conditions. This comparison will be useful since the depression of arsenopyrite would obviously not be of any real significance if most other sulphide minerals would be depressed under the same conditions. Consideration of the behaviour of pyrite therefore gives at least a limited measure of whether conditions for the depression of arsenopyrite are excessive. Another benefit of comparing the response of pyrite to that of arsenopyrite is that while arsenopyrite has received only very limited study, pyrite has been extensively investigated.

Sutherland and Wark (12) showed the critical pH (above which flotation did not occur) for flotation of arsenopyrite

with 25 mg. per litre of ethyl xanthate to be pH=8.4 compared to a value of pH=10.5 for pyrite.

Mitrofanov (13) indicated the maximum recovery of arsenopyrite to be achieved in the range of pH from 4 to 6.

Plaksin (14) and later Glembotski et al (15) discussed the influence of crystal structure on the oxidation of pyrite and arsenopyrite. The position of sulphur atoms in the pyrite was considered to be such that they could interact with oxygen and produce soluble species which left the surface as new pyrite, still able to react with reagents. The more complex structure of arsenopyrite was believed to result in slower oxidation rates than for pyrite. Prolonged oxidation was believed to result in decomposition of the arsenopyrite lattice with both sulphur and arsenic being oxidized. The arsenic oxide groups were postulated to remain at the mineral's surface.

The different susceptibility of the two minerals to oxidation has been exploited by Nekrasov (16) and Machovic (17) to achieve a separation. A bulk pyrite - arsenopyrite concentrate was produced and conditioned with an oxidizing agent. Nekrasov used an addition of MnO_2 followed by a two hour conditioning period with aeration to depress arsenopyrite. Machovic used additions of $KMnO_4$ to depress arsenopyrite while floating pyrite. Similar use of permanganate to depress arsenopyrite and pyrrhotite selectively from pyrite has been the subject of patents (18).

Glembotski et al. (15) related the greater oxygen concentration required for arsenopyrite flotation compared to that required for pyrite flotation to their different

susceptibility to oxidation. Rand (19) provided an explanation for the different oxygen requirements which is more in keeping with current flotation theory. He showed that pyrite has a greater oxygen reduction activity than has arsenopyrite. Pyrite therefore requires lower oxygen concentration in solution to provide the cathodic oxygen reduction reaction required to balance the anodic oxidation of xanthate. Similar results and interpretations were presented by Biegler et al. (20).

The use of magnesia mixture as a depressant for arsenopyrite has been proposed (21). The depressant mixture was prepared from magnesium chloride, ammonium chloride and ammonium hydroxide with distilled water. The mixture was found to give a high degree of arsenopyrite depression at pH values greater than 8. Chalcopyrite was also found to be depressed by this mixture if the mineral was first conditioned with AsI_3. Pyrite was found to be unaffected by the mixture. It was concluded that depression resulted from the formation of a strongly hydrophilic compound, $MgNH_4AsO_4 6H_2O$ on the surface of arsenopyrite. No direct evidence to support this conclusion was presented.

2.2 Nature of Adsorbed Xanthate Species

Very limited work has been reported in the literature with regard to the nature of adsorbed xanthate species on arsenopyrite. Allison et al. (22) reported dixanthogen to be the reaction product. The limits of detection were indicated to be such that up to 5 percent of the minor product (i.e. ferric xanthate) could be present.

Although additional investigations into the nature of the

reaction products of arsenopyrite with xanthate have not been reported, it is of interest to note the similarities with pyrite. Both minerals were reported to have dixanthogen as the predominant collector product and both have ferric xanthate as the alternative collector product (22,24). In the presence of oxygen, both minerals also have mixed potentials which are greater than the equilibrium potential for xanthate oxidation to dixanthogen.

In spite of the seeming consistency of these findings, controversy has continued as to the nature of the products formed by the interaction of pyrite with xanthate in solution. Various investigators (23,24,25,26) have studied the nature of the collector species on pyrite. Each of these studies has concluded the predominant surface product to be dixanthogen. The continued controversy appears to result from the determination of some investigators to establish a single adsorbed product and to neglect the role played by minor concentrations of other adsorbed species (27,28).

The majority of researchers now believe that dixanthogen is the active collector species in pyrite flotation while at the same time additional minor contributions to hydrophobicity can be made by ferric hydroxyxanthate or by elemental sulphur resulting from mineral oxidation.

The electrochemical oxidation of adsorbed xanthate to dixanthogen can be represented by:

$$X_2 + 2e^- == 2X^- \qquad (1)$$

The corresponding cathodic reaction is generally considered

to be the reduction of oxygen (23).

$$1/2\ O_2 + H_2O + 2e^- == 2OH^- \qquad (2)$$

$$O_2 + 4H^+ + 4e^- == 2H_2O \qquad (3)$$

The above reactions occuring via peroxide intermediate (23).

In the iron system, oxidants other than oxygen are also possible (24).

$$2Fe^{3+} + 2X^- == 2Fe^{2+} + X_2 \qquad (4)$$

$$2Fe(OH)_3 + 6H^+ + 2X^- == 2Fe^{2+} + 6H_2O + X_2 \qquad (5)$$

Although the preceding review was based on work with pyrite, it appears consistent to assume that the same conclusions can be made for the arsenopyrite - xanthate - oxygen system.

2.3 Crystal Structure

The structure of arsenopyrite has been investigated by Buerger (33,34) and Morimoto and Clark (36). Buerger determined the structure to be monoclinic, closely related to that of marcasite and loellingite (34,35). Each iron atom is surrounded by a distorted octahedron of which one face is a triangle of three arsenic atoms and the other a triangle of three sulphur atoms. The arsenopyrite structure is complex and is further

complicated by the fact that the mineral almost always occurs as twins. The effect of twinning is to give the mineral a pseudo-orthorhombic symmetry.

The structure of arsenopyrite as presented by Buerger is shown in Figure 4.

It can be seen that the structure is a body centered cubic structure with regard to iron. Sulphur and arsenic occur as As-S groups along cell edges.

Buerger(33) explained observed variations in interatomic spacing on the basis that iron in pyrite is in the ferrous state while iron in marcasite, loellingite and arsenopyrite is in the ferric state.

Although Glembotski (15) and Plaksin (14) based their arguments for oxidation of pyrite and arsenopyrite on the relative accessibility of the sulphur atoms to interaction with oxygen, it appears that significantly more complex considerations are controlling in this regard. While both marcasite and arsenopyrite are known to oxidize more readily than pyrite the results presented by those investigators indicate that arsenopyrite is passivated during oxidation while marcasite is not (37). The variation in behaviour of the various minerals under oxidizing conditions therefore appears to be controlled by the nature of both sulphur and iron oxidation products.

2.4 Electrochemical Oxidation of Arsenopyrite

The electrochemical oxidation of arsenopyrite has received limited study. Kostina and Chernyak (29,30,31) presented results

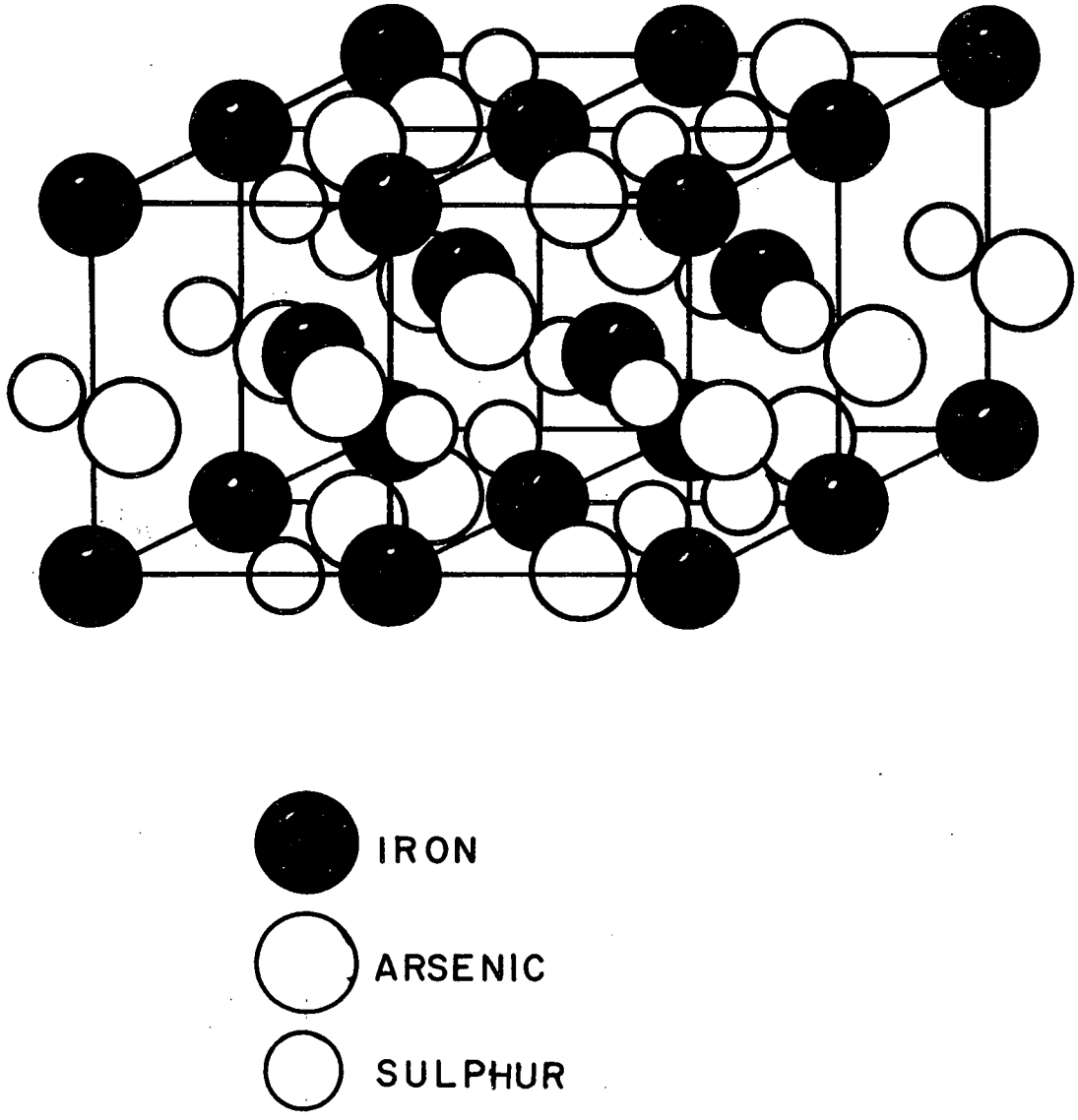

Figure 4

Crystal structure of arsenopyrite (after Buerger (33))

for oxidation experiments carried out with both pyrite and arsenopyrite. The objective of their work was to find conditions under which arsenopyrite would be rapidly oxidized and thereby release any entrapped gold. They demonstrated that the oxidation of both minerals occurred at lower potentials as conditions were changed from acid to alkaline pH. Arsenopyrite demonstrated a distinct oxidation peak in alkaline (sodium hydroxide) solution. Increasing temperature was found to increase the rate of oxidation at a given potential.

Pyrite was found to oxidize at a lower rate at a given potential than did arsenopyrite. It was also observed that the difference in oxidation rates increased with increasing potential (30). This contradicts the assumptions made by Glembotski (15) as previously discussed in section 2.1.

Analysis of solutions following prolonged oxidation in caustic solutions showed that under moderate oxidation conditions, arsenic and sulphur were leached from arsenopyrite. Almost equal amounts of tri-valent and penta-valent arsenic were formed. Sulphur oxidation resulted in varying ratios of sulphate to thiosulphate with varying oxidation potential (30).

Vakhontova and Grudnev (32) measured arsenopyrite electrode potential as a function of pH. Observed variations in the Eh-pH relationship were related to changes in the nature of decomposition products. Under acid conditions iron was concluded to go into solution as ferrous while under neutral and alkaline conditions it went into solution as ferric. In the supergene zone of ore deposits the alteration product of arsenopyrite under acidic conditions were found to be symplesite (ferrous

arsenate) while under neutral or alkaline conditions scorodite (ferric arsenate) was formed.

2.5 Arsenopyrite Composition and Phase Relations

The compositional variations of both synthetic and natural arsenopyrites have been considered in several investigations (38,36,39).

Clark (38) in studying phase relations in the Fe-As-S system observed that arsenopyrite synthesized under varying conditions of temperature and bulk composition deviated from the ideal FeAsS formula. X-ray diffraction data were used to determine the d_{131} spacing of arsenopyrite synthesized in various univariant assemblages as a function of temperature. It was observed that while at any given temperature the variation in arsenopyrite composition is small, throughout the range of temperatures investigated, the variation in composition is significant. Only a qualitative relation was established however, since insufficient compositional data were available to quantify the dependence of d_{131} on the S/As ratio in arsenopyrite.

In addition to compositional variations of arsenopyrite, Clark presented data which show the limits of stability of the various mineral assemblages. The maximum temperature of formation of arsenopyrite was shown to be 702° ± 3°C. If native arsenic coexists with arsenopyrite the deposition temperature was below 688° ± 3°C. The maximum temperature of pyrite - arsenopyrite coexistence is 491° ± 12°C.

Morimoto and Clark (36) presented chemical analyses for

sixteen naturally occuring arsenopyrites. From those analyses which were considered to be consistent with the associated mineral assemblages they determined the composition of naturally occurring arsenopyrite to vary from $FeAs_{0.9}S_{1.1}$ to $FeAs_{1.1}S_{0.9}$. The majority of analyses were shown to be on the sulfur-rich side of the ideal FeAsS composition which was considered to be consistent with the predominance of sulphide - type over arsenide - type mineral deposits.

Kretschmar and Scott (39) made a further contribution to determining the composition of natural arsenopyrite. In addition to a review of published studies on arsenopyrite composition they presented detailed analyses for 31 synthesized and 54 naturally occurring arsenopyrites.

Analyses were carried out by means of electron microprobe determinations.

The relation between atomic % arsenic and the d_{131} X-ray peak position was determined to be:

$As = 866.67d_{131} - 1381.12$

with an estimated standard deviation of ±0.45% As.

A temperature - composition section for arsenopyrite which was prepared (39) is shown in Figure 5. The data used to construct the diagram were obtained by synthesizing arsenopyrite at varying temperatures and equilibrium assemblages. The diagram illustrates the range of compositions for arsenopyrite depending on the conditions of formation. The diagram is also useful in the converse sense in that if an arsenopyrite is accurately analyzed and its equilibrium assemblage is determined then the temperature of formation can be established.

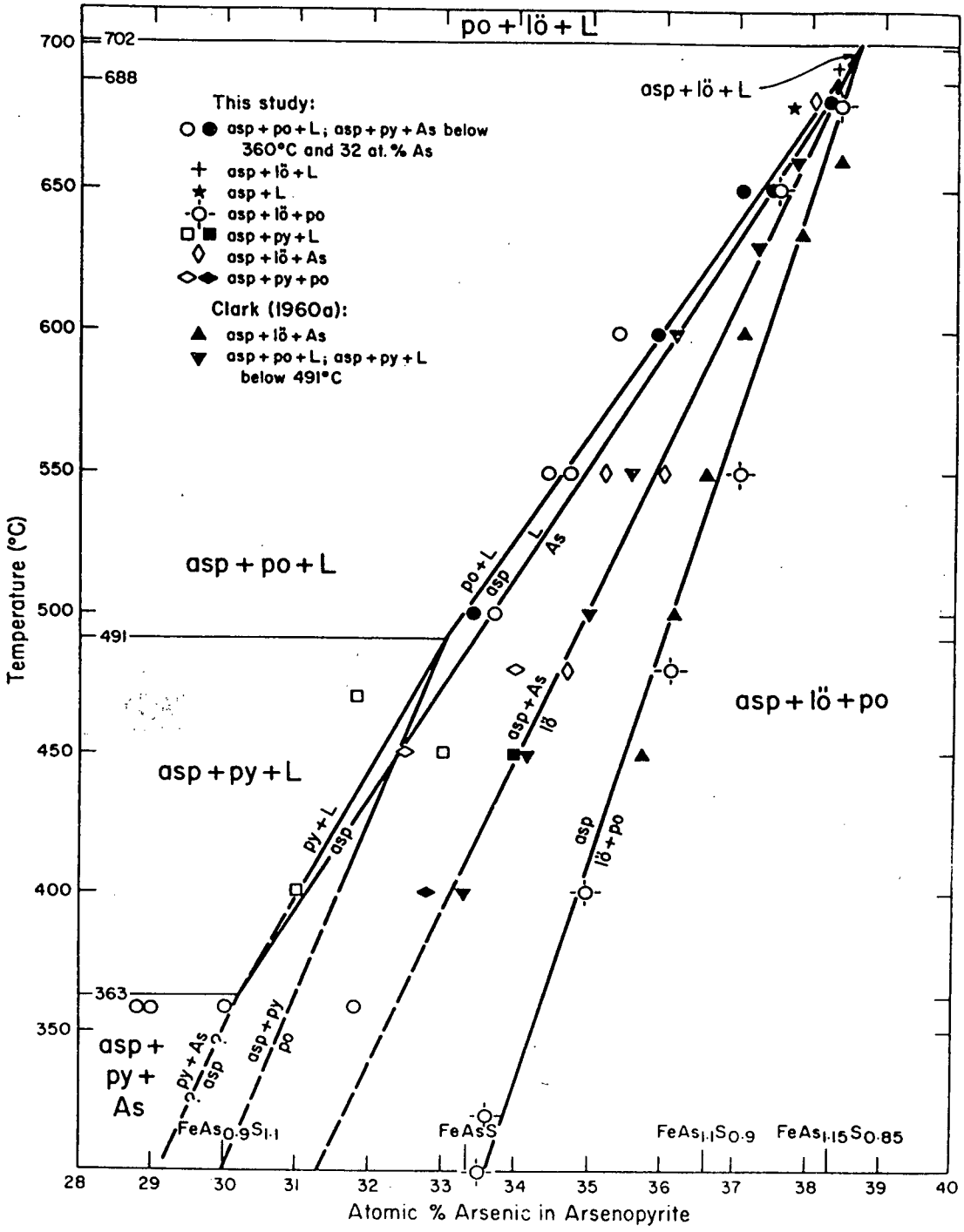

Figure 5

Atomic % arsenic in arsenopyrite

Arsenopyrite is slightly non-stoichiometric, showing an Fe deficiency. Morimoto and Clark (36) and Kretschmar and Scott (39) determined the Fe deficiency to be less than 0.7 atomic %.

The limits of arsenopyrite composition presented by Kretschmar and Scott are $FeAs_{0.9}S_{1.1}$ to $FeAs_{1.5}S_{0.85}$ corresponding to an approximate range in atomic % As of 30% to 38%.

Clark (38) and Kretschmar and Scott (39) observed that arsenopyrite formed with a given composition does not readily re-equilibrate if subjected to a new set of conditions. Arsenopyrite present in highly metamorphosed deposits will therefore be characteristic of the initial conditions of formation of the deposit.

Natural arsenopyrites are almost always compositionally zoned (39). In S-rich assemblages the centre of crystals are S-rich relative to the rims while in As-rich assemblages the centres are As-rich relative to the rims.

2.6 Electrophysical Properties of Arsenopyrite

Arsenopyrite is a semiconducting mineral with a band gap of about 0.2 eV (45). Shuey summarized the mineral as having a low carrier mobility and consistently high carrier concentration. Resistivity values reported by several investigators are presented in Table 3.

Arsenopyrite near stoichiometric composition is an intrinsic semiconductor at room temperature. Arsenic deficiency or the presence of impurities make most arsenopyrite n-type, but in arsenic-rich environments it is p-type.

Table 3
Arsenopyrite Resistivity Values

Source	Resistivity, ohm-cm.
42	$2.0 \times 10^{-3} - 3.0 \times 10^{-2}$
43	$1.10 \times 10^{-2} - 6.0 \times 10^{-2}$
44	$7.5 \times 10^{-2} - 4.5 \times 10^{-1}$
45	3.0×10^{-2}
46	$1.5 \times 10^{-3} - 7.0 \times 10^{-1}$

Krasnikov (40) determined that arsenopyrite in a gold ore deposit varied from p-type in high temperature, lower horizons to n-type in lower temperature, upper horizons. Favorov (41) discussed the results of a statistical treatment of spectral analysis and thermo-emf measurements for 2000 samples of pyrite and arsenopyrite. Arsenopyrite was found to vary from p-type for high temperature, low sulphur partial pressure associations to n-type for decreasing temperature and increasing sulphur partial pressure associations.

The possible influence of semiconductor properties on the flotation behaviour of arsenopyrite must be considered.

2.7 Electrophysical Effects in Flotation

Sulphide minerals are generally semiconductors. These minerals vary widely in their electrophysical properties such as resistivity, band gap, carrier concentration and conductor-type (45). These varying electrophysical properties could be expected to influence the adsorption or electrooxidation of collector molecules at the mineral surfaces.

Plaksin and Shafeev (46) were the first to study the nature of charge carriers in sulphide minerals (in particular galena)

and the effect of charge carrier type on xanthate adsorption They considered that the presence of free electrons in the surface layer of sulphides prevents the formation of adsorption bonds with xanthate. The action of oxygen on galena was believed to result from an inversion of the surface layer from n-type to p-type.

Subsequent investigators in this field proposed alternate roles for oxygen and concluded that semiconductor properties were not controlling with regard to xanthate - mineral interaction (47,48,49).

Recently, Biegler (50) concluded that there was no obvious correlation between kinetic parameters for oxygen reduction on pyrite and the nature of semiconduction. He further concluded that if impurities were the primary influence on differences in electrochemical behaviour their influence was not exerted through their effects on the semiconducting properties.

It appears therefore that while sulphide minerals are semiconductors and display all the electrical properties associated with this class of conductors, the flotation response of these sulphide minerals is not controlled primarily by these electrical properties. Although the influence of semiconducting properties on the electrochemical behaviour of arsenopyrite has not been reported in the literature, a reasonable deduction can be made. The behaviour of arsenopyrite as an electrocatalyst for oxygen reduction has been shown (20) to be similar to that of other sulphides such as pyrite and galena. It is therefore a reasonable assumption that the semiconducting properties of arsenopyrite will not be a principal influence on

electrochemical behaviour throughout the potential range relevant to flotation of the mineral.

Chapter 3

OBJECTIVES OF THE PRESENT INVESTIGATION

The objective of the present research program was to study the surface chemistry of arsenopyrite so that its flotation or depression could be more effectively controlled than has been possible to date.

A review of the literature revealed that the flotation response of arsenopyrite had received only limited study. Fundamental investigations of the nature of surface reactions of arsenopyrite under flotation conditions had not been carried out previously.

Information obtained from the literature and preliminary investigations for the present research program indicated that surface oxidation reactions could be significant in controlling arsenopyrite flotation. In addition, the adsorption of xanthate at the arsenopyrite surface involves electron transfer reactions. Electrochemical investigations have therefore been a principal research method for this program. In particular, cyclic voltammetry of stationary and rotating arsenopyrite electrodes has been used to study surface oxidation reactions.

Electron spectroscopy (ESCA) has been used to augment these surface oxidation studies. This technique enables surface oxidation films to be analyzed. In addition to verifying the formation of surface iron hydroxide films, the behaviour of arsenic and sulphur during the formation of these films was determined. The behaviour of arsenic and sulphur could not be

resolved through the use of voltammetry alone.

Since arsenopyrite is most commonly recovered in flotation systems employing xanthate as the collector, the influence of the surface oxidation of arsenopyrite on its interaction with xanthate was also considered.

Flotation experiments to evaluate the effectiveness of various oxidation procedures on arsenopyrite have been carried out. Arsenopyrite which had not been floated previously with xanthate as well as some which had been floated was investigated.

Compositional variations of arsenopyrite used for electrochemical or flotation experiments have not been considered since these are not expected to control the oxidation of the mineral or its interaction with xanthate, provided large amounts of impurities are not present.

Chapter 4

ELECTROCHEMICAL STUDIES

4.1 Electrode Potential Measurements

The potential achieved in the absence of oxidizing agents gives an indication of the tendency of the mineral to oxidize in the presence of aeration (51). Potentials achieved in the presence of oxidizing agents can be correlated with results of electrochemical investigations to predict relative oxidation rates as well as the nature of oxidation products.

Mixed potential measurements were carried out in order to determine the potential achieved by the mineral in the absence of any well defined redox couple and then to observe the effects of various oxidizing agents on electrode potential.

Measurements were carried out across the range of pH values commonly encountered in sulphide flotation circuits (pH = 4 to pH = 12).

4.1.1 Experimental

Electrode potential measurements were carried out in a spherical glass cell containing 1.25 litres of solution at room temperature (25-28°C.). Test solutions were prepared from single distilled water with a standard addition of 0.1 molar KCl. The desired pH value for each test was achieved through the use of

sodium tetraborate (0.05 M) with sodium hydroxide or sulphuric acid to raise or lower the pH respectively.

Solutions were deoxygenated by bubbling argon through them. Bubbling was continued throughout the test and was the only source of solution stirring. Traces of oxygen (3 to 5 ppm), present in the argon were removed by passing the gas through a pyrogallol solution.

Potential measurements were carried out relative to a saturated calomel electrode and converted to the hydrogen scale by taking the potential of the SCE to be -0.243 volts relative to a hydrogen electrode at 25°C.

Potentials were measured with a Beckman Electroscan 30. A potential having a drift of less than 2 mV over a ten minute period was generally achieved within 5 minutes. The potential was recorded after 20 minutes to ensure stable conditions had been achieved in each case. Potentials could be determined within ±5 mV. The reproducibility of potentials at a given pH value was found to be ±20 mV.

In tests involving oxidizing agents the electrode was first placed in distilled water and was allowed a 20 minute period to achieve a stable potential. After this period the oxidizing agent was added to the solution and again a 20 minute period was allowed before the potential was recorded.

Electrodes were constructed using arsenopyrite crystals from two sources.

One sample was obtained from Ward's Scientific and was indicated to come from Parral, Chihuahua. This material was analyzed as follows:

Measured	Theoretical
As = 46.0 ±0.2%	46.01
Fe = 34.0 ±1.0%	34.30
S = 19.8 ±0.1%	19.69
Co = not detected (<0.02%)	
Ni = not detected (<0.02%)	
Sb = not detected (<0.04%)	
Cu = not detected (<0.01%)	
Pb = 0.27%	
Zn = 0.06%	

This composition shows a slight iron deficiency compared to stoichiometric composition, as has generally been noted for arsenopyrite (39). The composition also shows a slight excess in the sulphur to arsenic ratio and would be expected to be an n-type semiconductor.

The electrode prepared from this sample had an exposed area of approximately 0.7 cm^2.

The second sample of arsenopyrite was supplied by Mr. Joe Nagel of the UBC Department of Geological Sciences and came from Riondel, B.C. There was insufficient sample to carry out a chemical analysis of this material but a comparative analysis to the sample from Mexico was carried out by means of a scanning electron microscope equipped with an energy dispersive analyzer (SEM-EDX). The analysis gave similar iron, arsenic and sulphur peaks as the Mexican material and did not exhibit any peaks indicative of excessive concentrations of any impurities.

The electrode prepared from this material had an exposed area of approximately 0.74 cm^2.

The semiconductor type of each material was determined by means of a simple determination employing the Seebeck effect. A millivoltmeter was used to measure the potential across a hot probe and a cold probe in contact with the arsenopyrite crystal.

In each case the hot junction was found to be positive relative to the cold junction indicating the samples to be n-type semiconductors.

A pyrite electrode was prepared using material from Hanaoka, Japan. The polished electrode was examined microscopically and was determined to be free from inclusions of other sulphide minerals. The exposed area of this electrode was approximately 0.38 cm^2.

The method of electrode construction is shown in Figure 6. A section of the mineral was mounted in epoxy consisting of one part diethylene triamine to 10 parts Epon 828. Immediately after placing the liquid epoxy on the sample it was placed in a vacuum to eliminate air bubbles and to enable the epoxy to seal cracks in the sample. Both sides of the mounted section were ground down to expose the mineral. One side then had a thin layer of gold vacuum deposited in two areas. A copper wire was fastened to each area with silver conducting cement.

A second epoxy section was prepared with a glass tube inserted through one side. The wires from the mineral sample were inserted through the glass tube and the two sections were glued together using a fast setting epoxy.

Prior to each experiment the section was wet ground on 600 mesh paper and then rinsed with distilled water before being inserted into the test solution.

4.1.2 Oxidizing Agents

A variety of oxidizing agents are used in industry to carry out reactions ranging from pulp bleaching to effluent control.

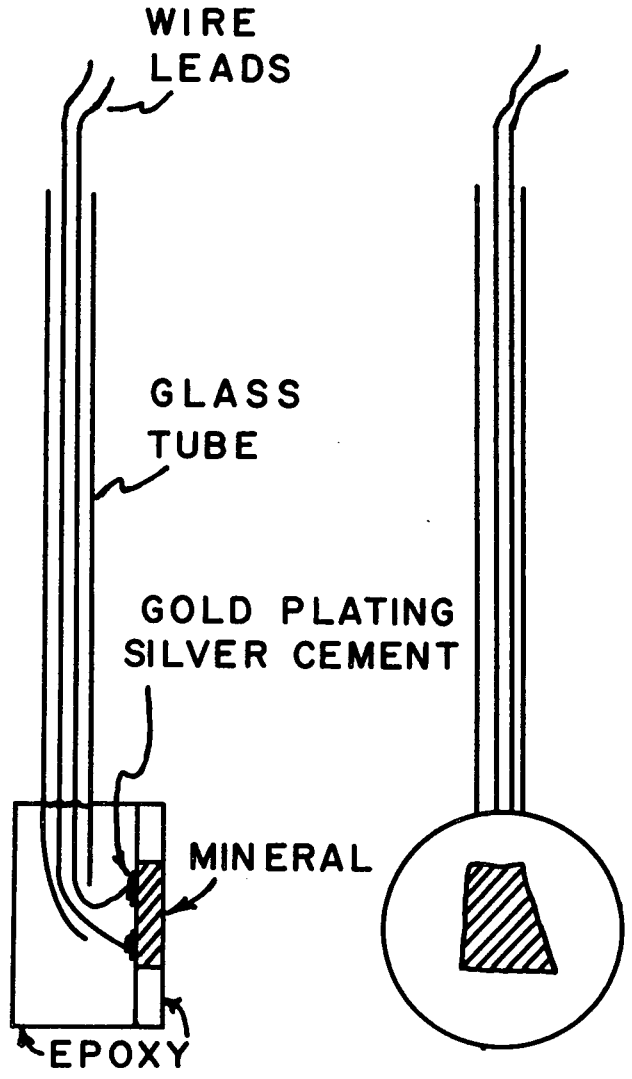

Figure 6

Method of electrode construction

Only limited use is made of oxidizing agents in the mineral processing industry. These are used primarily for alkaline chlorination of cyanide solutions and as oxidants for the leaching of uranium ore (54). Use has also been made of potassium permanganate to increase the oxidation of pyrrhotite during grinding and thereby decrease its floatability (52).

In order for an oxidizing agent to be acceptable for use in controlling the flotation response of minerals it must meet several criteria in addition to being an effective oxidant. Among these criteria are that it must be cost competitive, must not be exceedingly difficult or dangerous to handle and mustnnot result in pollution problems.

The oxidizing agents used in the present study were selected on the basis of either already having some application in processing plants (NaClO, $KMnO_4$) or being considered to be a non-polluting, cost competitive reagent (H_2O_2). While additional oxidizing agents such as chlorine or Caro's acid (H_2SO_5) could also be appropriate, the range of mixed potentials achieved by the present series of agents was found to cover the range of interest as determined by electrochemical experiments described in subsequent sections. The current (1982) costs for the reagents used in the study are shown in Table 4. Table 4 also shows the available oxidizing units per kilogram. These units are the product of the number of moles of oxidant per kilogram times the number of electrons transferred assuming alkaline conditions.

The variation in oxidizing power of these reagents can be determined from a series of oxidation state diagrams (53). These

Table 4
Cost of Oxidizing Agents

OXIDIZING AGENT	COST $/kg. Oxidant	OXIDIZING units/kg
Hydrogen Peroxide (50% Solution)	1.10 - 1.32	58.8
Potassium Permanganate	3.75 - 4.75	25.3
Sodium hypochlorite (12% Solution)	3.48 - 5.61	26.8

diagrams graphically present the volt equivalent of a compound or ion as a function of its oxidation state. The volt equivalent is the product of the oxidation state and the redox potential relative to the element in its standard state and is related to the free energy for the species according to $\Delta G = -nFE$. The gradient of the line joining two points on such a diagram is the redox potential of the couple represented by the points. A large positive gradient represents a strong oxidizing couple and a large negative gradient, a strong reducing couple.

Diagrams for the chlorine, manganese and oxygen-water systems are shown in Figures 7,8 and 9. The diagrams include both acid ($a_{OH^+}=1$) and alkaline ($a_{OH^-}=1$) conditions. The variation of the oxidizing power with pH is an important consideration since flotation of sulphides is generally carried out at pH values greater than pH=4 and more commonly in the range of pH=8 to pH=11. Thus the diagram for manganese indicates that while in acid media permanganate represents a strong oxidizing agent capable of being reduced to Mn^{++} ions, in alkaline media a much lower gradient is apparent and manganese oxides and hydroxides are formed. The use of MnO_2 in acid media could be expected to result in reasonable oxidation while at high pH this reagent would be ineffective as an oxidant. This

could in part explain the two hour conditioning period which Nekrasov (16) required when using MnO_2 for arsenopyrite oxidation.

In the case of the chloride system hypochlorite is indicated to be a stronger oxidizing agent than chlorate.

While the diagrams are useful for representing the oxidation potential of various reagents it must be held in mind that particularly in a heterogeneous system, kinetic factors may in fact control their relative effectiveness.

4.2 Results and Discussion

Preliminary experiments with a platinum electrode in deoxygenated distilled water gave the relation

$$Eh = 850 - 62.3\ pH \quad ,mV$$
$$r = -1.00$$

Since this is in reasonable agreement with the relationship

$$Eh = 800 - 59\ pH \quad ,mV$$

which has been developed elsewhere (55) the recording equipment was considered to be capable of providing reliable measurements. A variation of up to 100 mV in the intercept potential can be expected because while the pH is buffered and therefore accurately controlled, the potential is to some extent controlled by kinetic factors and may therefore deviate from thermodynamically derived values. The experimental relation was achieved by varying the pH and then measuring the electrode potential without repolishing or cleaning the electrode between measurements. Slow kinetics with regard to equilibration of the system could account for the deviation of both the intercept and

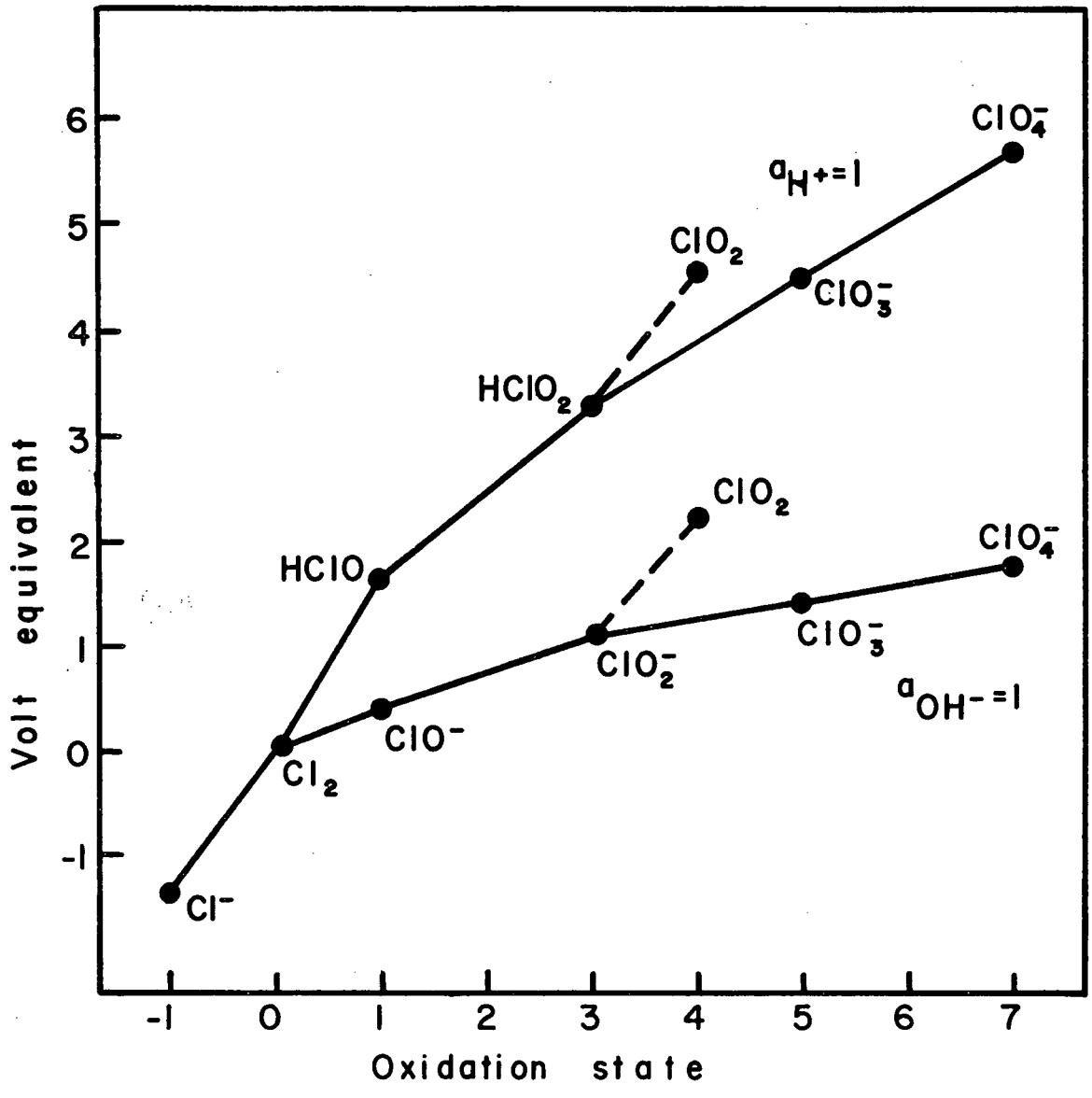

Figure 7

Oxidation state diagram for the chlorine system

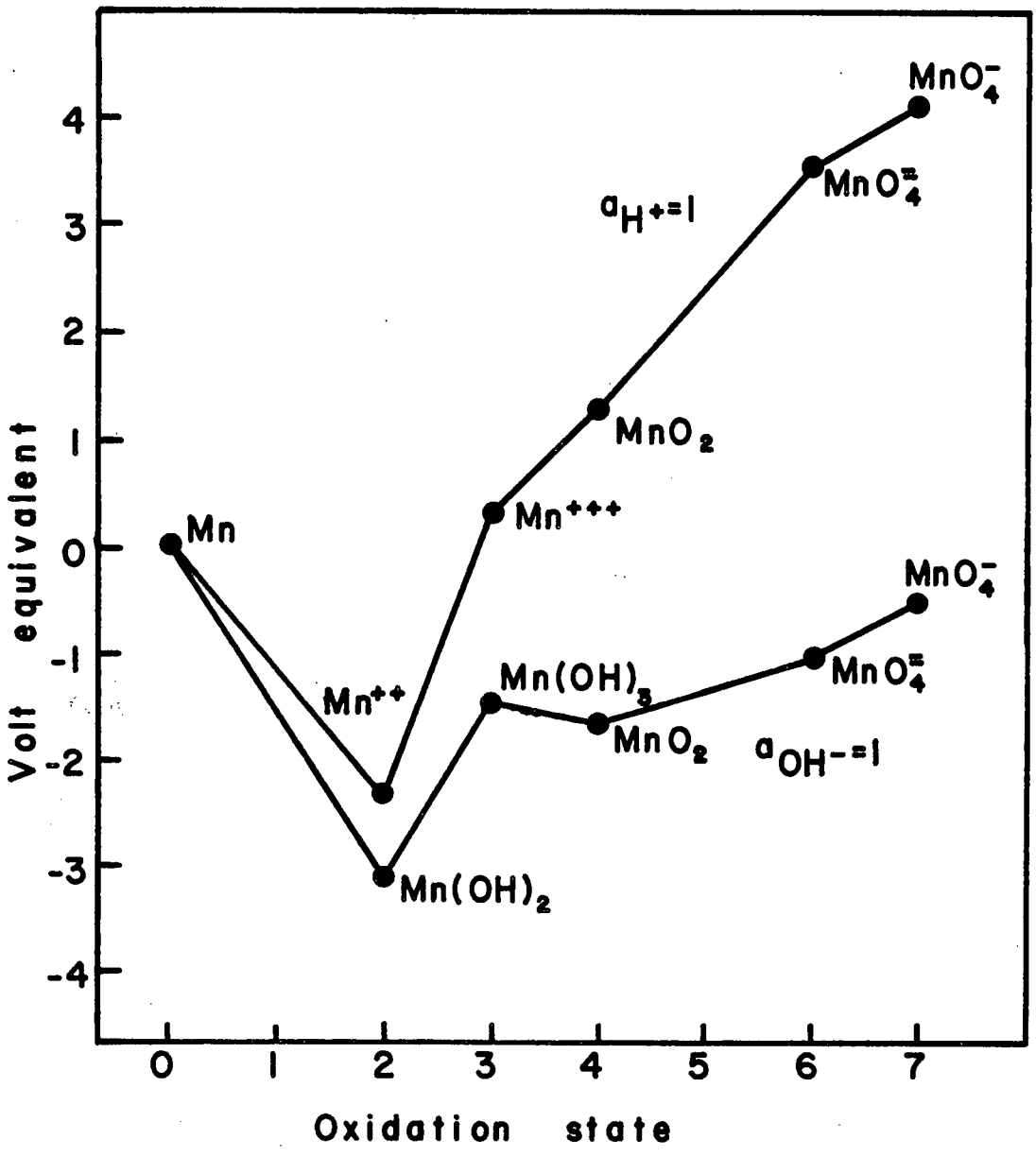

Figure 8

Oxidation state diagram for manganese system

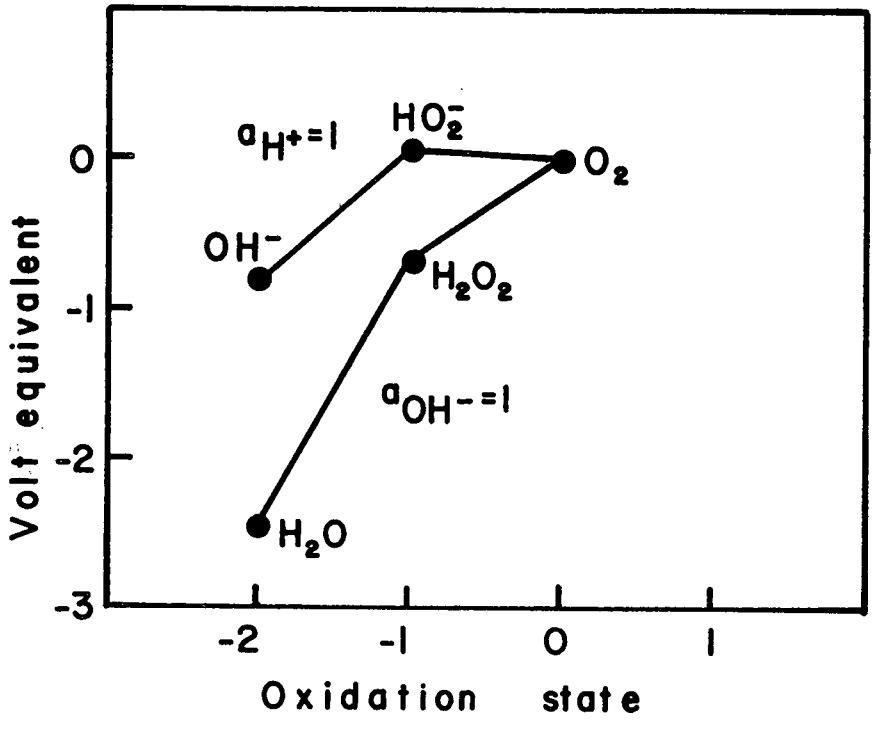

Figure 9

Oxidation state diagram for the oxygen system

slope of the experimental relation from theoretical values.

Mixed potentials measured with arsenopyrite and pyrite electrodes are shown in Figures 10 and 11.

The potential measured with arsenopyrite in deoxygenated water over the pH range from 3.8 to 11.2 gives the relation

$$Eh = 586 - 48.2\ pH \quad ,mV$$
$$r = -0.9976$$

At pH greater than 11.2 the potentials fall below this line with increasing deviation as the pH increases. At the same time an electrode which was allowed to reach a stable potential at pH greater than 11.2 was observed to develop a visible surface oxide layer. This surface deposit had a brown appearance when the electrode was allowed to dry.

Another observation was that if the pH of the solution was lowered after the electrode had reached a stable potential at pH greater than 11.2, the electrode potential followed along the same curve as for freshly polished electrode measurements. The points obtained in this way are shown in Figure 10. The deviation from a straight line at pH greater than 11.2 indicates arsenopyrite to be inherently unstable in this region. The mineral decomposes, leaving a surface oxide layer. Since the electrode potentials in the presence of this visible oxide follow the same relation as obtained for a freshly polished electrode, the same oxide film must be present with the fresh electrode but is too thin to be readily observed. The composition of this surface oxide will be discussed in the section on voltammetry.

There are several differences in the behaviour of the pyrite electrode compared to the arsenopyrite electrode. Over

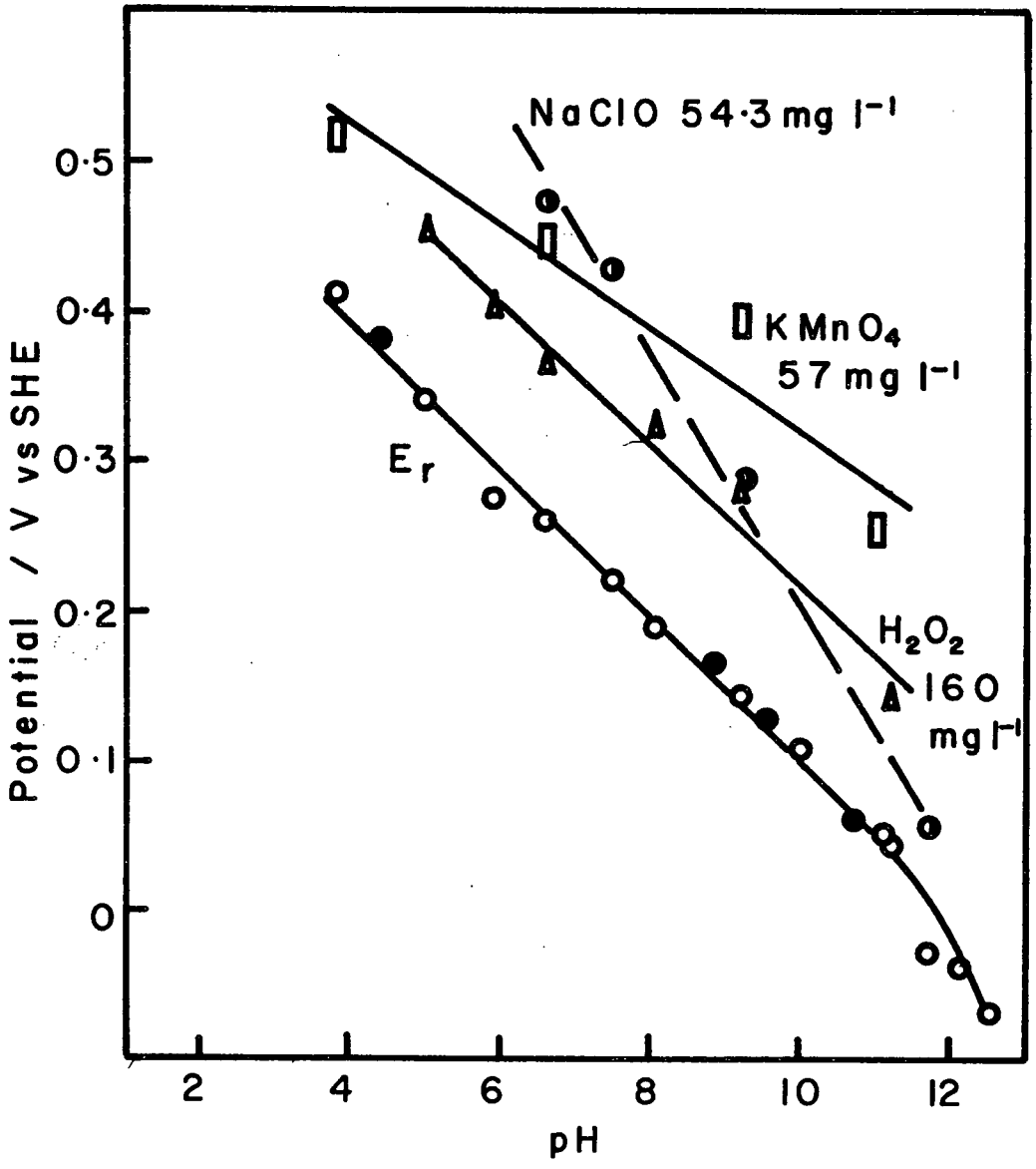

○ Individual measurement

● Titration point

Figure 10

Eh versus pH for arsenopyrite

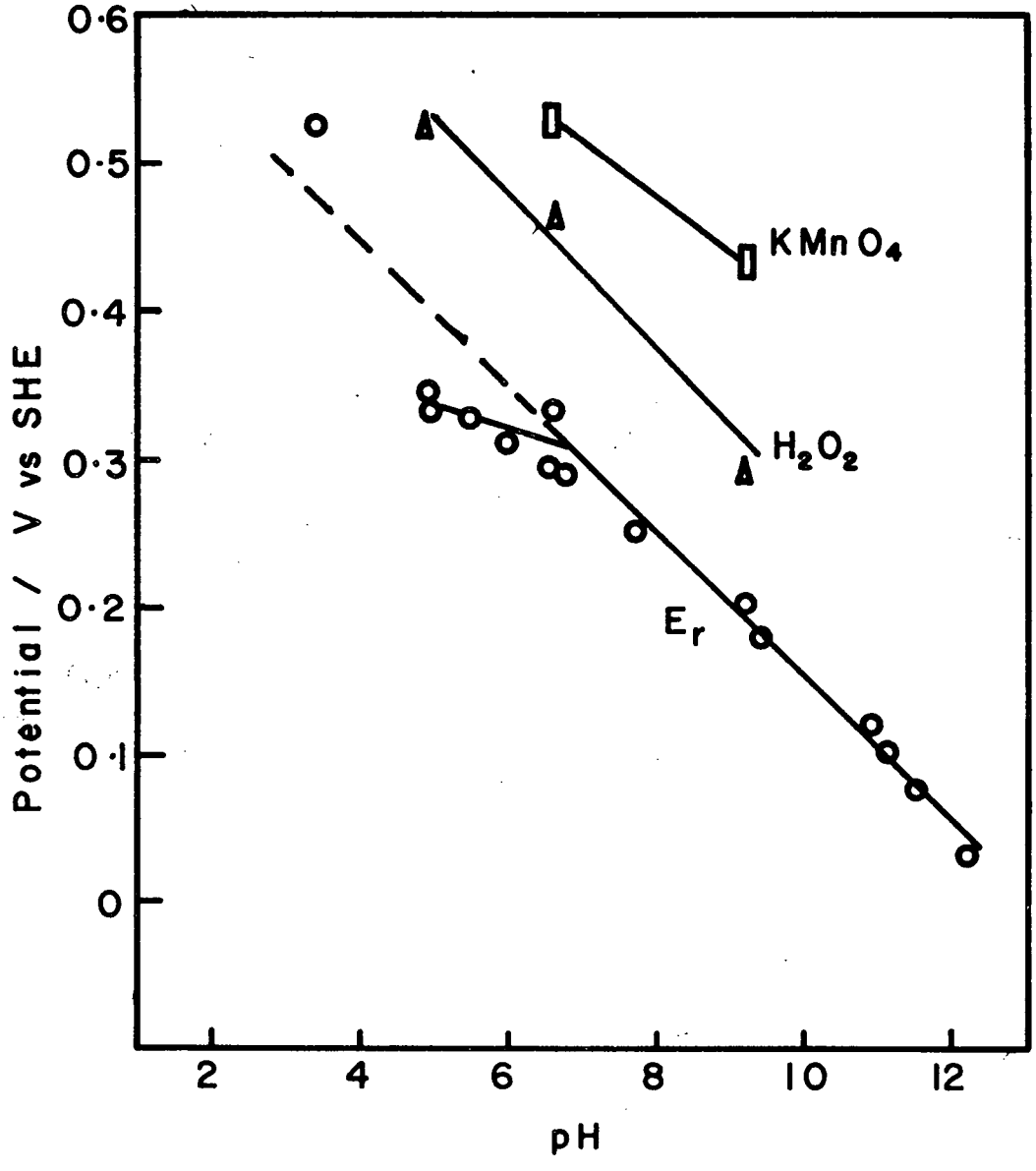

Figure 11

Eh versus pH for pyrite

the pH range from 7 to 12.2 the potential followed the relation

$$Eh = 643 - 49.0\ pH$$
$$r = -0.993$$

indicating pyrite to be a more noble mineral than arsenopyrite. Unlike arsenopyrite, pyrite shows no deviation from this relation at high pH. The potential of an electrode which had reached a stable potential at pH = 12.2 followed the same Eh-pH relation down to pH = 3.4. Only a slight tarnish was visible for the pyrite electrode at pH = 12.2.

Potentials measured with a clean pyrite electrode at pH less than 7 fall below the line represented by the above relation. Similar observations have been made for pyrite and other sulphides by other investigators (55). The deviation from the relation below pH = 7 was explained on the basis that below this pH the passivating oxide layer was not forming and the electrode is in a corrosion region.

The concentration of each oxidizing agent which was used in tests involving these additions was based on the results of preliminary flotation experiments. The flotation experiments had indicated that these concentrations of oxidizing agent were in the range which could be required for arsenopyrite depression.

Potential measurements made with an arsenopyrite electrode in the presence of oxidizing agents are shown in Figure 10. In the case of potassium chlorate the potentials in the region of pH from 7 to 10 were found to fall on the same line as those obtained in the absence of any oxidizing agents.

The remaining potentials follow the relations:

With 160 mg/l Hydrogen Peroxide

$$Eh = 688 - 46.9\ pH$$
$$r = -0.9886.$$

With 57 mg/l Potassium Permanganate

$$Eh = 663 - 34.1\ pH$$
$$r = -0.9533$$

With 54.3 mg/l Sodium Hypochlorite

$$Eh = 1037 - 82.9\ pH$$
$$r = -0.9966$$

A few measurements were carried out with the pyrite electrode in the presence of hydrogen peroxide and potassium permanganate. As in the case of arsenopyrite the potential achieved with pyrite in the presence of permanganate is higher than with peroxide over the pH region of interest.

4.3 Cyclic Voltammetry

References cited in the literature review on arsenopyrite flotation indicate that the surface oxidation of the mineral could play a major role in controlling its flotation response. The results of electrode measurements presented in the previous section indicate that surface oxide deposits are formed on arsenopyrite at high pH or under moderate oxidizing conditions. It is therefore of interest to determine the nature of these surface oxide deposits so that their formation and therefore the flotation response of arsenopyrite can be better controlled than has previously been possible.

Cyclic voltammetry, in addition to enabling the interaction of electrodes with dissolved electroactive species such as xanthate to be studied, provides a means for studying surface oxidation reactions of electrodes. By carrying out repetitive scans the influence on surface changes of excursions to various potential ranges can be observed.

Cyclic voltammetry has been used to study the oxidation of

ethyl xanthate and the influence of flotation depressants on pyrite electrodes (23). The interaction of flotation reagents with (57) and the surface oxidation (58) of galena has also been studied by this technique.

Electrochemical reactions involving particular species in the absence of chemical reaction mechanisms have been studied using noble metal electrodes (23,49) and employing cyclic voltammetry.

Cyclic voltammetry is similar to linear sweep polarization but with the added feature that the potential variation with time is reversed at some point and returned to the starting potential. In this way both the oxidation and reduction of electroactive species at the electrode surface can be studied. For example, if xanthate is oxidized to dixanthogen at an electrode during an anodic potential sweep and the sweep is then reversed, the reduction reaction can be monitored. By measuring both anodic and cathodic currents, it can be determined that the dixanthogen formed at the electrode remains at the surface and does not diffuse into the bulk solution.

Several figures which are essential to the discussion in this thesis are included on a fold - out page as Appendix II. Figure 1 in Appendix II is taken from reference 49 to illustrate the essential features of a voltammogram. In the presence of xanthate an anodic potential sweep starting at -0.4V shows essentially no current being passed until a potential of 0.2V is exceeded. Beyond this potential there is a rapid rise in current to a peak, followed by a gradual decline. Once the potential falls below 0 V dixanthogen is reduced, at which point a

cathodic peak is observed. The reversible potential for the xanthate - dixanthogen couple is 0.15 V at the concentration of xanthate used. The anodic peak can be associated with the oxidation of xanthate to dixanthogen while the cathodic peak can be associated with the reverse reaction. In the presence of xanthate, hydrogen and oxygen adsorption is inhibited and peaks associated with these species are therefore not observed.

The height of the xanthate peaks would be increased by stirring of the solution or by increasing the xanthate concentration. Both of these actions would increase the supply of xanthate to the electrode surface.

Although voltammetric sweeps are sometimes carried out at slow scan speeds (less than 1mV/sec.) in general the scan speeds employed are greater than 1 mV/sec. At increasing scan speeds the current peaks due to charge transfer reactions are increased and may be more fully studied.

For a fixed sweeprate and current scale, increased peak height is associated with an increased reaction rate. An increase in the area under a peak indicates an increase in the reaction products (i.e. a greater total current is passed).

4.3.1 Experimental

Voltammetry was carried out with both stationary and rotating electrodes. For stationary electrode experiments the electrodes were the same ones as used for electrode potential measurements.

The rotating electrode was constructed as shown in Figure 12. An arsenopyrite disc was prepared using a diamond

impregnated glass drill. The crystal used for this electrode was the same one from Riondel, B.C. as was used for the stationary electrode. One face of the disc was gold coated and this face was fastened to the end of the brass rod which formed the centre of the electrode. The space between the arsenopyrite and the surrounding teflon tube was filled in three stages using a hypodermic syringe filled with epoxy. The electrode was equipped with a gold ring which was silver soldered to a brass sleeve leading to the electrode connections. The remaining physical features and manner of connection was as for a standard Pine Instruments rotating electrode (84).

The measurement circuit employed for voltammetry is shown in Figure 13. The potentiostat used was a Wenking 68 TS10. Cyclic potential functions were controlled by means of a Princeton Applied Research Model 175 Universal programmer. Currents were recorded by means of a Keithley Model 171 digital multimeter in series with the platinum counter electrode. Current - potential scans were recorded with an Electro Instruments Model 520 XY recorder. Rotating experiments were carried out by means of a Pine Instruments Model ASR 2 rotator. All instruments were plugged into a multi- outlet extension to eliminate ground - loop problems.

Tests were carried out in a convential H - cell with the working electrode compartment having a volume of 850 cc and being separated from the counter electrode by a fritted glass disc. All tests were carried out at room temperature (22±2 °C). A standard addition of 0.1M potassium chloride was made to each test. The pH was adjusted by means of sodium tetraborate with

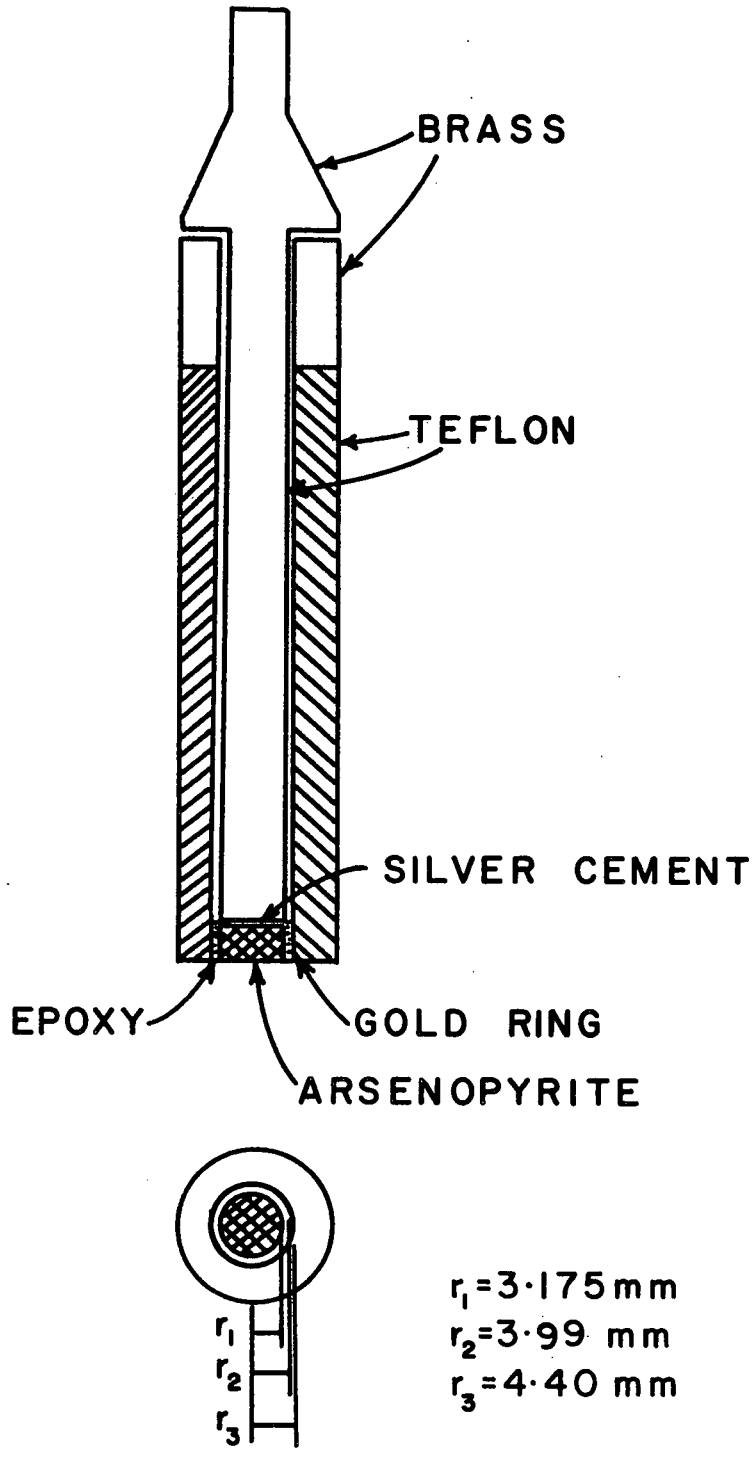

Figure 12

Construction of rotating arsenopyrite electrode

sodium hydroxide or sulphuric acid. All reagents used for preparation of solutions or for addition of specific ions were reagent or analytical grade.

4.3.2 Results and Discussion

A. Single Sweep Voltammograms

By carring out voltammetry across a wide range of pH, variations in both anodic and cathodic peak positions can be observed. By noting both peak positions and shifts in peak position with pH, possible elecrochemical surface reactions associated with these peaks can be postulated. Reversible potentials for postulated reactions can be calculated and correlated with peak positions.

Voltammograms resulting from the application of triangular potential cycles to arsenopyrite across the range of pH = 5.85 to pH = 11.95 are shown in Figures 14 and 15.

Between pH = 6.6 and 7.3 an anodic peak becomes apparent in the region of 0.6 to 0.7 volts. This peak becomes more prominent and shifts to more cathodic potentials with increasing pH according to the relation.

$$Ep = 1216 - 78.6\ pH\ mV.$$

$$r = -0.99$$

The scans shown in figures 14 and 15 start well below the rest potential of arsenopyrite. Additional anodic scans were carried out starting from the rest potential to ensure that the anodic peak is not associated with products resulting from cathodic currents observed at the start of the scans. Anodic peaks for

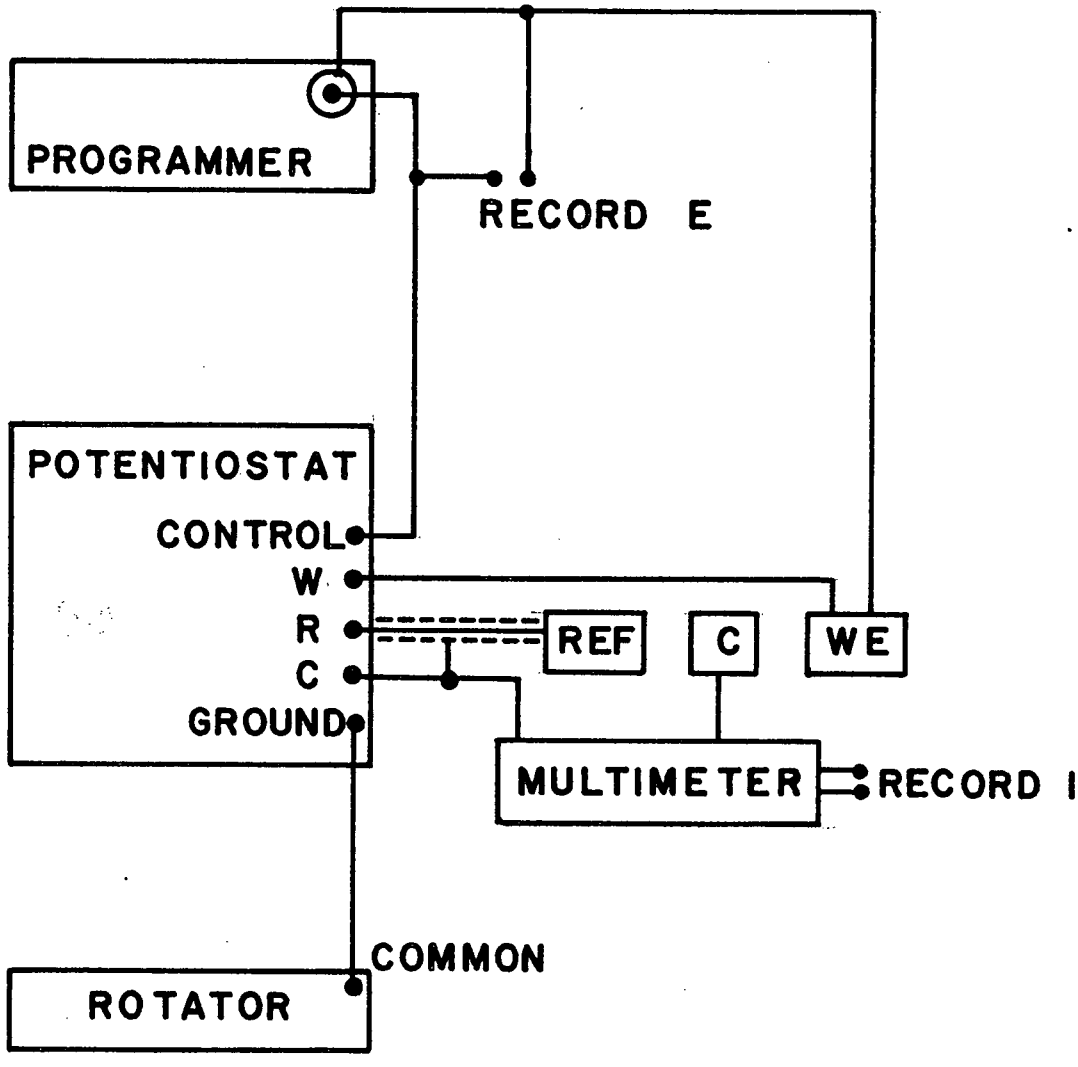

Figure 13

Control and measurement circuit used for voltammetry

scans starting at the rest potential were found to occur at the same potential and to be of the same magnitude as those for scans starting at the lower potentials.

The anodic peak lies in the potential region which is relevant to flotation systems. The electrode potentials which were measured in the presence of hydrogen peroxide and permanganate are indicated in Figure 16 and Figure 2, Appendix II, on a voltammogram obtained at pH = 8.2. The potentials achieved with these oxidizing agents should result in the reaction associated with the anodic peak proceeding at a significant rate.

Since a KCl supporting electrolyte was used and good connections to the electrode were made and the resisitivity of the electrode material is low (ie. 10^{-2} ohm - cm) peak potentials are believed to be accurate even at the relatively high currents (800 microamperes) observed for some scans.

The repeatability of scans was found to be within 10 millivolts and was limited primarily by the ability to determine accurately the peak position on the chart recorder. Peak currents were found to be sensitive to the condition of the grinding paper used to prepare the electrode surface. Provided a fresh area of grinding paper was used to finish the electrode preparation, currents could be reproduced to within 20 microamperes.

A small anodic prewave becomes apparent at approximately -0.1 V at pH = 9.6 in Figure 14. This prewave becomes more apparent over the pH range from 9.6 to 10.55 and then decreases over the range of pH 11.05 to 11.95. The peak position shifts to

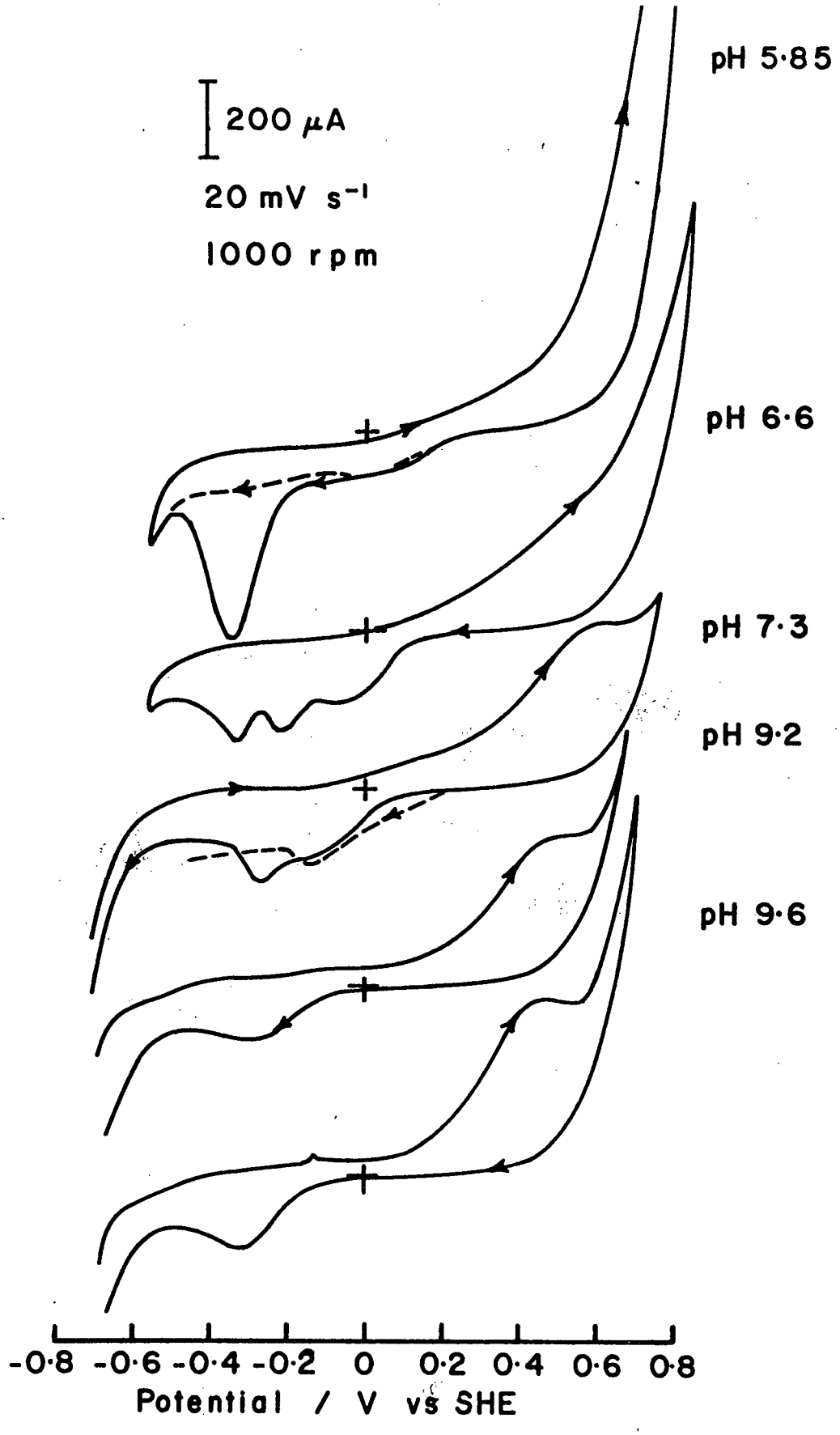

Figure 14

Voltammograms for arsenopyrite at increasing pH values

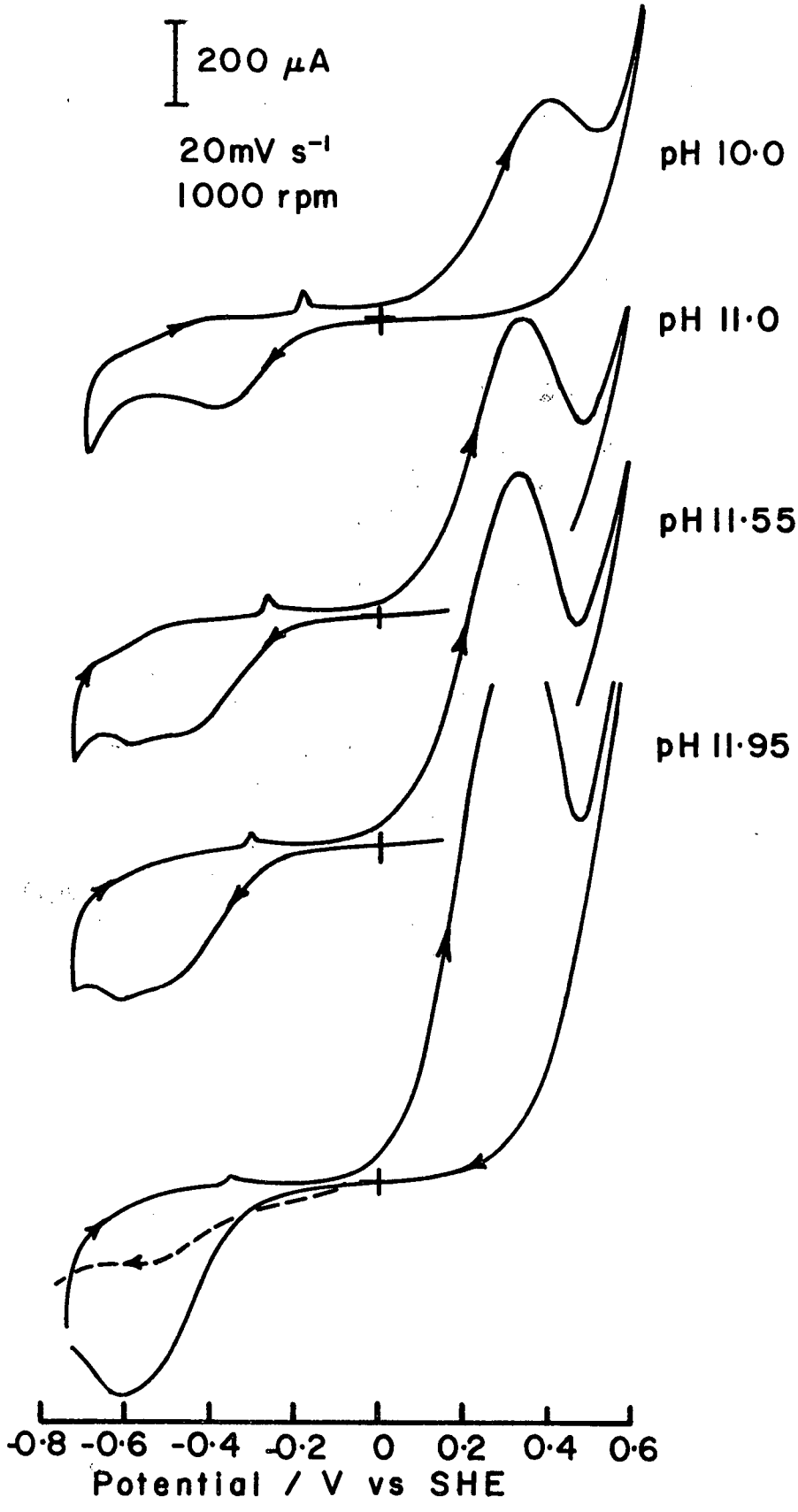

Figure 15

Voltammograms for arsenopyrite at high pH

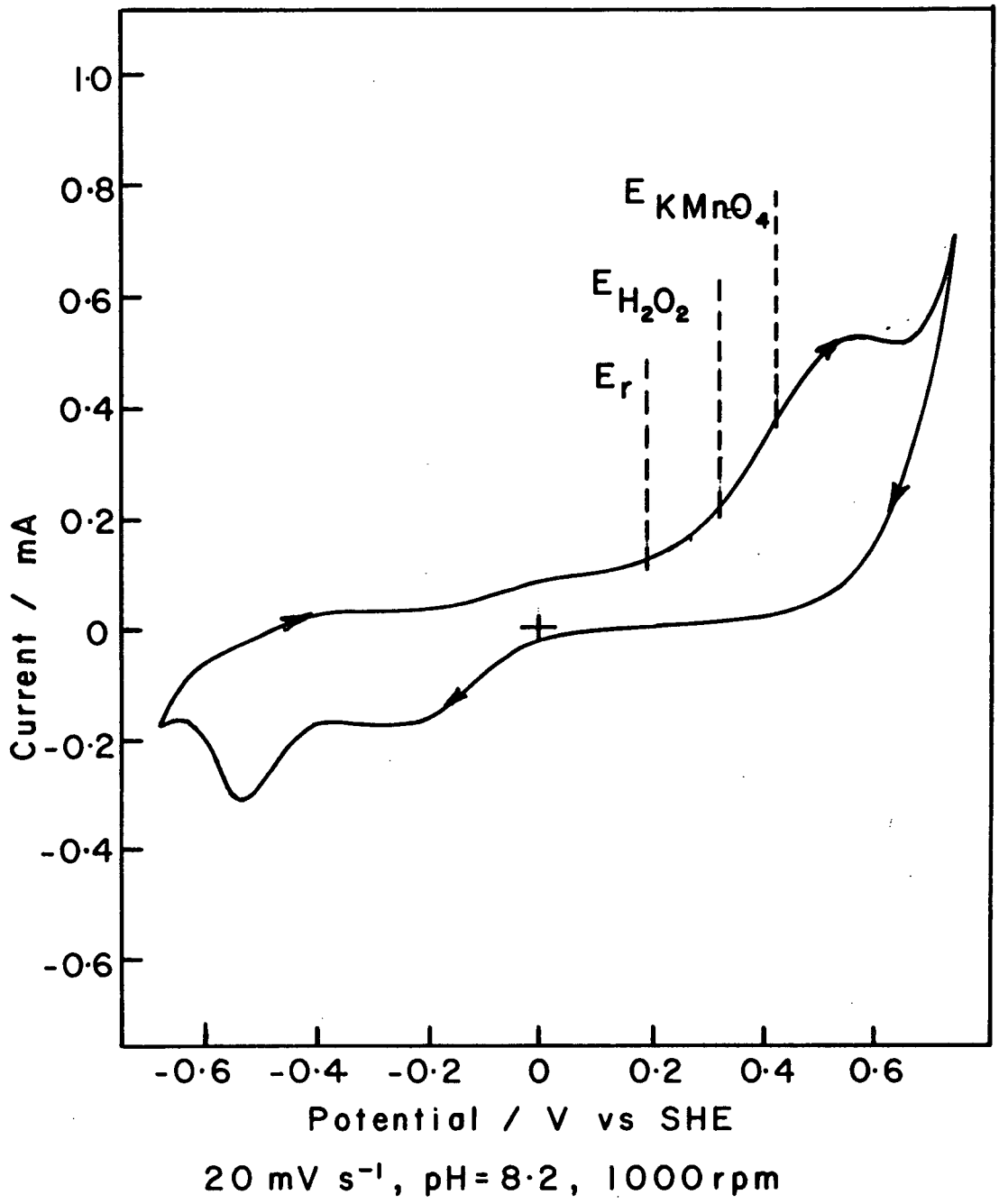

Figure 16

Voltammogram for arsenopyrite at pH = 8.2 showing potentials achieved with oxidizing agents

more cathodic potentials with increasing pH. Such prewaves previously have been interpreted as being associated with thin oxidation layers (79). In the present study the peak is believed to result from the presence of iron hydroxide films formed during electrode preparation as will subsequently be discussed.

The behaviour of arsenopyrite and pyrite across the potential region of interest is compared in Figure 17. The oxidation of arsenopyrite is observed to commence at potentials approximately 200 mV lower that those required for pyrite oxidation. The main pyrite oxidation reaction becomes significant at potentials greater than that of the arsenopyrite oxidation peak. This difference in the behaviour of these two minerals further indicates that the anodic peak observed for arsenopyrite could be significant in attempting to control the selective flotation or depression of arsenopyrite.

Possible reactions associated with the oxidation of arsenopyrite can be determined by considering the stability diagram for arsenopyrite shown in Figure 18. Thermodynamic data used to construct the diagram and additional stability considerations for arsenopyrite are presented in Appendix I. These diagrams were constructed as part of the present study.

At pH = 4 to pH = 7

$$1/2\ As_2S_3 + Fe^{++} + H^+ + 3e^- = FeAsS + 1/2\ H_2S \quad (6)$$

$$E = -0.012 - 0.0295 \log \frac{(H_2S)^{1/2}}{(Fe^{++})} - 0.0197\ pH$$

or if oxidation to form H_3AsO_3 and SO_4^{--} is considered

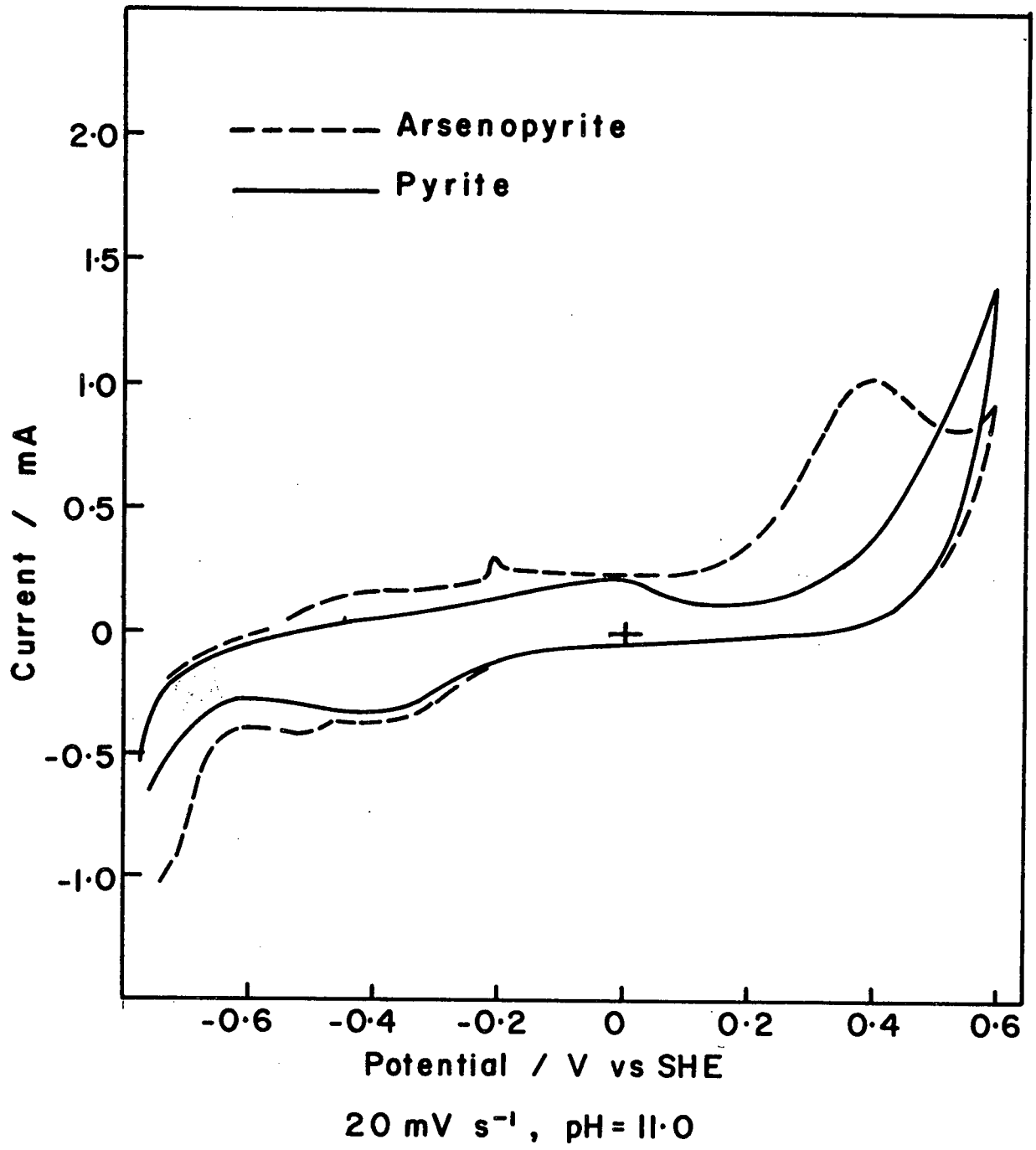

Figure 17

Voltammograms for pyrite and arsenopyrite at pH = 11.

$$Fe^{++} + H_3AsO_3 + SO_4^{--} + 11H^+ + 11e^- = FeAsS + 7H_2O \quad (7)$$

$E = 0.283 + 0.005 \log(Fe^{++})(H_3AsO_3)(SO_4^{--}) - 0.0591$ pH At pH greater than 7

$$Fe(OH)_2 + H_3AsO_3 + SO_4^{--} + 13H^+ + 11e^- = FeAsS + 9H_2O \quad (8)$$

$E = 0.346 + 0.005 \log(H_3AsO_3)(SO_4^{--}) - 0.070$ pH

The appearance of the anodic peak at 0.6 V between pH = 6.6 and 7.3 can be related to the formation of $Fe(OH)_2$ at pH greater than approximately 7. The exact pH at which $Fe(OH)_2$ becomes stable relative to Fe^{++} depends on the activity of Fe at the surface of the electrode.

The observed anodic peak or half wave potentials are considerably anodic to the reversible potentials calculated from the above equations. Assuming activities of 10^{-3} M for example equation 8 predicts a reversible potential of -0.422 volts. Such a shift in peak potential may be due to irreversibility of the reaction, to the formation of a passive layer or to both.

At the observed peak potentials the iron hydroxide which should be formed is $Fe(OH)_3$ rather than the $Fe(OH)_2$ indicated by equation 8. The reversible potential for $Fe(OH)_2$ to $Fe(OH)_3$ oxidation is given by

$$Fe(OH)_3 + H^+ + e^- = Fe(OH)_2 + H_2O \quad (9)$$

$E = 0.28 - 0.059$ pH from which a value of $E = -0.342$ V is obtained at pH = 10.55.

It can be seen in Figure 18 that at the observed peak

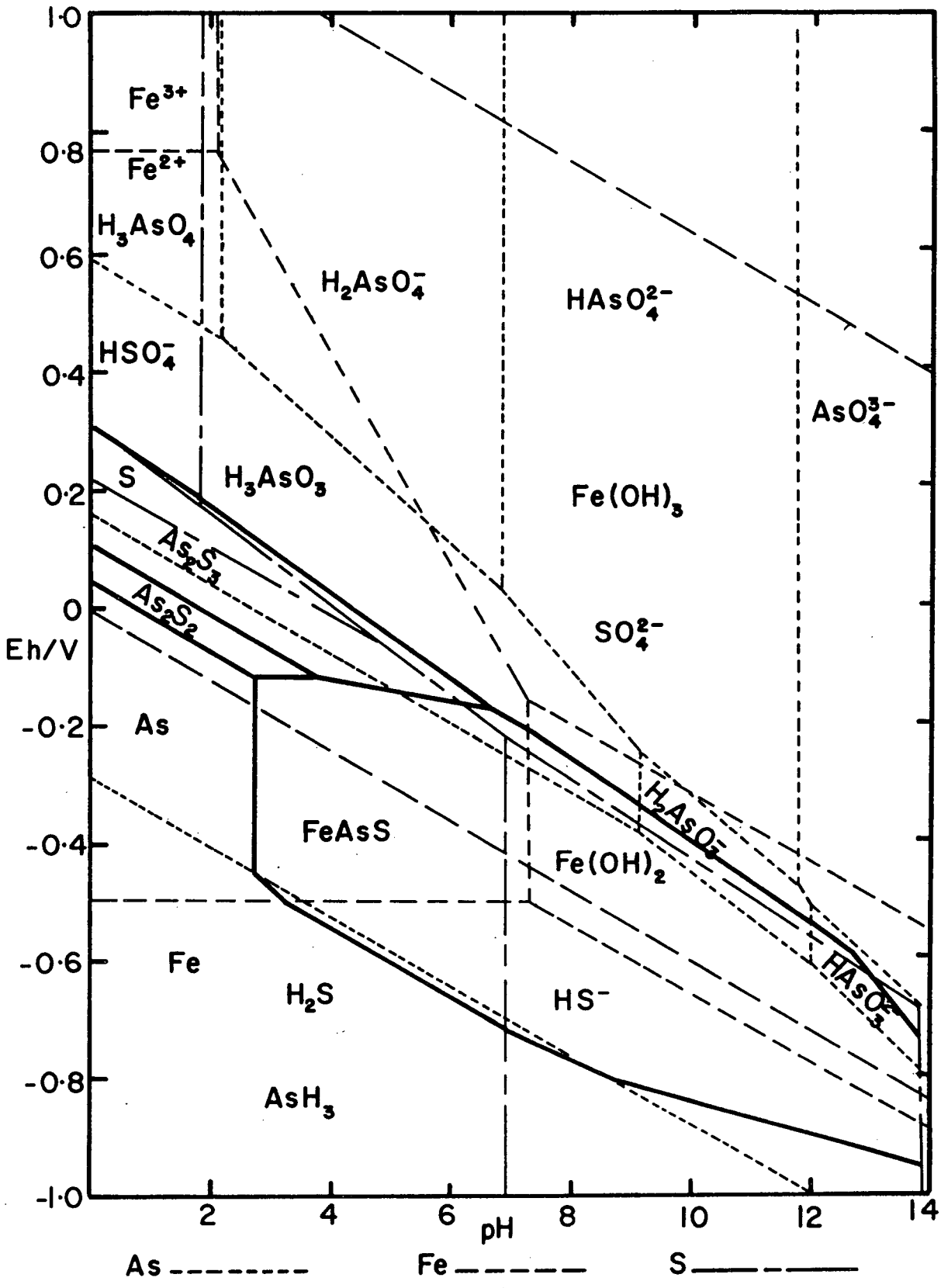

Figure 18

Eh - pH diagram for arsenopyrite. Activity for each species taken to be 10^{-3} M.

potentials arsenic is expected to be oxidized to arsenate and sulphur is expected to be oxidized to sulphate.

The formation of $Fe(OH)_3$ during the anodic process is consistent with certain additional features of the voltammograms shown in Figures 14 and 15. A cathodic potential sweep starting near the rest potential is shown at pH = 11.95. The cathodic peaks for the complete potential sweeps show significatly greater currents than those for cathodic sweeps only. The increased cathodic peak current for the complete sweeps indicates that species formed during the anodic part of the potential cycle are being reduced. These cathodic peaks occur at potentials consistent with equation 9 and can be interpreted to represent the reduction of $Fe(OH)_3$ formed during the oxidation reaction.

The cathodic peak at pH greater than 11.0 in Figure 15 is actually a double peak. This could represent a two step reduction of $Fe(OH)_3$ or could indicate that additional species such as sulphur are being reduced.

Voltammograms at lower pH and particularly at pH = 5.85 in Figure 14 show a prominent cathodic peak although no anodic peak associated with iron hydroxide formation is evident. It is believed that this cathodic peak results from the formation of sulphur or a sulphur compound during the anodic sweep.

The small prewave observed during the anodic scan results from the oxidation of a small amount of $Fe(OH)_2$ formed on the electrode during electrode polishing and preparation as discussed in Chapter 5.

Figure 19 shows a current - decay curve for an arsenopyrite

electrode which was stepped from the rest potential to +343 mV at pH = 10.6. This potential represents the anodic peak potential at this pH. The current decays from the initial value of several thousand microamps to less than 100 microamps in less than one minute. Such a current decay is associated with the build-up of oxidation products at the surface of the electrode. The presence of these oxidation products at the surface of the electrode passivates it, making further reaction increasingly difficult. This rapid decay of current confirms that the oxidation of arsenopyrite results in solid products which remain at the electrode surface.

An estimate was made of the quantity of iron hydroxide formed on the surface during an anodic scan. The area under the anodic peak at pH = 11.55 was determined in order to determine the current passed. From the start of the oxidation peak to the inflection in the curve just past the peak, a current of approximately 11700 micro coulombs was passed. Using equation 8, which shows 11 electrons per mole of arsenopyrite oxidized, together with equation 9, which indicates an extra electron for every mole of $Fe(OH)_2$ oxidized to $Fe(OH)_3$, the quantity of FeAsS which is oxidized during the scan is 0.102×10^{-7} mole. Assuming a stochiometric composition, this means that the same amount of iron is oxidized to the ferric state. Using the projected area of the electrode of 28.3 sq. mm. and assuming a solid product of Fe_2O_3 with a density of 5 (60) an oxide thickness of 40 A° is determined. This is an order of magnitude estimate only since the structure could differ from the assumed one and since the real surface area can be expected to be several times greater

than the projected area.

Taking into account the real surface area could result in an estimate of the oxide thickness as low as 10 A^{o}. A less dense iron hydroxide structure than has been assumed in the calculation on the other hand could result in the actual oxide thickness being several times the calculated value.

B. Multiple Sweep (Cyclic) Voltammetry

By allowing the triangular potential cycle to repeat a number of times, changes with time in the surface composition of the electrode can be detected. In this way the build-up of surface oxides or other electroactive species can be detected.

Cyclic voltammograms for stationary and rotating arsenopyrite electrodes at pH = 10.6 are shown in Figure 20. The anodic peak at 0.35 V is observed to decrease with continued cycling while the initially small anodic peak at -0.025 V and the cathodic peak at about -0.4 V steadily increase in height. These observations are consistent with the formation of $Fe(OH)_3$ during the anodic decomposition peak.

The oxidation peak at 0.35 V decreases with each subsequent cycle due to the electrode becoming passivated by the build-up of surface hydroxide. At the same time the cathodic peak increases in height since there is an increasing amount of hydroxide to be reduced from $Fe(OH)_3$ to $Fe(OH)_2$. The increasing amount of $Fe(OH)_2$ thus formed results in the anodic peak at −0.25 V increasing in height with subsequent cycles.

Similar peaks and changes with cycling were obtained with arsenopyrite electrodes from the two different localities.

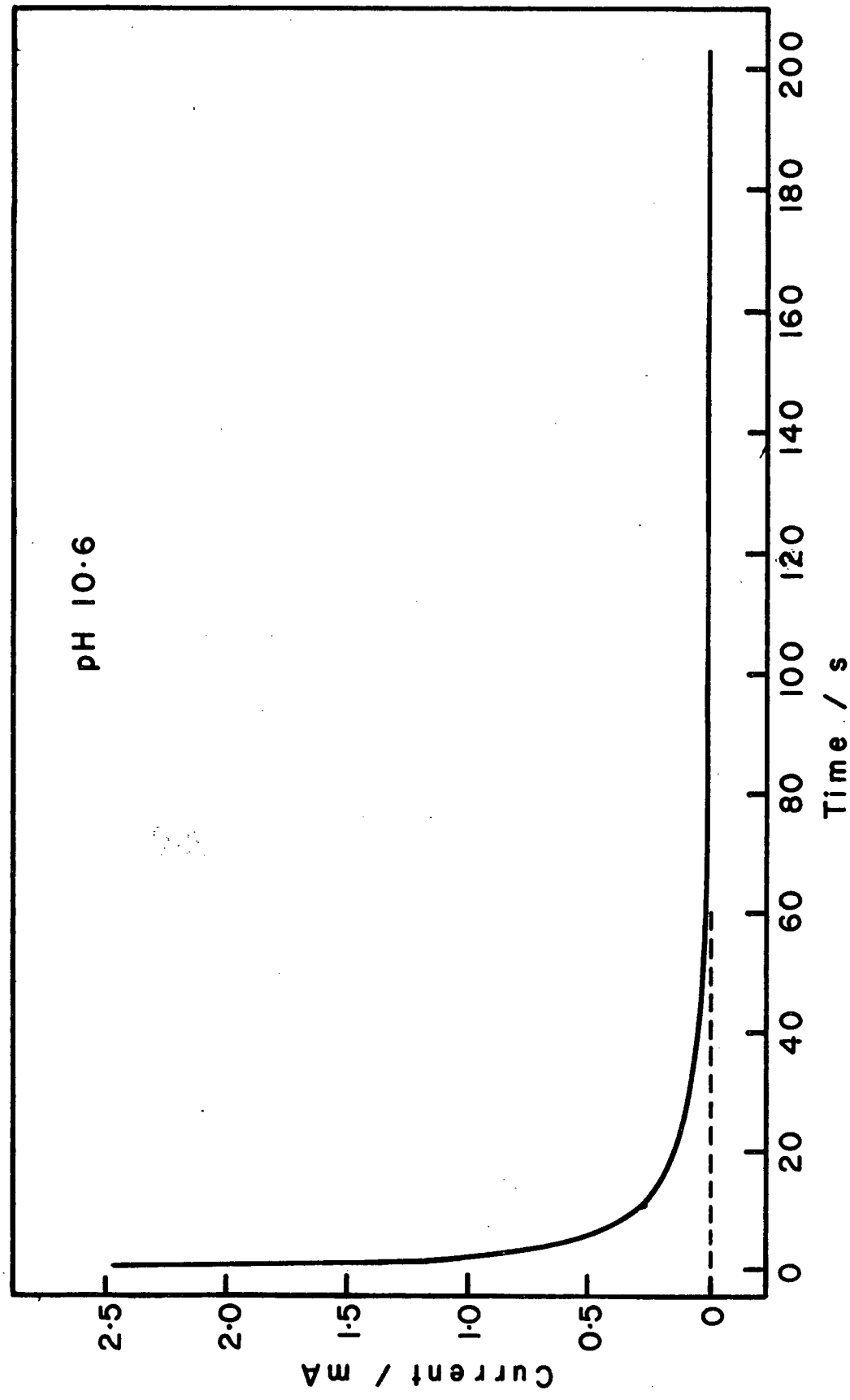

Figure 19

Current - decay curve for arsenopyrite at +0.0343 V.

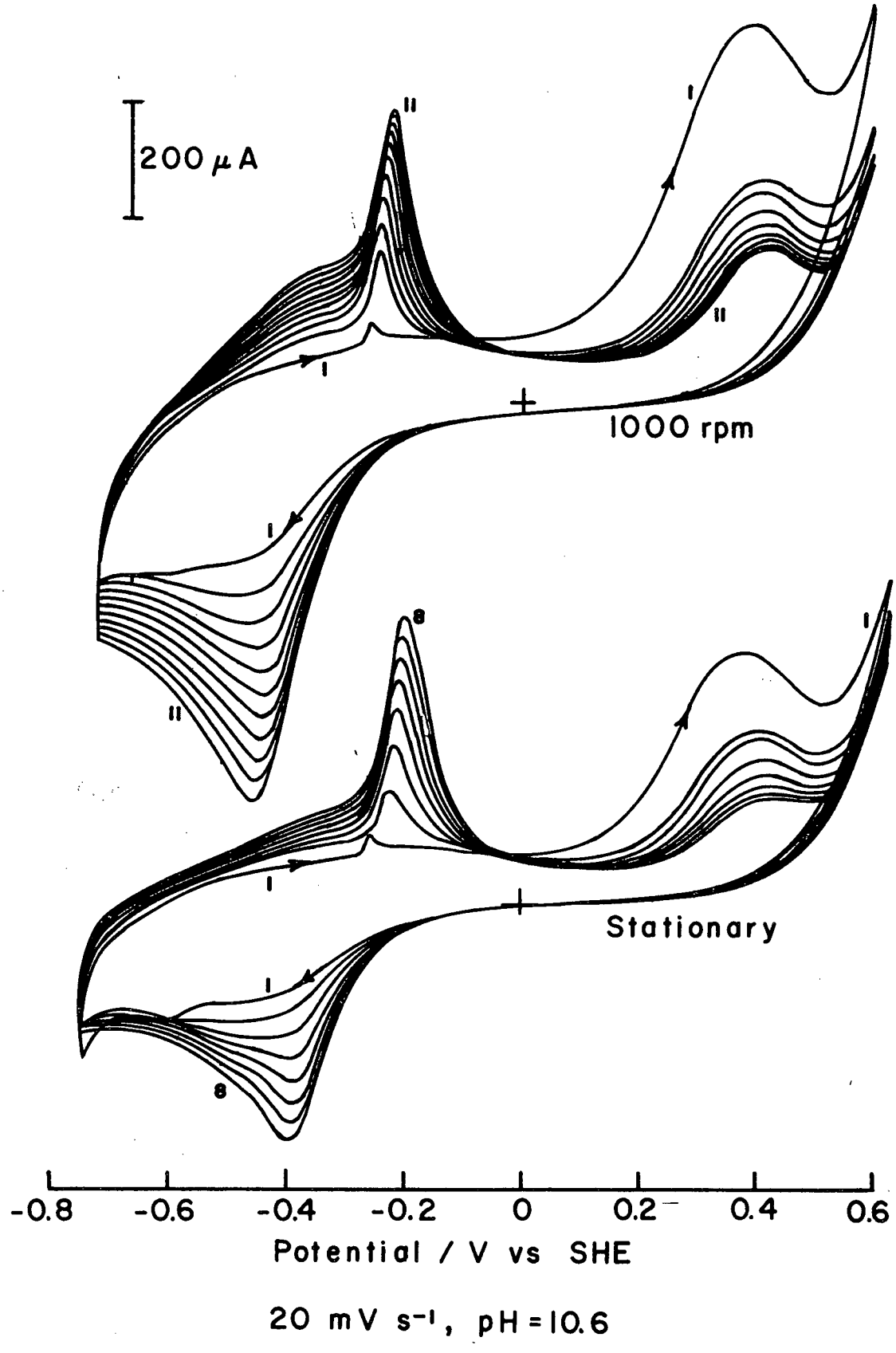

Figure 20

Multiple sweep voltammograms for stationary and rotating electrodes at pH = 10.6

The effect of rotating the electrode is that the oxidation peaks at 0.35 in Figure 20 are increased in height. At the same time the anodic peak at - 0.25 V becomes narrower and an additional anodic peak at -0.35 V becomes evident with continued cycling. This additional anodic peak suggests that the $Fe(OH)_2/Fe(OH)_3$ redox reaction results in the formation of additional iron species than these hydroxides. The effect of rotation is discussed more fully following the discussion of a reaction mechanism.

Cyclic voltammograms at pH = 11.7 are shown in Figure 21 and Figure 3, Appendix II. The vertical scale in this figure represents greater currents than that of Figure 20. As for the results obtained at pH = 10.6 the effect of rotating the electrode is to increase the currents associated with the oxidation peak at 0.35 V, to result in the anodic peak at - 0.35 V becoming narrower and, the formation of additional anodic and cathodic peaks in the region of iron hydroxide oxidation and reduction. These additional peaks at pH = 11.7 are much more apparent than those which result from stirring at lower pH. The reason why these peaks are more apparent at high pH is explained later in this chapter.

An additional feature of the voltammogram for the rotating electrode at pH = 11.7 is that while the oxidation peak at 0.35 V decreases from the first to the second cycle, it increases on subsequent cycles.

For each of the tests shown in Figures 20 and 21, the electrode became covered with a visible brown oxide during the multiple potential cycles. This oxide layer became irridescent

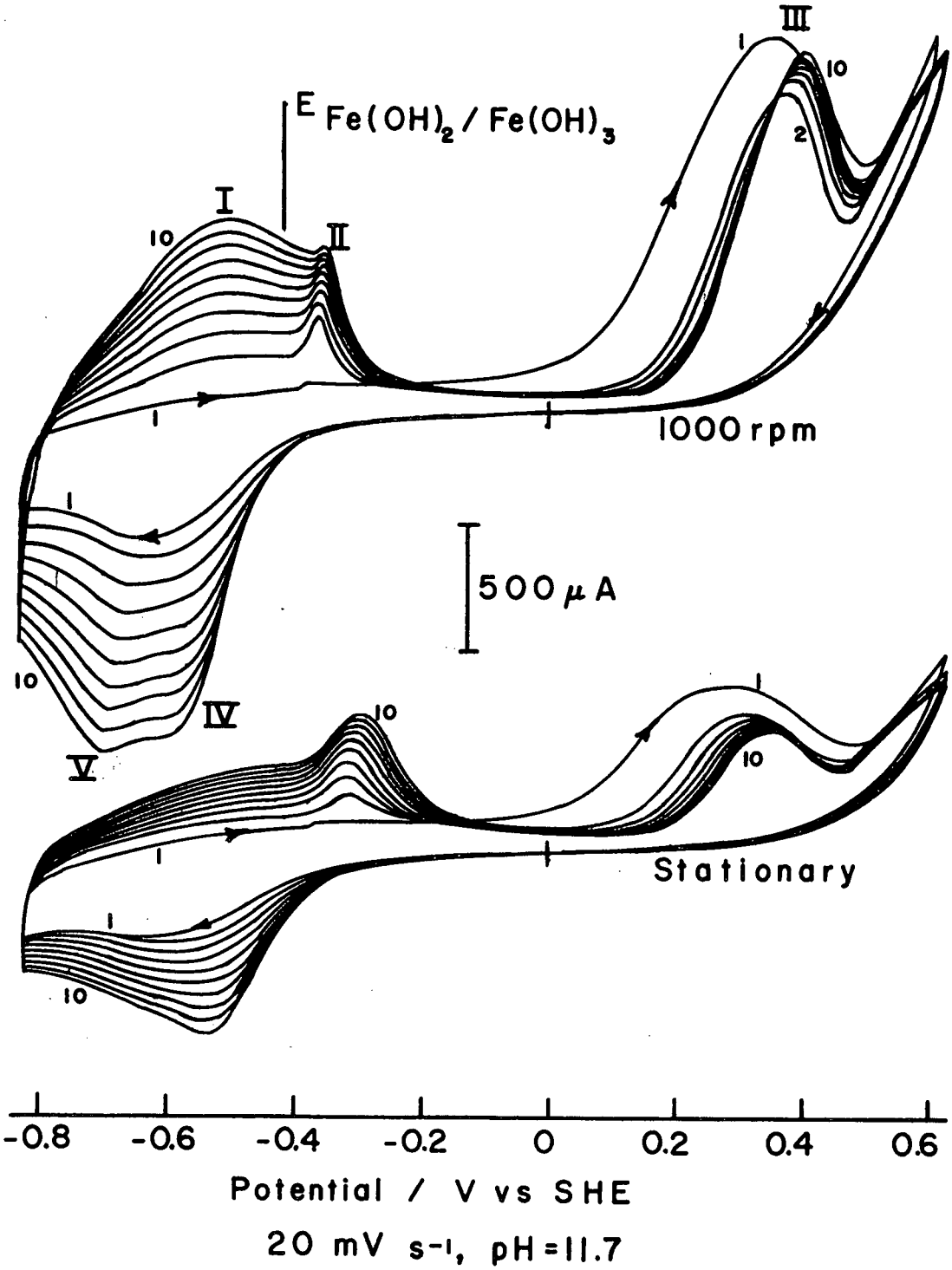

Figure 21

Multiple sweep voltammograms for stationary and rotating electrodes at pH = 11.7

in color, varying from blue at low pH to yellow - green at high pH. Such colors have been shown to relate to iron oxide layers in the range of 200 to 400 angstroms in thickness (60).

Since the peaks have been related to redox reactions involving iron species, a reaction sequence from Fe to iron hydroxides will be considered. Such a reaction sequence has been proposed for an iron electrode (61).

In the following equations brackets denote reaction intermediates whose surface coverage is of the order of a fraction of a monolayer and braces indicate species eventually related to the formation of new phases and which may undergo ageing (61).

$$[Fe(OH)]ad + e = Fe + OH^- \quad (10)$$

$$[Fe(OH)]^+ad + e = [Fe(OH)]ad \quad (11)$$

$$\{Fe(OH)_2\} = [Fe(OH)]^+ad + OH^- \quad (12)$$

$$HFeO_2^- + H_2O = \{Fe(OH)_2\} + OH^- \quad (13)$$

$$FeO_2^{2-} + H_2O = HFeO_2^- + OH^- \quad (14)$$

$$\{FeOOH\} + H_2O + e = \{Fe(OH)_2\} + OH^- \quad (15)$$

$$\{Fe_2O_3 \cdot H_2O\} = \{FeOOH\} + \{FeOOH\} \quad (16)$$

The above equations are written with FeOOH as the oxidized hydroxide while the discussion so far has considered $Fe(OH)_3$. The precise form present on the electrode cannot be determined from results of the present investigation. Throughout the literature relating to iron electrodes the preferred structure is FeOOH. The two forms will be used interchangeably as referring to ferric hydroxide.

In considering the reaction sequence during a potential cycle from the cathodic limit to the anodic limit and back to the starting point, the reactions would occur in the following order as shown in Figure 21 and in Figure 3, Appendix II.

1. The initial anodic potential sweep results in the oxidation of arsenopyrite to form FeOOH. The oxidation is associated with peak III. At the same time arsenic is released as arsenate ions and sulphate is released as sulphate ions. Arsenate is electroinactivè and therefore does not participate in reactions associated with the remaining peaks. This will be more fully discussed in section 4.3.2C. Based on the results of ESCA experiments presented in Chapter 5, it is believed that arsenate precipitates in the ferric hydroxide deposits. The composition of the arsenic complex so formed is not known. Sulphate is also electroinactive and is believed to diffuse slowly through the ferric hydroxide layer.
2. On the reduction cycle FeOOH is reduced to $Fe(OH)_2$ according to reaction 15. This reaction is associated with peak IV.
3. A further reduction of the $Fe(OH)_2$ according to equations

12, 11 and 10 is indicated by peak V. This peak has a somewhat greater current associated with it than does peak IV because although some $Fe(OH)_2$ is solubilized according to reactions 13 and 14, equations 10 and 11 involve a two electron transfer reaction while equation 15 involves only one.

4. The second and successive anodic scans involve the conjugated reaction to that associated with peak V as peak I, namely the formation of $Fe(OH)_2$ from reduced iron - hydroxy species.
5. The $Fe(OH)_2$ formed at peak I is oxidized to FeOOH according to reaction 15 at peak II. As for peaks IV and V, peak II is again less than peak I since only a one electron transfer is involved.
6. At high pH the hydroxide concentration is such that a considerable amount of $Fe(OH)_2$ is dissolved according to reactions 13 and 14, so that the current associated with peak III increases on subsequent scans. In the case of a stationary electrode these products are not swept away and as a consequence the peak current becomes depressed with continued cycling due to a greater build-up of hydroxide at the surface.

The influence of electrode rotation and increasing pH can now be correlated to the above reaction sequence. Reaction 15 can be rewritten in terms of proton transfer as follows.

$$FeOOH + H^+ + e = Fe(OH)_2 \qquad (17)$$

and

$$H^+ + OH^- = H_2O \qquad (18)$$

The formation of ferric hydroxide according to reaction 17 then results in formation of H^+ in addition to FeOOH. The H^+ so formed is neutralized according to reaction 18 either by diffusion of H^+ away from the reaction site due to concentration gradients or by diffusion of OH^- to the site. Conditions which promote the diffusion or transport of these species should therefore increase the rate of FeOOH production. This is in fact observed since the effect of rotation is to increase the height of peak III. At the same time increasing pH increases the peak height since a greater concentration of OH^- is available for H^+ neutralization.

Reaction 10 can similarly be written in terms of proton transfer and the same arguments as presented above explain the appearance of peaks I and V with stirring or increasing pH.

Similar arguments have been presented elsewhere (62) for the formation of nickel hydroxide films according to.

$$NiOOH + H_2O + e = Ni(OH)_2 + OH^- \qquad (19)$$

or

$$NiOOH + H^+ + e = Ni(OH)_2 \qquad (20)$$

and

$$H^+ + OH^- = H_2O \qquad (21)$$

To this point apart from the arsenopyrite oxidation peak (peak III) no peaks have been assigned to arsenic or sulphur

species. At the peak potentials observed for the main oxidation peak for arsenopyrite (peak III) arsenic oxidation to the arsenate state and sulphur oxidation to the sulphate state are expected.

The irreversibility of sulphate formation is well established and reduction peaks associated with this species are not expected. In the case of pyrite and pyrrhotite, elemental sulphur has been shown to be formed even at high pH and high overpotential (63). The presence of sulphur was shown to result in the formation of FeS during continued cycling (63). Although the formation of sulphur during arsenopyrite oxidation is a reasonable expectation there is no evidence in the present results that this is in fact occuring in the pH range where iron hydroxide films are formed since no peaks associated with FeS are observed.

In addition to the formation of FeS, the presence of elemental sulphur could be expected to result in increasing thiosulphate formation with increasing pH according to

$$S_2O_3^{2-} + 6H^+ + 4e = 2S + 3H_2O \qquad (22)$$

$$E = + 0.26 + 0.015 \log(S_2O_3^{2-}) - 0.089\ pH$$

$$2SO_4^{2-} + 10\ H^+ + 8\ e = S_2O_3^{2-} + 5\ H_2O \qquad (23)$$

$$E = + 0.04 - 0.007 \log\frac{(S_2O_3^{2-})}{(SO_4^{2-})^2} - 0.074\ pH$$

The peaks associated with the above reactions would lie within the peaks assigned to iron species as would any peaks resulting from the reduction of thiosulphate to sulphide. The

effect of electrode rotation would be to reduce peaks associated with thiosulphate reduction and subsequent sulphide oxidation. No peaks whose height decreases with electrode rotation are observed and therefore thiosulphate and sulphur do not appear to be produced.

The formation of arsenate during arsenopyrite oxidation is also irreversible and peaks associated with arsenate reduction are not expected. This will be discussed more fully in the next section.

The irreversibility of both sulphate and arsenate formation in part accounts for the deviation of the observed peak potential for arsenopyrite oxidation from the calculated reversible value.

Since both arsenic and sulphur form soluble species the effect of stirring or electrode rotation is expected to be that the anodic peak height increases, as is observed. This observation is therefore consistent with the oxidation of all three elements in arsenopyrite.

Consideration has also been given to the possiblity of ferric arsenate precipitation at the electrode surface according to

$$FeAsO_4 + 3H^+ = H_3AsO_4 + Fe^{3+} \qquad (24)$$

$$pH = 0.12 - 1/3 \log(H_3AsO_4)(Fe^{3+})$$

or

$$FeAsO_4 + 3H_2O = Fe(OH)_3 + H_2AsO_4^- + H^+ \qquad (25)$$

$$pH = 5.30 + \log(H_2AsO_4^-)$$

At the pH values being considered in the present work the formation of ferric arsenate would not be expected. The minimum solubility of ferric arsenate lies at about pH = 2.2 and at greater pH it decomposes to give $Fe(OH)_3$ and $H_2AsO_4^-$ according to reaction 25 (64).

The oxidation of arsenopyrite to form hydroxide results in the release of H^+. Equation 8 for instance indicates the formation of 13 moles of H^+ for every mole of FeAsS which is oxidized. At the rapid sweep rates (20 mV/sec.) employed the pH at the electrode surface could therefore be significantly lower than the bulk solution pH. Ferric arsenate could form at the electrode surface in the presence of such high H^+ concentration.

Voltammograms produced at decreasing pH values should have enhanced peaks due to the formation of $FeAsO_4$ since the bulk pH would be approaching the pH generated at the electrode surface. Figure 22 shows a multiple sweep voltammogram carried out at pH = 5.8. The absence of the peaks which are observed at higher pH at -0.35V indicates that those peaks are not associated with $FeAsO_4$ formation.

The cathodic limit of the potential cycles were kept within the stability limits for FeAsS which are shown in Figure 18. It was recognized however that the activities of dissolved species at the electrode could be different from those assumed in construction of the diagram. Cathodic decomposition reactions could therefore be occurring if the limits of cycling were actually beyond the stability limits of the mineral.

Figure 23 shows voltammograms produced with cathodic limits of -0.7 V and -0.55 V. The same peaks are evident in each case

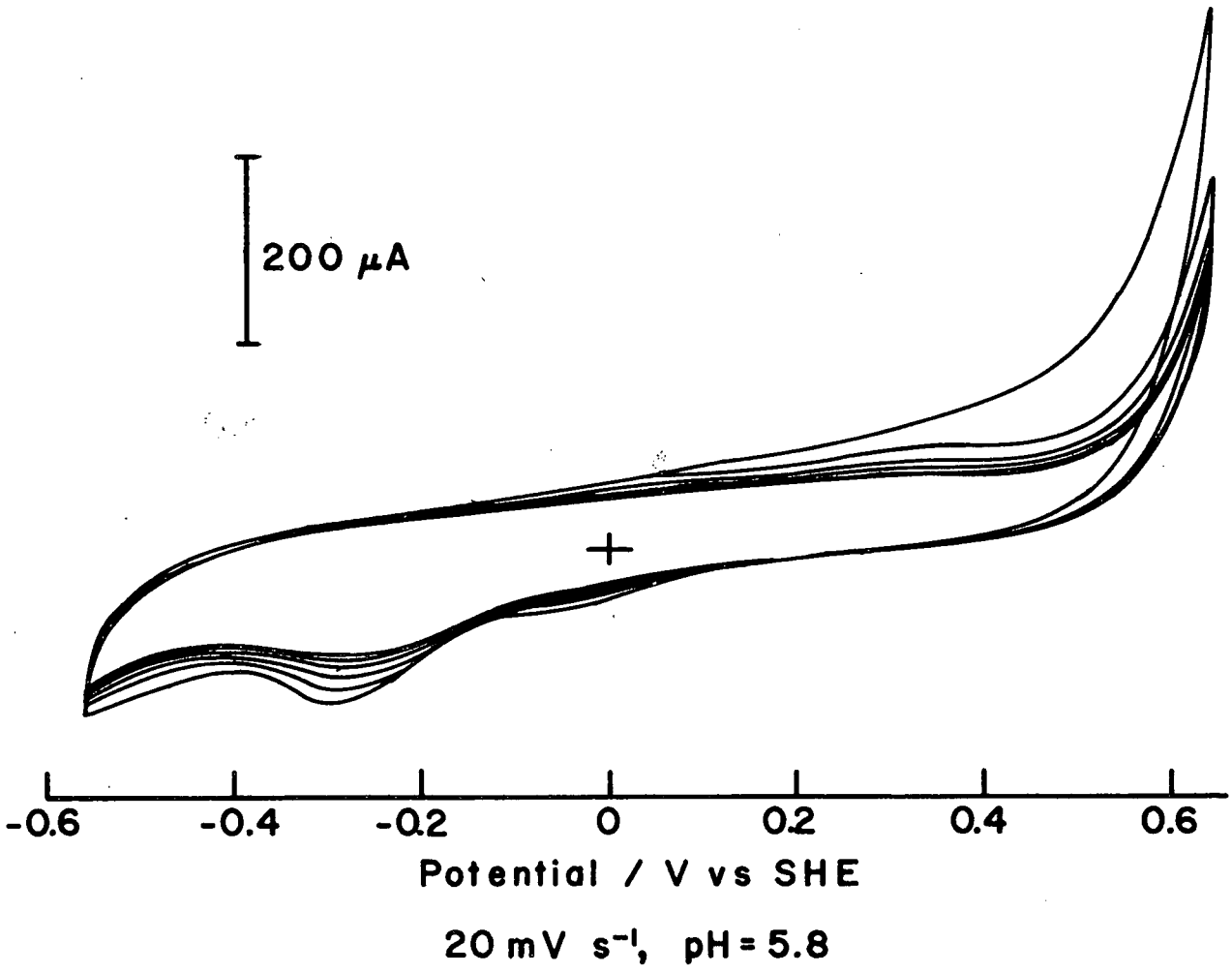

Figure 22

Multiple sweep voltammograms at pH = 5.8.

although the shape of the peaks and the rate at which peak currents change differ somewhat due to a decrease in total cathodic current passed with the less negative cathodic limit. A less cathodic limit does not result in elimination of any peaks.

Figure 24 shows a voltammogram produced with a cathodic limit of -0.55 V and an anodic limit of +0.24 V. The anodic peaks at -0.2 V which are evident in Figure 23 are completely absent in Figure 24. A portion of a scan carried out after the electrode was held at the cathodic limit for 5 minutes is also shown in Figure 24. Only a minor peak associated with $Fe(OH)_2$ oxidation is evident. It is therefore reasonable to assume that the peaks at -0.2 V are associated with anodic oxidation products when the anodic limit is 0.6V.

C. Irreversibility of Arsenate Formation

While arsenic (III) can be oxidized or reduced in solution (65), arsenic (V) has been reported to be electroinactive (66,67). The determination of arsenic by polarographic or voltammetric methods requires the reduction of arsenic (V) with reducing agents prior to determination (67).

Figure 25 demonstrates the irreversibilty of arsenate formation at pH = 9.2 and 10.7. Peak A in this figure represents the oxidation of As to As (III) while peak B represents the oxidation of As (III) to As (V). It can be seen that there is no cathodic peak representing As(V) reduction to As (III) corresponding to peak B. Peak C represents the deposition of arsenic onto the gold electrode. The effect of holding the

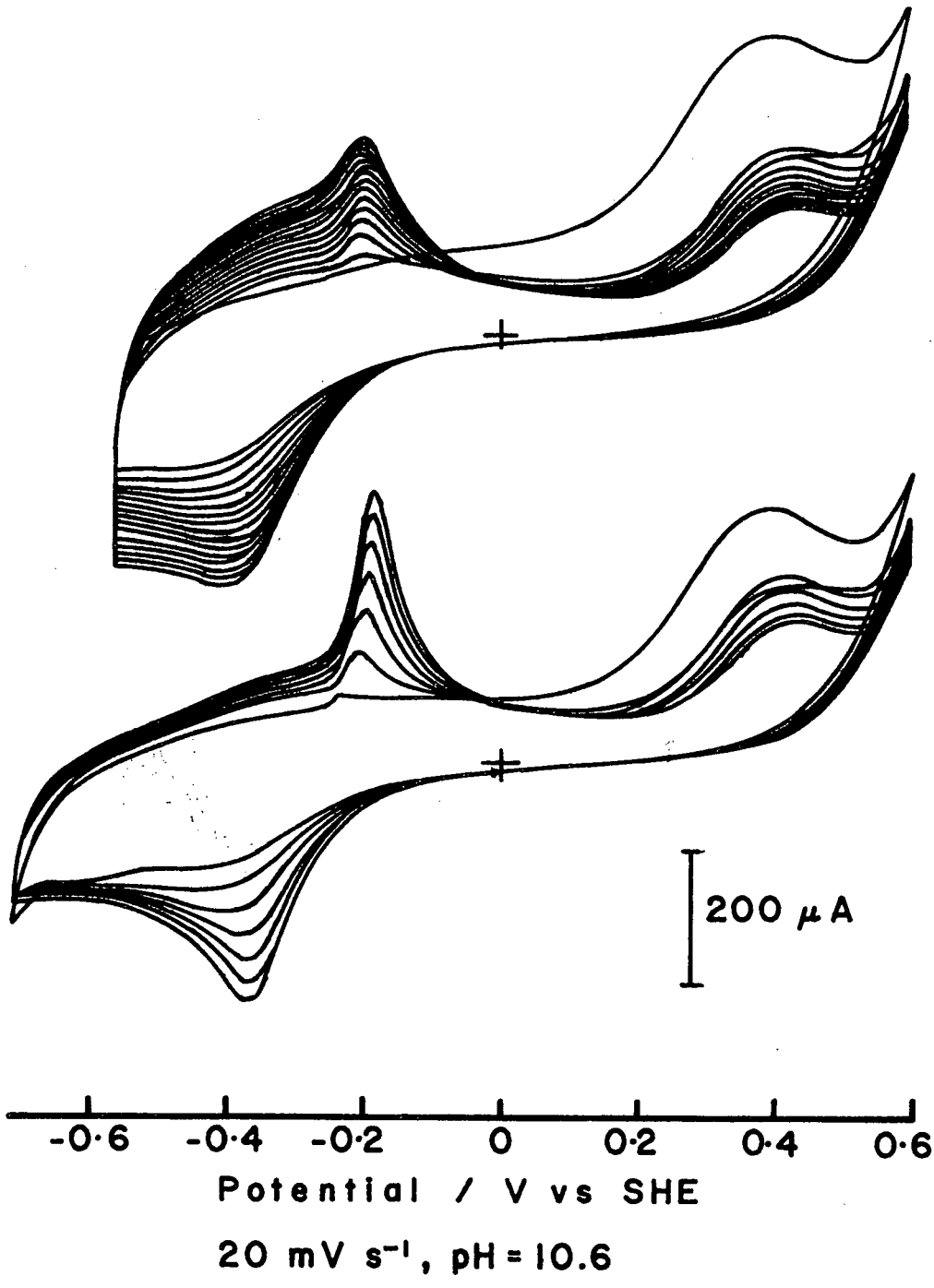

Figure 23

Influence of cathodic limit on voltammogram

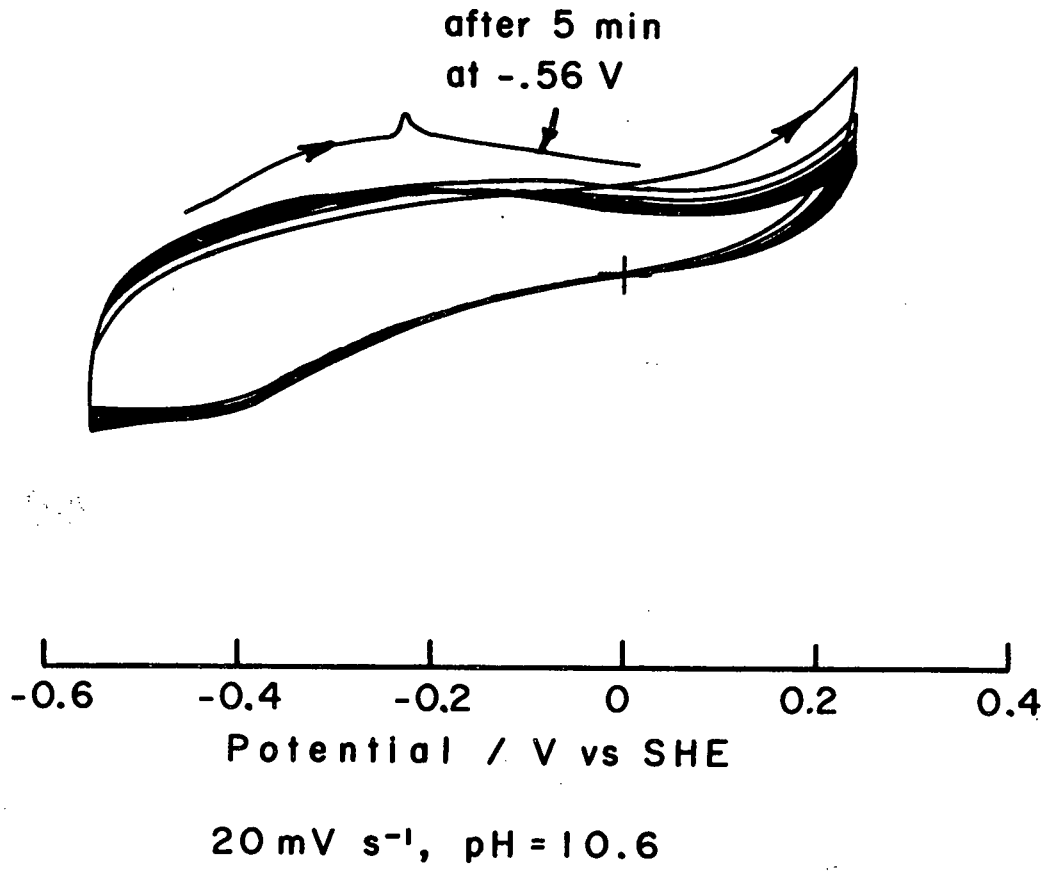

Figure 24

Influence of anodic limit on voltammogram

electrode at the cathodic limit for 5 minutes prior to carrying out the potential sweep is to deposit a greater quantity of arsenic onto the electrode. This is made evident by the increase in the height of peak A in this case. Peak B at the same time is unnaffected since the concentration of As (III) available for oxidation to As (V) is not changed.

D. Influence of Dissolved Arsenic on Voltammetry

The oxidation of arsenopyrite according to equations such as 8 shows soluble arsenic as a product. The influence of increasing dissolved arsenic in solution should therefore be to depress the anodic peak and to shift it to higher potentials.

At the same time by carrying out voltammetry in the presence of dissolved arsenic, peaks due to arsenic oxidation or reduction should be enhanced. The absence of peak enhancement will confirm the previous conclusion that all observed peaks at pH greater than 7 are due to iron species.

Figure 26 shows the influence of arsenic additions to solution. As expected the arsenopyrite oxidation peak at 0.35V is diminished by such addition as well as being shifted to more anodic potentials. As a consequence of the diminished anodic reaction, the cathodic peak associated with ferric hydroxide reduction also becomes diminished.

None of the observed peaks are enhanced by increasing arsenic additions. The conclusion that none of the peaks are associated with arsenic oxidation or reduction is therefore

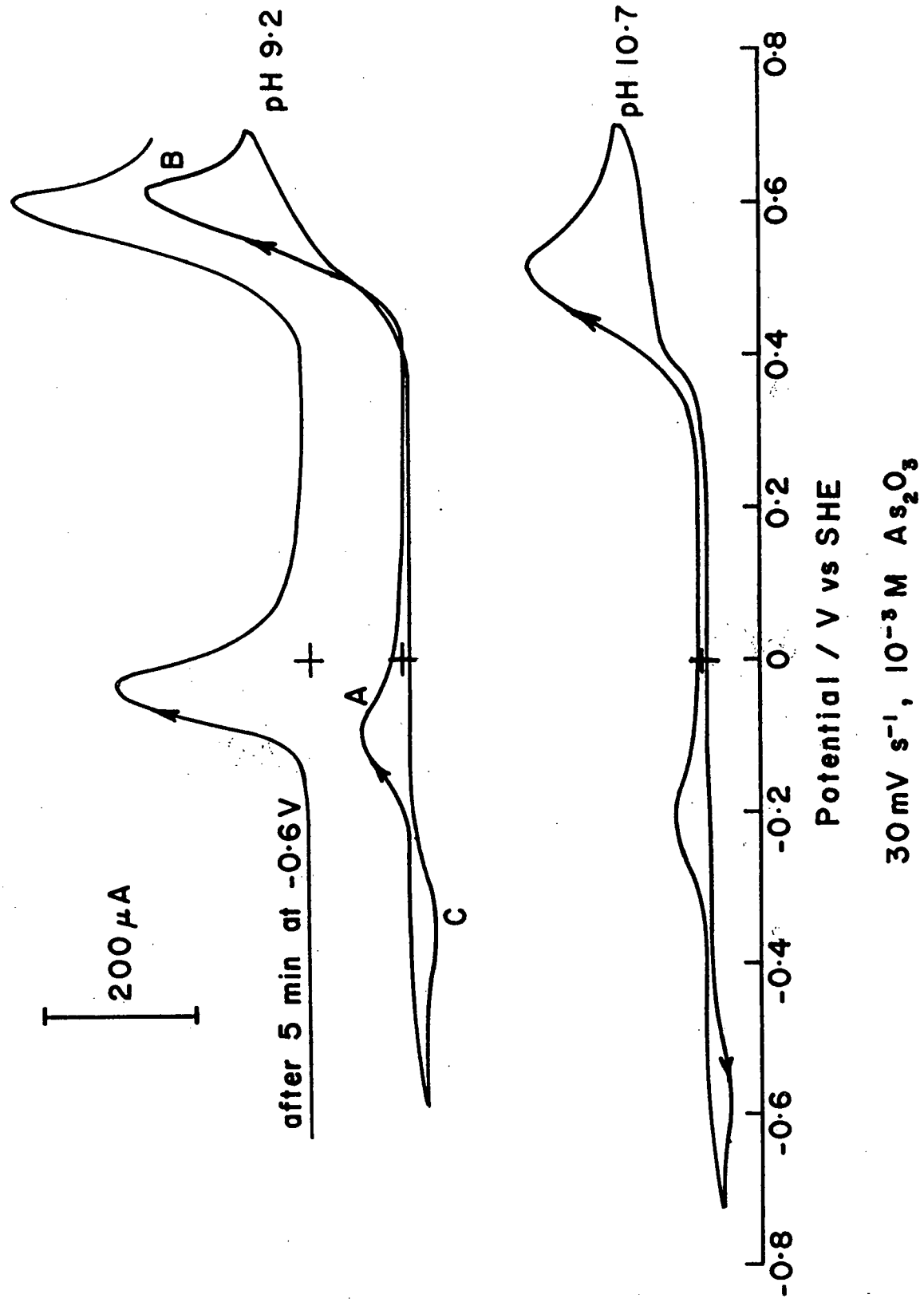

Figure 25

Voltammogram for gold electrode in arsenic solution

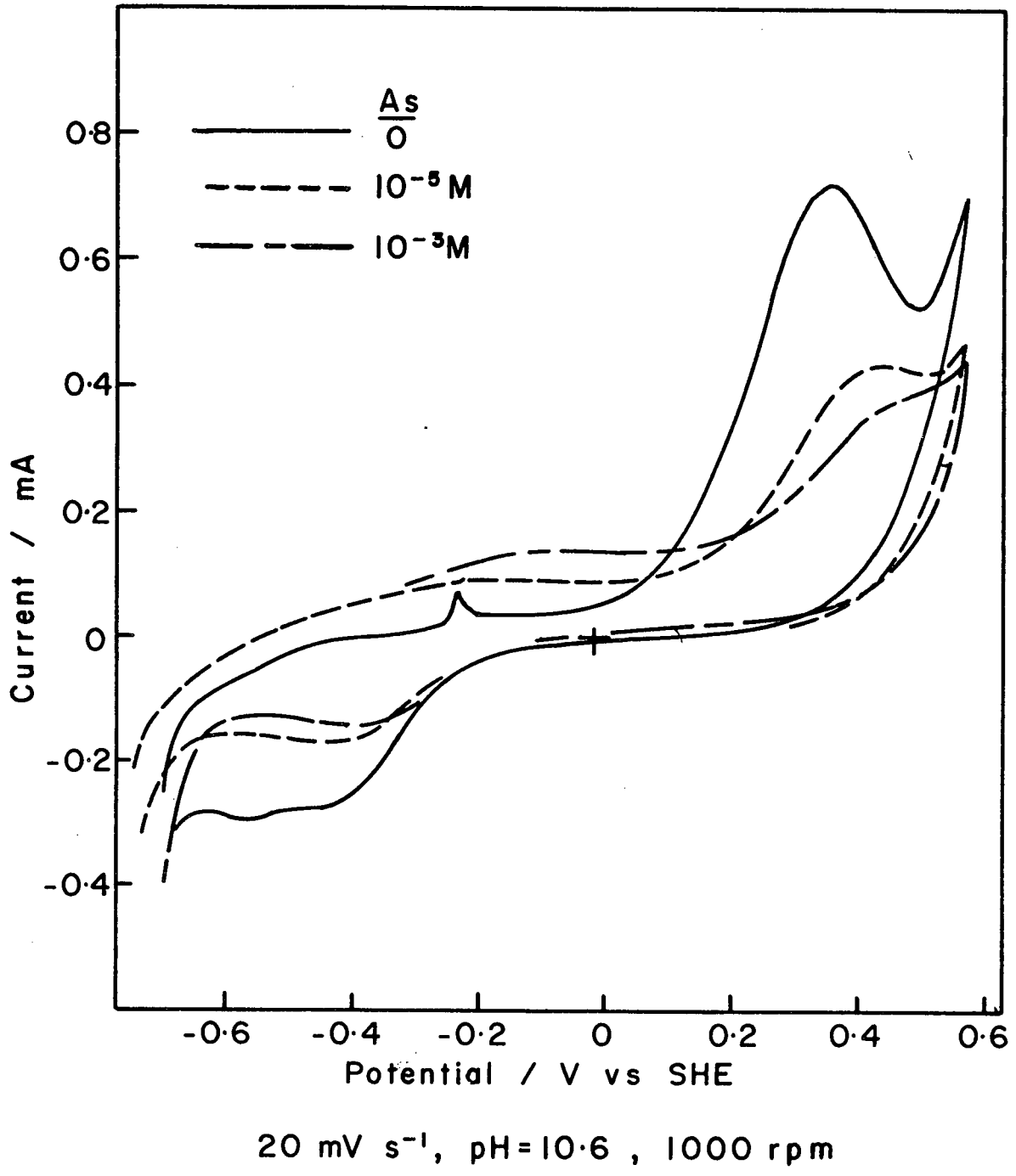

Figure 26

Effect of arsenic additions on arsenopyrite potential sweeps

supported.

Peaks due to the oxidation of arsenic III to arsenic V are not observed although considerable arsenic III is present in solution. This is expected since the potentials required for As(III) oxidation which are presented in the previous section lie in the region where currents due to arsenopyrite oxidation are already substantial.

E. Effect of Sweep Rate.

The model which has been developed for the oxidation of arsenopyrite across the pH range of interest is that iron in the mineral is oxidized to form a surface deposit of ferric hydroxide which increases in thickness with time. At the same time arsenic and sulphur in the mineral are oxidized to soluble arsenate and sulphate respectively.

The formation of such an ever - thickening surface hydroxide layer has implications to the electrochemical behaviour of arsenopyrite. The hydroxide layer will tend to inhibit activation controlled reactions and further oxidation will become diffusion limited.

By analyzing the influence of sweep rate on peak current and potential, kinetic parameters and the extent to which they are affected by the hydroxide layer may be determined.

Under linear diffusion conditions reversible charge transfer processes give peak potentials which are independent of sweep rate.

Voltammograms were obtained at pH = 10.6 for sweep rates

from 1 mV/sec. to 80 mV/sec. The results at 2, 30 and 80 mV/sec are shown in Figure 27 and all the results are plotted in Figure 28. It is apparent that the anodic peak associated with mineral oxidation is greatly affected by sweep rate indicating this oxidation process to be irreversible.

The cathodic peak associated with the reduction of $Fe(OH)_3$ is insensitive to sweep rate indicating this reaction to be reversible, as expected. At low sweep rates the cathodic peak exhibits the fact that it represents a two stage reaction, displaying a double peak. This is consistent with the argument presented in the section on multiple sweep voltammetry that improving the conditions for proton or hydroxide diffusion will make the ferrous hydroxide reduction reaction more favoured.

If the anodic reaction is considered to be a totally irreversible electrode process involving a single rate determining step, the following relations should apply (56,68)

$$Ep = E_0 + (RT/\beta naF)(0.78 + \ln(Db)^{1/2} - \ln Ks) \qquad (26)$$

$$Ep - Ep_2 = 1.857\ (RT/\beta naF) = 0.048/\beta na \qquad (27)$$

$$ip = 3 \times 10^5 n(\beta na)^{1/2} A D^{1/2} C^0 v^{1/2} \qquad (28)$$

where

Ks = rate constant when electrode is at E^0

n = total number of electrons involved in the electrode process

na=number of electrons involved in the rate - determining step

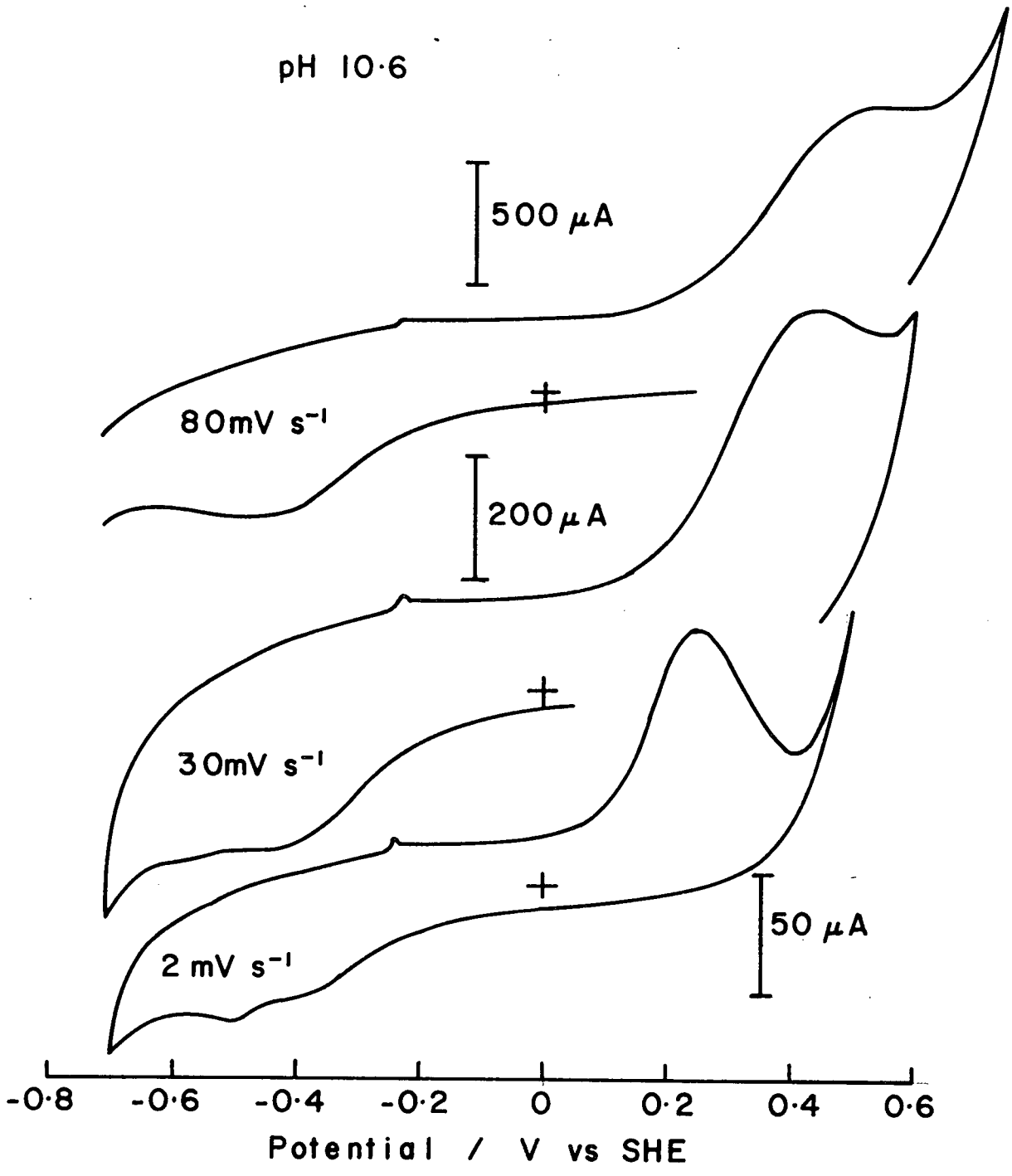

Figure 27

Voltammograms at increasing sweep rate

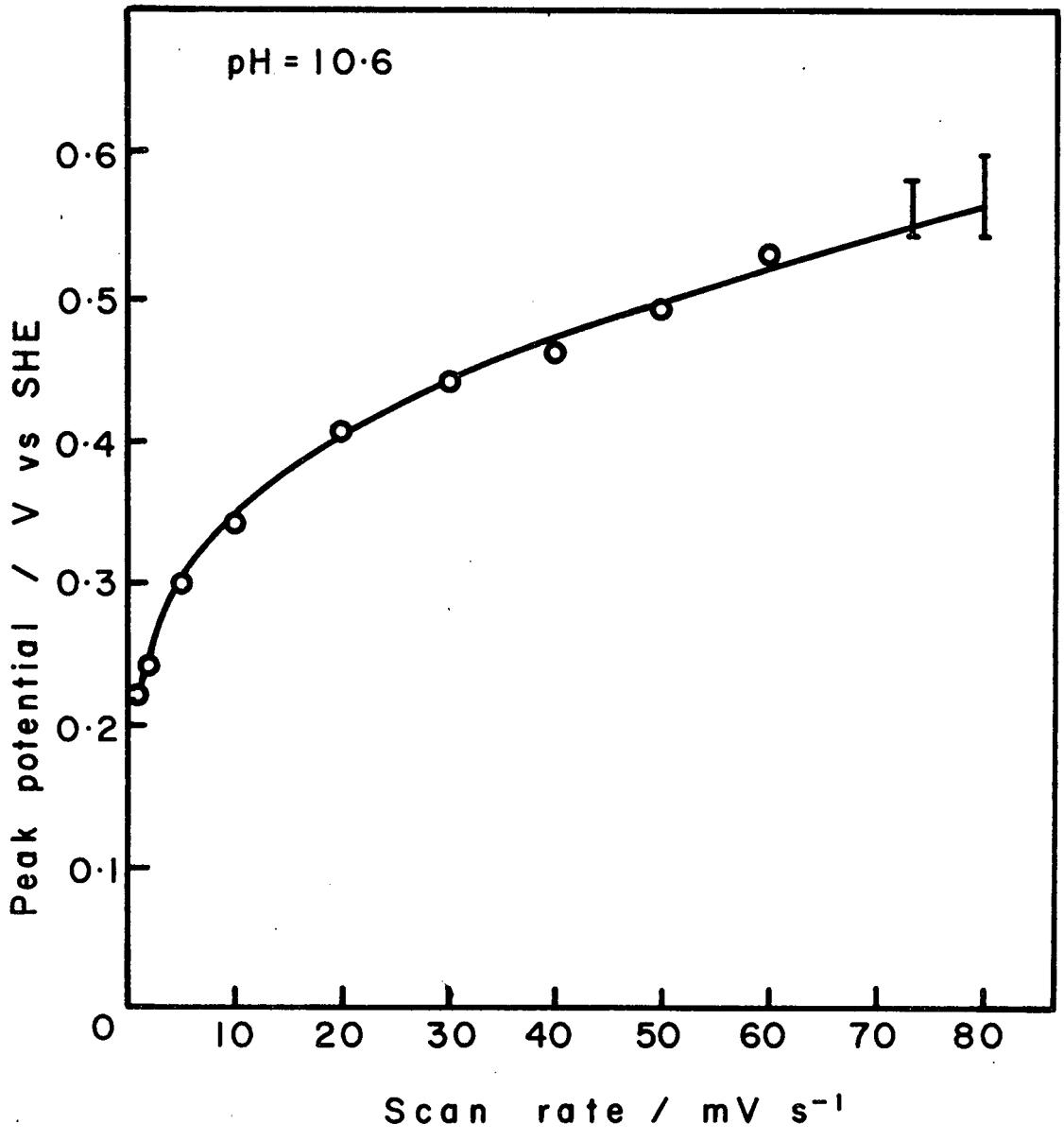

Figure 28

Influence of sweep rate on peak potential

of the electrode process, for a single step process n = na

C^0 = bulk concentration of the reactant

α = transfer coefficient

E = Electrode potential = $E^0 + \nu t$

E^0 = standard electrode potential

D = diffusion constant

A = electrode area

Ep = peak potential corresponding to the oxidation peak

Ep_2 = half peak potential where i = 1/2 ip

ip = maximum current in the current peak

β = $1 - \alpha$

b = $\beta naFv/RT$

v = scan rate

According to equation 26, a plot of Ep vs. log ν is expected to be a straight line. The plot shown in Figure 29 is clearly not linear and equation 26 therefore does not apply to the oxidizing arsenopyrite. At the two highest scan rates shown the peaks were very broad and are therefore represented by bars rather than by points.

Additional consideration of the results indicates that equations 27 and 28 also do not apply. Values of na β determined according to equation 27 are shown in Table 5. While a constant value should be obtained for an activation controlled process, the results are observed to decrease continuously over the range of sweep rates considered.

Equation 28 indicates that a plot of log ip versus log ν should give a straight line having a slope of 0.5. Figure 30 shows a straight line but having a slope of 0.77.

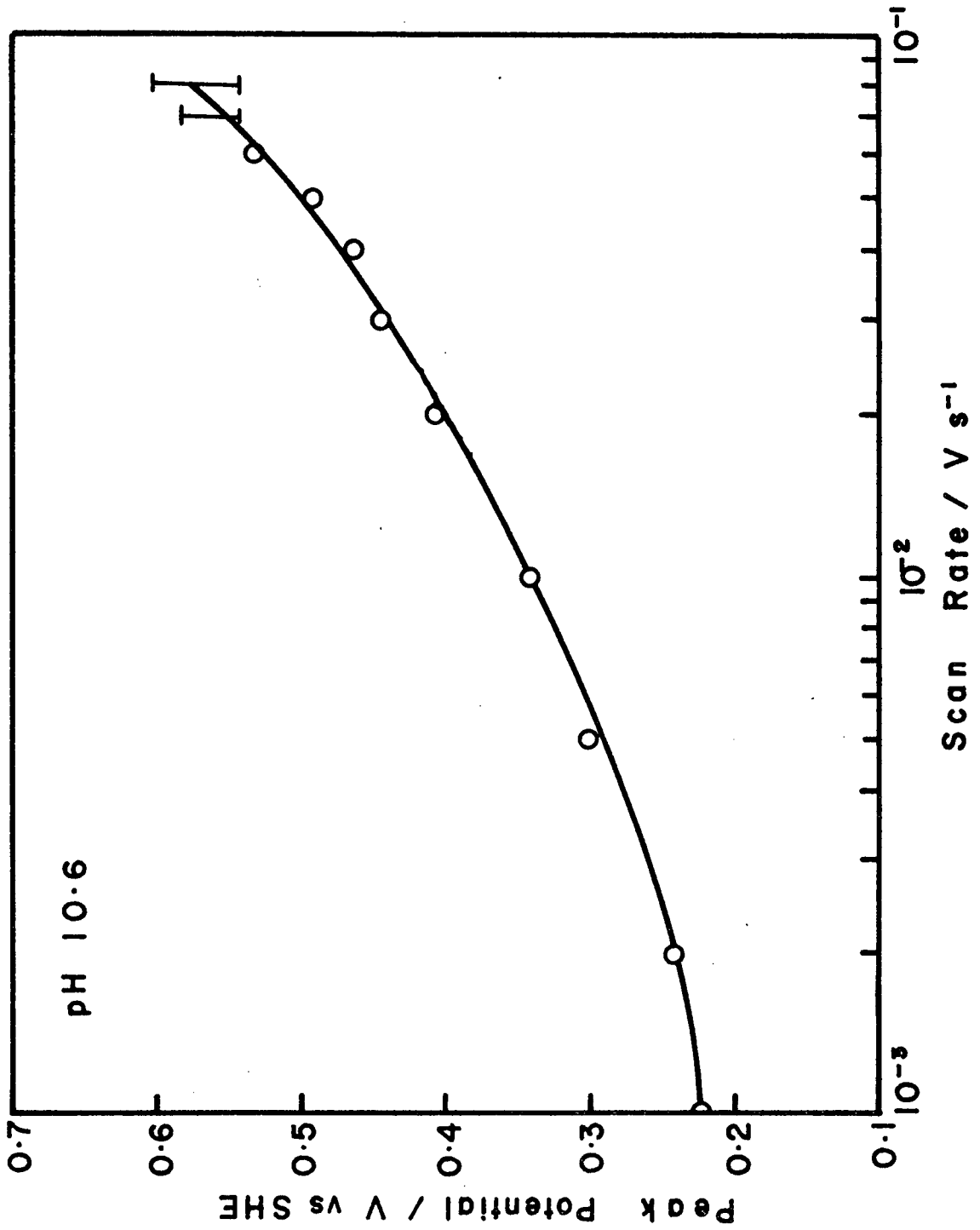

Figure 29

Plot of peak potential as a function of log scan rate

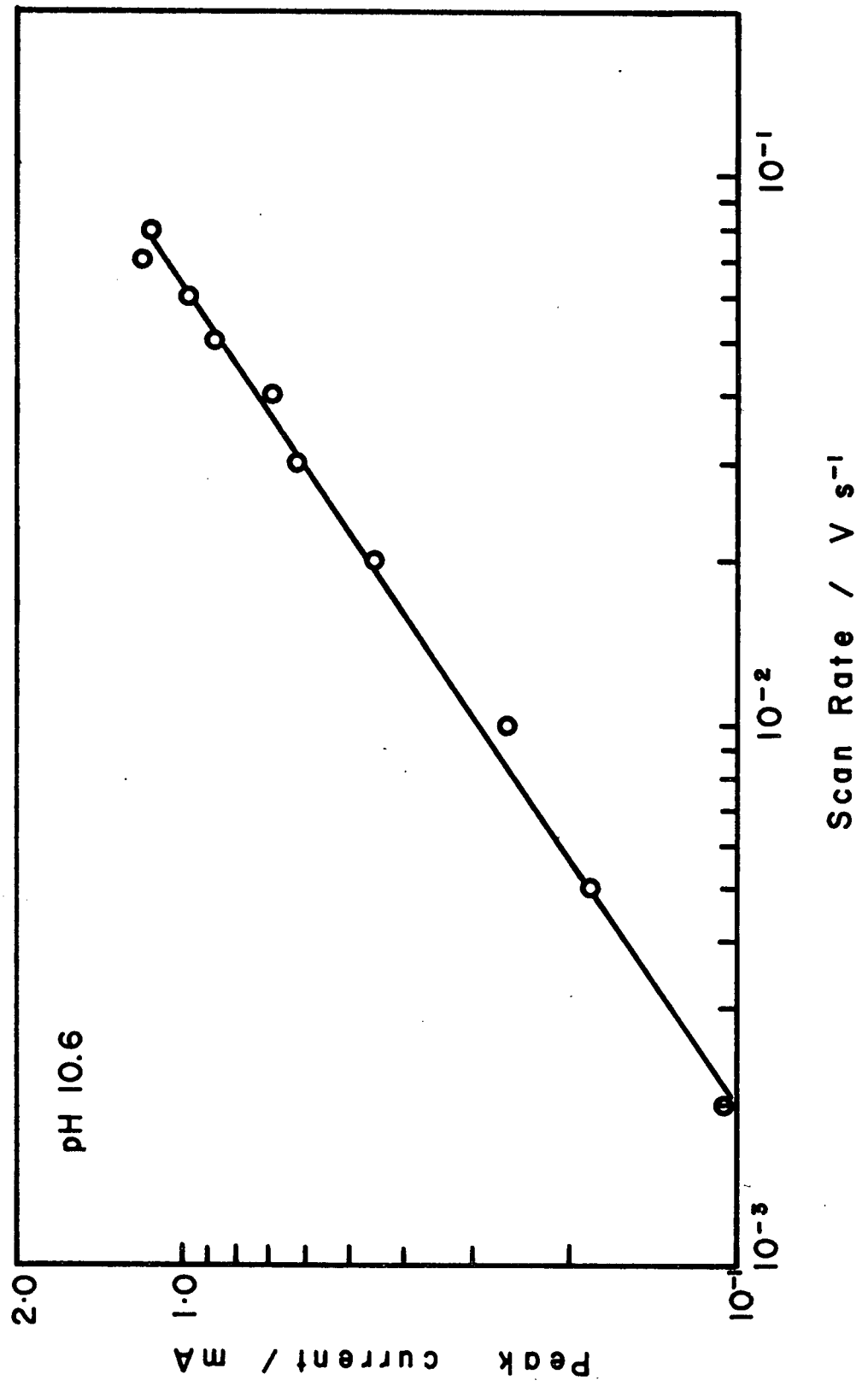

Figure 30

Log peak current versus log scan rate

It is apparent that the model used for these equations does not apply in the present case. Deviation from the model may in part result from the existence of more than one rate determining step. A more significant cause of deviation from the model likely results from the proposed oxidation mechanism. The formation of the ferric hydroxide surface deposit during oxidation results in a process controlled by diffusion rather than by activation processes.

Table 5
Influence of Scan Rate on Kinetic Parameters

Scan Rate mV/sec.	Imax mA.	Ep V	Ep_2 V	$Ep-Ep_2$	$n\beta$
1	.055	.223	.138	.085	0.56
2	.105	.243	.148	.095	0.51
5	.185	.301	.177	.124	0.39
10	.260	.343	.201	.142	0.34
20	.450	.408	.223	.185	0.26
30	.630	.443	.248	.195	0.25
40	.695	.463	.250	.205	0.23
50	.880	.493	.263	.230	0.21
60	.990	.533	.278	.255	0.19
70	1.200	(.543)	.286	.267	0.18
80	1.150	(.603)	.310	.268	0.18

F. Effect of Temperature

Since the flotation of arsenopyrite appears to be controlled by the formation of surface oxidation layers, it is of interest to determine the influence of temperature on the formation of these layers. The results of this study should indicate the extent to which temperature can be used to control

the flotation of arsenopyrite.

(i) Experimental

The same polarization equipment and test set - up as was described in the section on voltammetry was used for experiments at different temperatures. In this case the cell was equipped with a water jacket connected to a Colora Type K thermostat. The solution in the cell could be controlled to within ± 1°C.

(ii) Results and Discussion

A series of voltammograms was obtained across the range of temperature from 19°C to 60.5°C. The solution used for the test sequence was pH = 10.75 at 22°C. The voltammograms obtained at the two temperature extremes are shown in Figure 31. The most apparent difference in the two voltammograms is the cathodic shift and increased peak current associated with the arsenopyrite oxidation peak.

The peak potential, half wave potential and peak current across the temperature range are shown in Figure 32.

The peak potential decreases with temperature according to

$Ep = 479 - 4T$

$r = - 0.9957$ where T = temperature, °C

While the half wave potential decreases according to

$Ep_2 = 274.2 - 2.8T$

$r = - 0.9756$

The difference in slopes of the two relations indicates the peak to become steeper with increasing temperature.

The dependence of peak current on temperature shows a complex relationship. If the nature of the surface hydroxide layer was consistent across the temperature range the peak

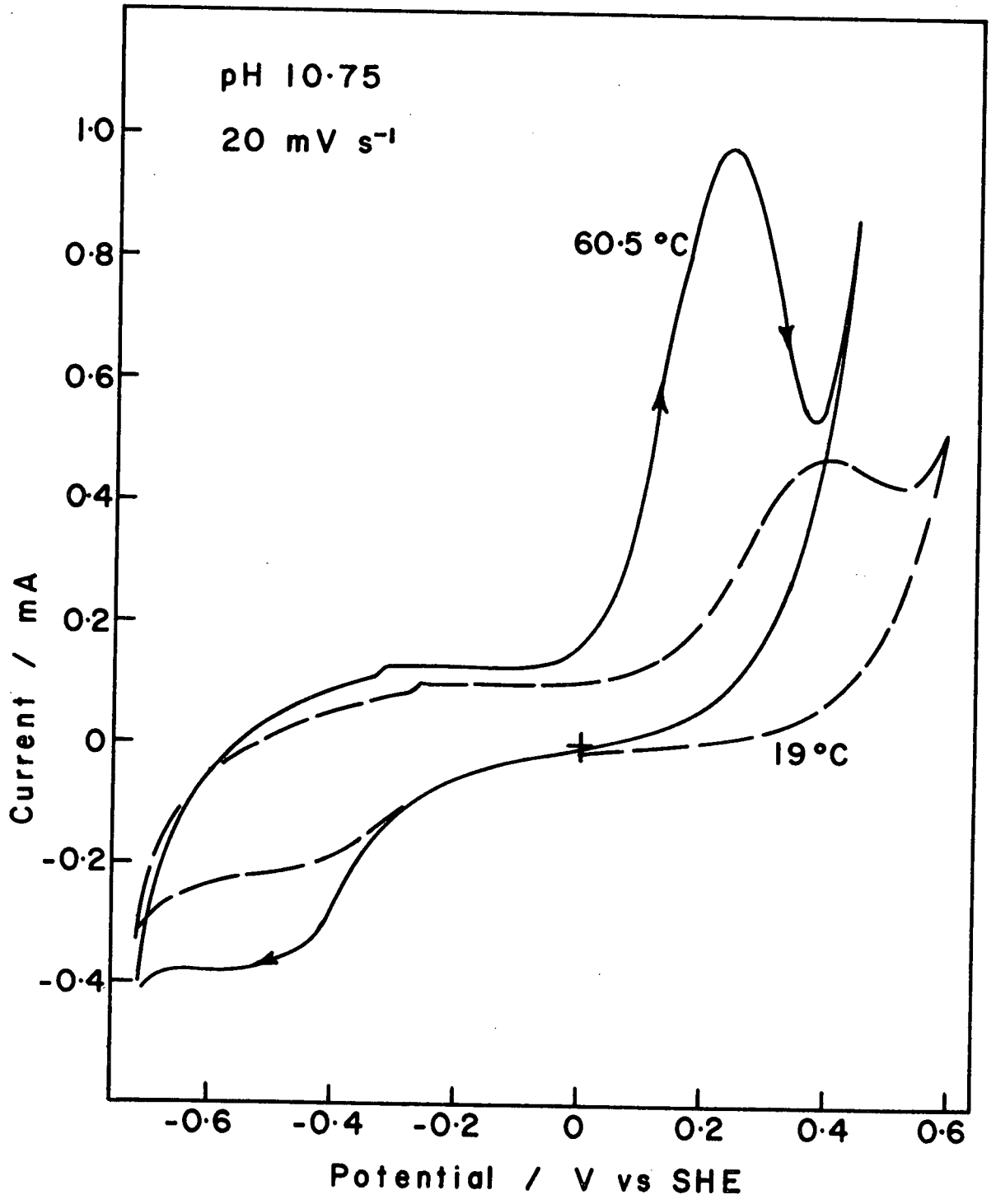

Figure 31

Voltammograms at 19°C and at 60.5°C.

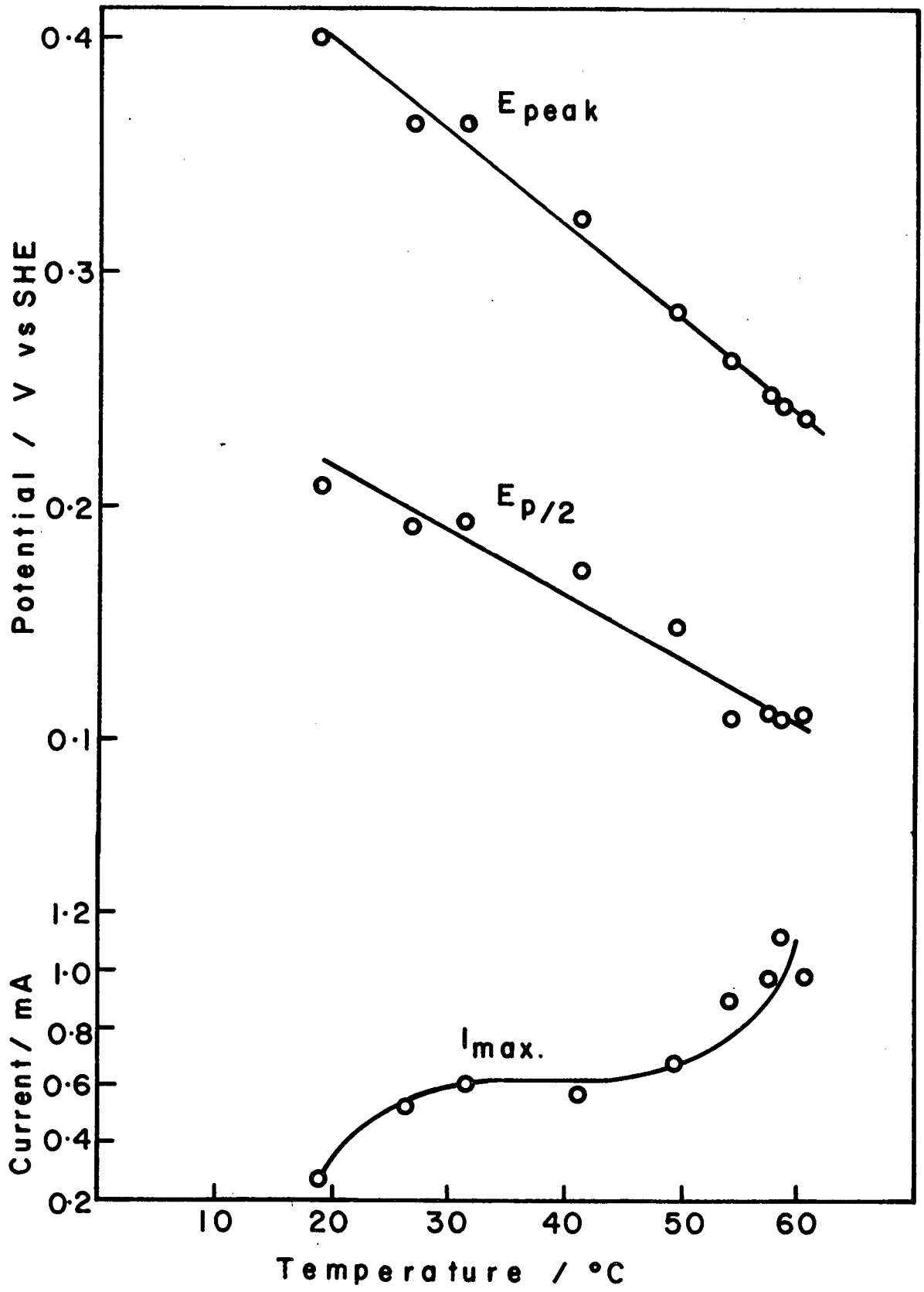

Figure 32

Influence of temperature on peak potential and peak current

current could be expected to be constant under diffusion control. The present results indicate a deviation from this behaviour.

At temperatures below approximately 30°C the hydroxide film development is incomplete and the current therefore increases with increasing temperature. Across the range from 30°C to approximately 45°C a constant film thickness is developed. Above 45°C an increase in current is observed indicating the diffusion barrier to be diminished. It is postulated that this increase results from a change in the morphology of the hydroxide film, a more porous film being developed. Thus while the film builds rapidly in thickness, its porous nature allows the anodic process to continue.

This is confirmed by Figure 33 which shows a multiple sweep voltammogram obtained at 58.5°C. While there is a decrease in current associated with the anodic peak (III) from the 1st. to 2nd. cycles, on subsequent cycles the current stays essentially constant while the peak shifts to slightly more anodic potentials. Both these observations are consistent with the presence of a steadily thickening but porous film. The increase in the peak height of the peaks I and V is consistent with the presence of an increasing amount of surface hydroxide. The electrode at the completion of this experiment was observed to be very heavily tarnished.

The formation of a porous film results in peaks I and V becoming more prominent than peaks II and IV. This is consistent with the effects noted upon electrode rotation or increasing pH (section 4.3.2 -B) and confirms improved conditions for

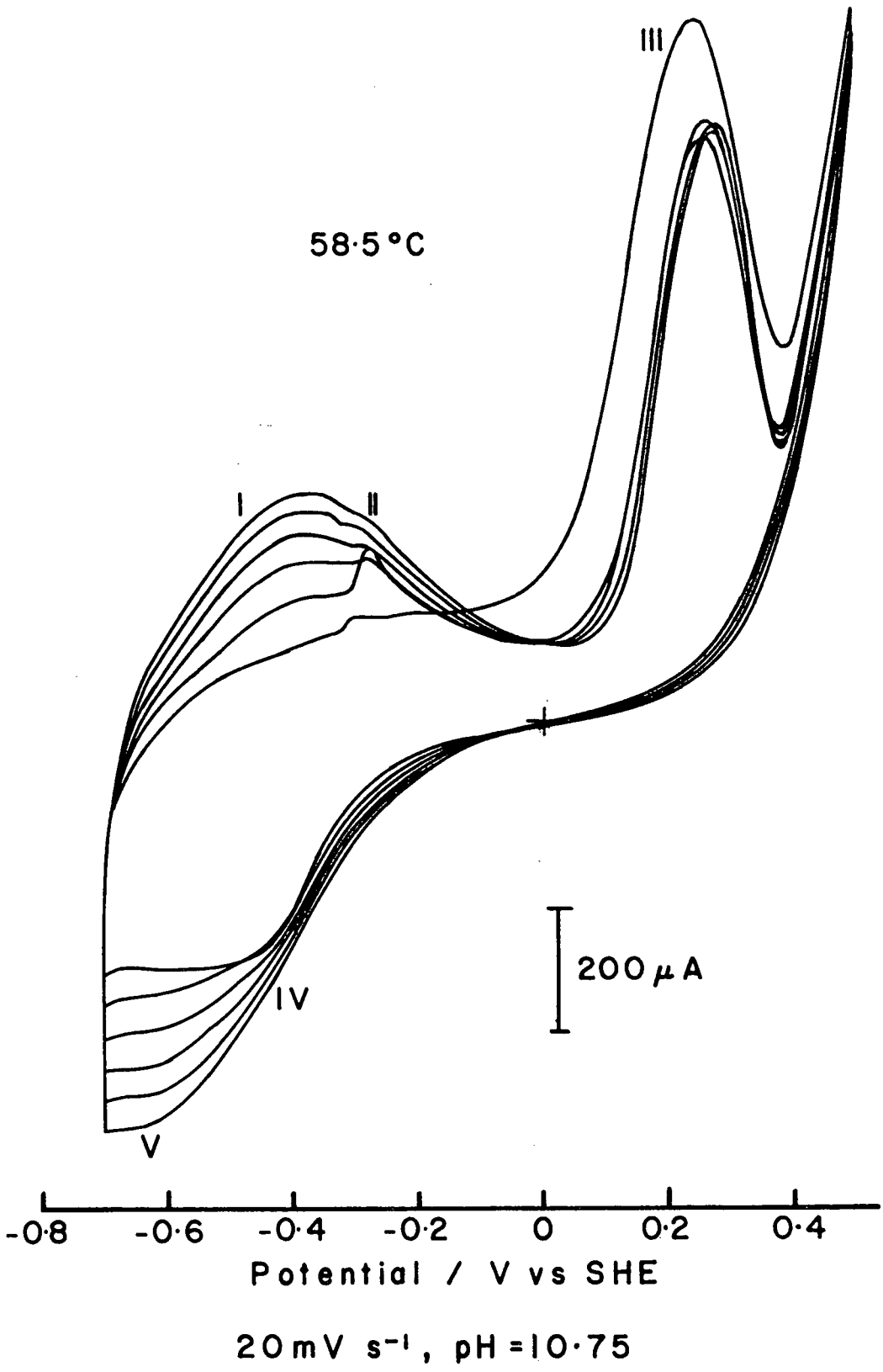

Figure 33

Multiple sweep voltammogram at 58.5°C

diffusion of species to and from the electrode.

Anodic scans for pyrite and arsenopyrite at 60°C are shown in Figure 34. The difference in potential between the two curves at the half peak potential for arsenopyrite is 30 mV. The difference observed at the same point at 22°C and pH 11 was 190 mV (Figure 17).

G. Influence of Cyanide

Cyanide is used as a flotation depressant for gangue sulphides such as pyrite. It is therefore of interest to determine the extent to which cyanide may be effective at depressing arsenopyrite.

The interaction of cyanide with pyrite has been studied by measuring the zeta potential and mixed potential of pyrite at varying pH with increasing addition of cyanide, ferrocyanide and ferricyanide (69). The zeta potential was observed to decrease with increasing cyanide additions indicating that the cyanide species adsorb chemically on pyrite. Mixed potential measurements for pyrite in the presence of cyanide were determined to lie in the region of stability of the compound $Fe_4[Fe(CN)_6]_3$. The formation of surface ferric ferrocyanide was therefore concluded to be responsible for the depression of pyrite by cyanide.

These investigators (69) also determined that variations in the degree of depression achieved with equal cyanide additions to various pyrite samples resulted from varying pyrite solubility. More soluble pyrite samples were found to be

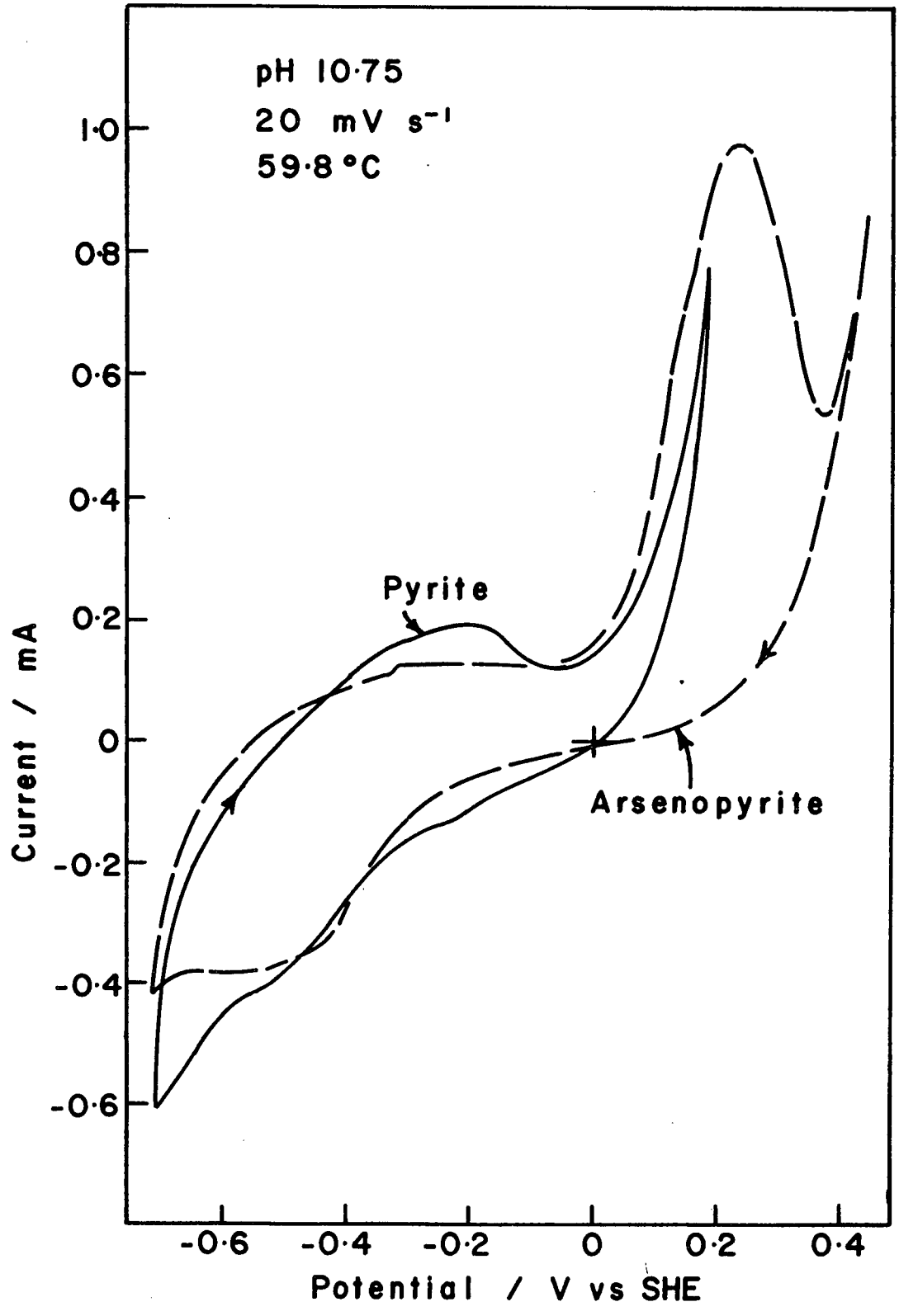

Figure 34

Comparison of pyrite and arsenopyrite voltammograms at 59.8°C

depressed to a lesser degree by cyanide than was less soluble pyrite. More soluble pyrite was postulated to result in higher levels of dissolved iron in solution, resulting in ineffective cyanide consumption. The results of electrochemical investigations into pyrite - cyanide interaction (23) were interpreted on the basis that the ferric ferrocyanide which formed on pyrite inhibited the electrochemical oxidation of xanthate and thus resulted in diminished floatability.

A series of voltammograms was obtained for arsenopyrite in the presence of increasing cyanide concentration at pH = 10.6. The cyanide concentration was varied from 1×10^{-4} M to 8×10^{-4} M sodium cyanide. Across this range of cyanide concentration the only significant change in multiple sweep voltammograms is that the anodic peak associated with the oxidation of ferrous hydroxide to ferric hydroxide becomes diminished with increasing cyanide concentration.

Figure 35 shows a multiple sweep voltammogram obtained at a cyanide concentration of 2.8×10^{-3} molar. At this cyanide concentration the ferrous hydroxide oxidation peak disappears completely. Comparison of Figure 35 with Figure 20 reveals that in the presence of cyanide the electrode becomes passivated to a much lesser degree than in the absence of cyanide. It appears therefore that cyanide acts to dissolve ferrous hydroxide formed at the surface of the electrode. Any iron - cyanide complexes which are formed are less effective inhibitors to further oxidation than is the hydroxide.

Curve A in Figure 36 represents a potential sweep on arsenopyrite carried out after the electrode had been held at

+343 mV for 15 minutes. This potential is just below the peak potential for arsenopyrite oxidation. The effect of holding the electrode at this anodic potential is to enhance the $Fe(OH)_2/Fe(OH)_3$ peaks while diminishing the arsenopyrite oxidation peak.

The peak for the oxidation of ferrous hydroxide to ferric hydroxide is believed to result from the formation of a small amount of ferrous hydroxide at the start of the potential sweep.

Curves B and C in Figure 36 represent potential sweeps carried out after holding the electrode at +343 mV for 15 minutes in the presence of $2X10^{-4}$ M and $2.8X10^{-3}$ M cyanide. Increasing cyanide concentration results in the ferrous hydroxide oxidation peak becoming diminished, the arsenopyrite peak becoming enhanced and the ferric hydroxide reduction peak being unaffected.

Curve D represents a potential sweep carried out after holding the electrode at +343 mV for 15 minutes followed by conditioning the electrode for 5 minutes in the presence of $1.63X10^{-3}$ M cyanide with no applied potential. Compared to curve A the ferrous peak is diminished while the arsenopyrite and ferric peaks are enhanced.

It is apparent that the action of cyanide is to dissolve ferrous hydroxide from the electrode. This decreases the effect of oxidation by removing the oxidation products from the surface. The arsenopyrite oxidation currents after holding the electrode at a corroding potential are therefore increased in the presence of cyanide.

The implication of this removal of surface hydroxide

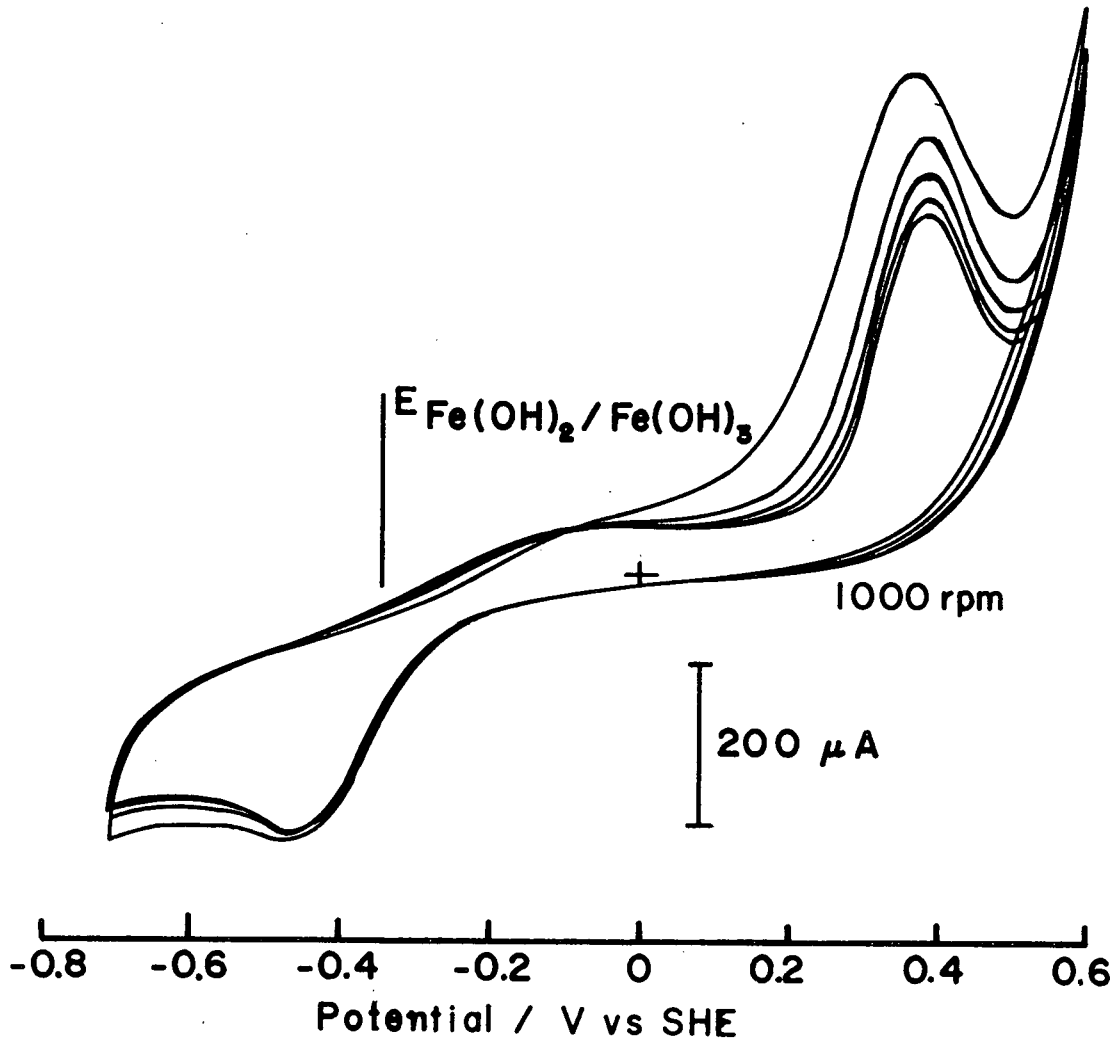

Figure 35

Multiple sweep voltammogram for arsenopyrite in the presence of 2.82×10^{-3} M NaCN

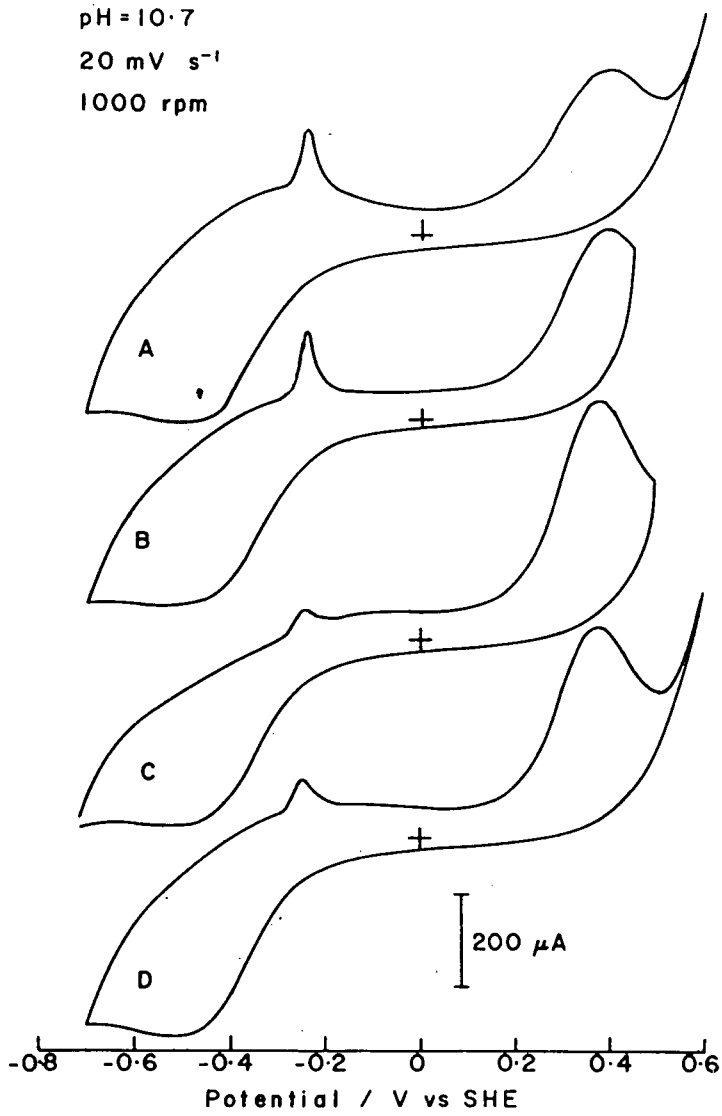

Figure 36

Influence of cyanide on formation of iron hydroxide films on arsenopyrite

deposits from arsenopyrite by cyanide is that cyanide may act as an activating agent rather than as a depressant for arsenopyrite.

A similar elimination of $Fe(OH)_2/Fe(OH)_3$ peaks in the presence of cyanide is observed for pyrite as shown in Figure 37. Pyrite in the presence of $1.63X10^{-3}$ M cyanide does not show any ferrous hydroxide peak. It was determined however that the anodic current at 0.443 V in the presence of cyanide was only 400μA while in the absence of cyanide it was 640μA. The cyanide therefore acts as an oxidation inhibitor in the case of pyrite. Such a decrease in anodic current in the presence of cyanide is not observed for arsenopyrite. The cyanide complexes which are known to be formed on pyrite are apparently not formed on arsenopyrite.

H. Other Minerals in the Fe - As - S System.

Multiple sweep voltammograms were obtained at pH = 10.6 for several other minerals in the Fe - As - S system as well as for iron. The purpose of this series of experiments was to determine whether ferric hydroxide formed during the oxidation of these minerals. Differences in floatability of these minerals can then be related to the variation in surface composition.

(i) Experimental

The pyrite electrode was the same electrode as was previously described. The marcasite electrode was made from a marcasite sample obtained from Wards' Scientific. The electrode was irregular in shape with an exposed surface of approximately

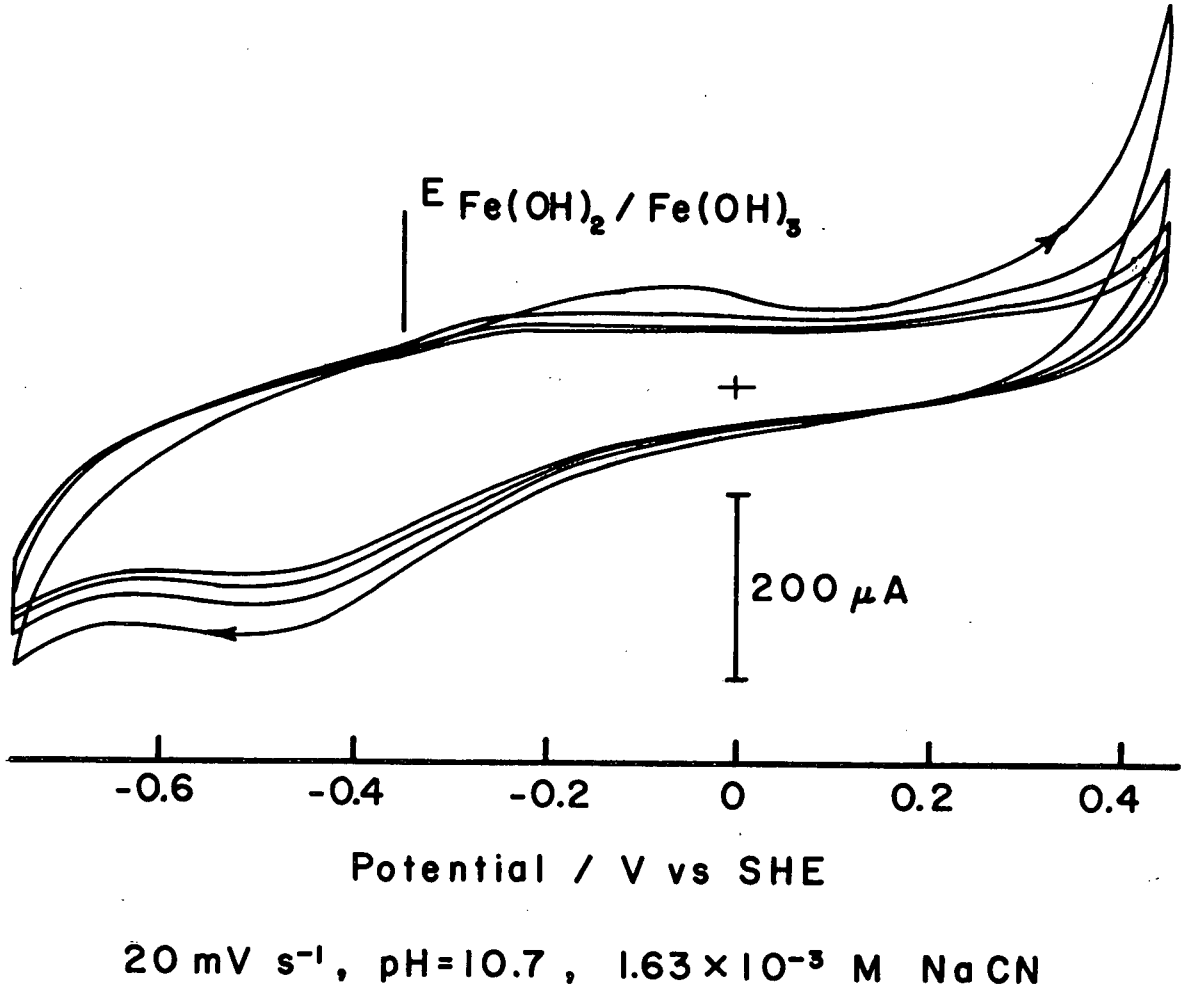

Figure 37

Voltammogram for pyrite in the presence of 1.62×10^{-3} M NaCN

4 square millimeters.

The loellingite sample was obtained from the UBC Department of Geological Sciences and was indicated to come from Cobalt, Ontario. The electrode was irregular in shape with an exposed area of approximately 59 square millimeters. The loellingite sample was analyzed by means of an SEM - EDX analysis. The major constituents were found to be arsenic and iron and the only trace constituent which was detected was antimony.

Electrodes were prepared as was previously described but with only one wire connected to them.

The iron electrode was made from a piece of Armco pure iron. The electrode was square in shape with an exposed area of approximately 14 square millimeters. This electrode was made by soldering a copper wire to one face of the iron cube and then encasing the assembly in epoxy. The face opposite the attached wire was ground down to 600 grit paper prior to use.

(ii) Results

Voltammograms for pyrite and marcasite are shown in Figure 38. The results for pyrite are similar to those for arsenopyrite in that the $Fe(OH)_2/Fe(OH)_3$ peaks are prominent but differ in that no anodic peak due to oxidation of pyrite itself is apparent. As previously discussed, the oxidation of pyrite occurs at higher potentials than does oxidation of arsenopyrite.

Peak A for pyrite has been attributed (63) to the formation of sulphur during pyrite oxidation. This peak is observed to become diminished with continued cycling.

The results for marcasite show less significant $Fe(OH)_2/Fe(OH)_3$ peaks but enhanced peaks associated with reduced

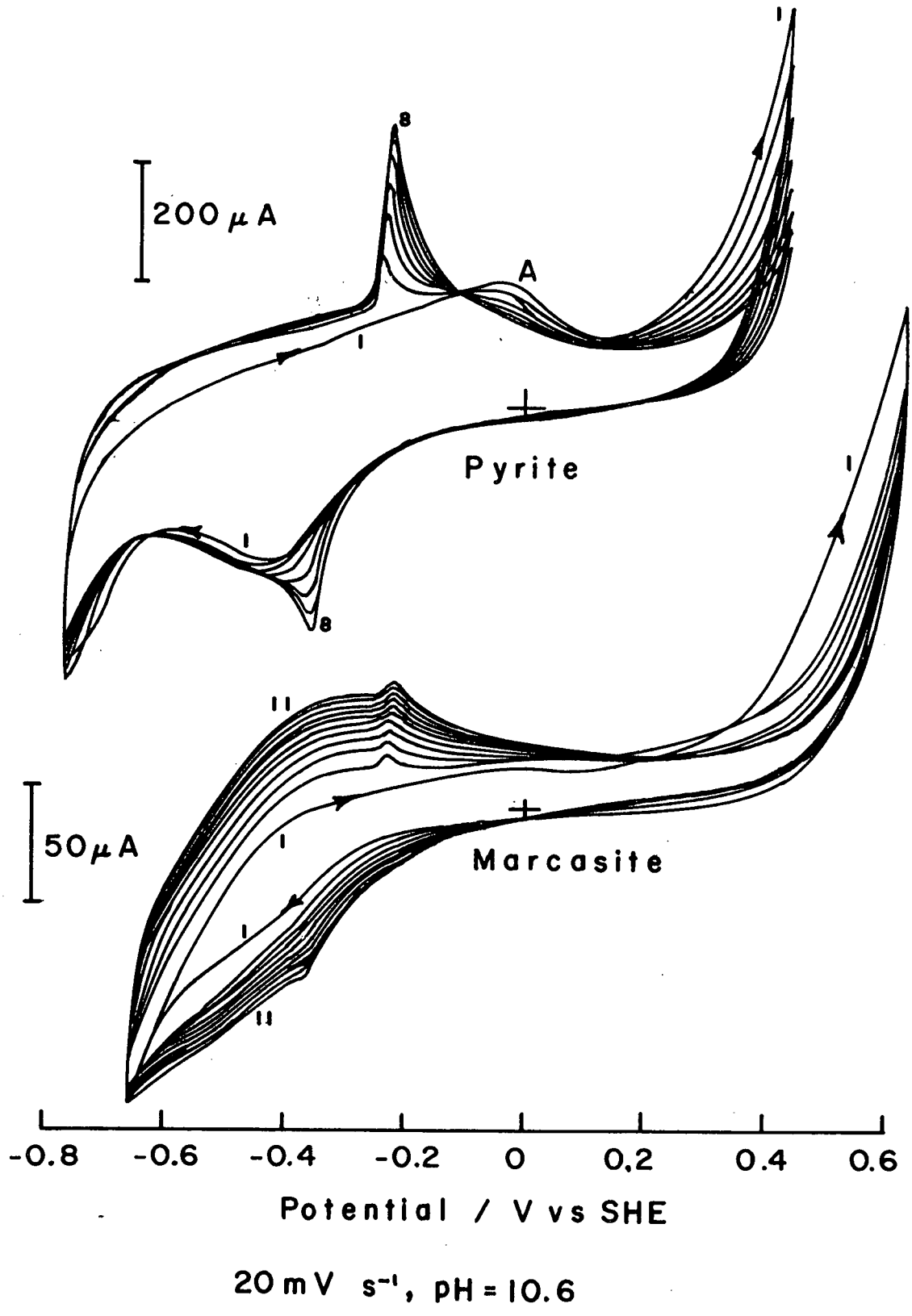

Figure 38

Voltammograms for pyrite and marcasite at pH = 10.6

iron - hydroxy species. The oxidation of marcasite occurs at more anodic potentials than pyrite. Marcasite shows a much lower tendency to passivate with continued scanning than does pyrite or arsenopyrite. The results are consistent with the formation of more soluble iron species during marcasite oxidation. This observation is consistent with the fact that marcasite is known to decompose with the formation of ferrous sulphate (37). The rate of oxidation of marcasite has been reported to be nine times as fast as pyrite (37).

Figure 39 shows a voltammogram for loellingite. The $Fe(OH)_2/Fe(OH)_3$ peaks are apparent as is an anodic peak associated with with loellingite oxidation. The loellingite oxidation peak is approximately 100 mV more anodic than the arsenopyrite oxidation peak under similar conditions (Figure 20).

A minor reversible reaction is apparent in Figure 39 at 0.2 to 0.3 V. The peaks result from a species which is oxidized on the first anodic sweep and then reversibly reduced and oxidized on subsequent sweeps. Although antimony was detected as a minor constituent in the loellingite, the peak potentials cannot be related to antimony reactions. Considering the fact that the loellingite originated in a silver producing area in Canada it was considered possible that the peaks were due to trace concentrations of silver which had not been detected during the sample analysis.

A voltammogram for a gold electrode in the presence of dissolved silver is shown in Figure 39. The peak positions show good agreement with those observed for loellingite.

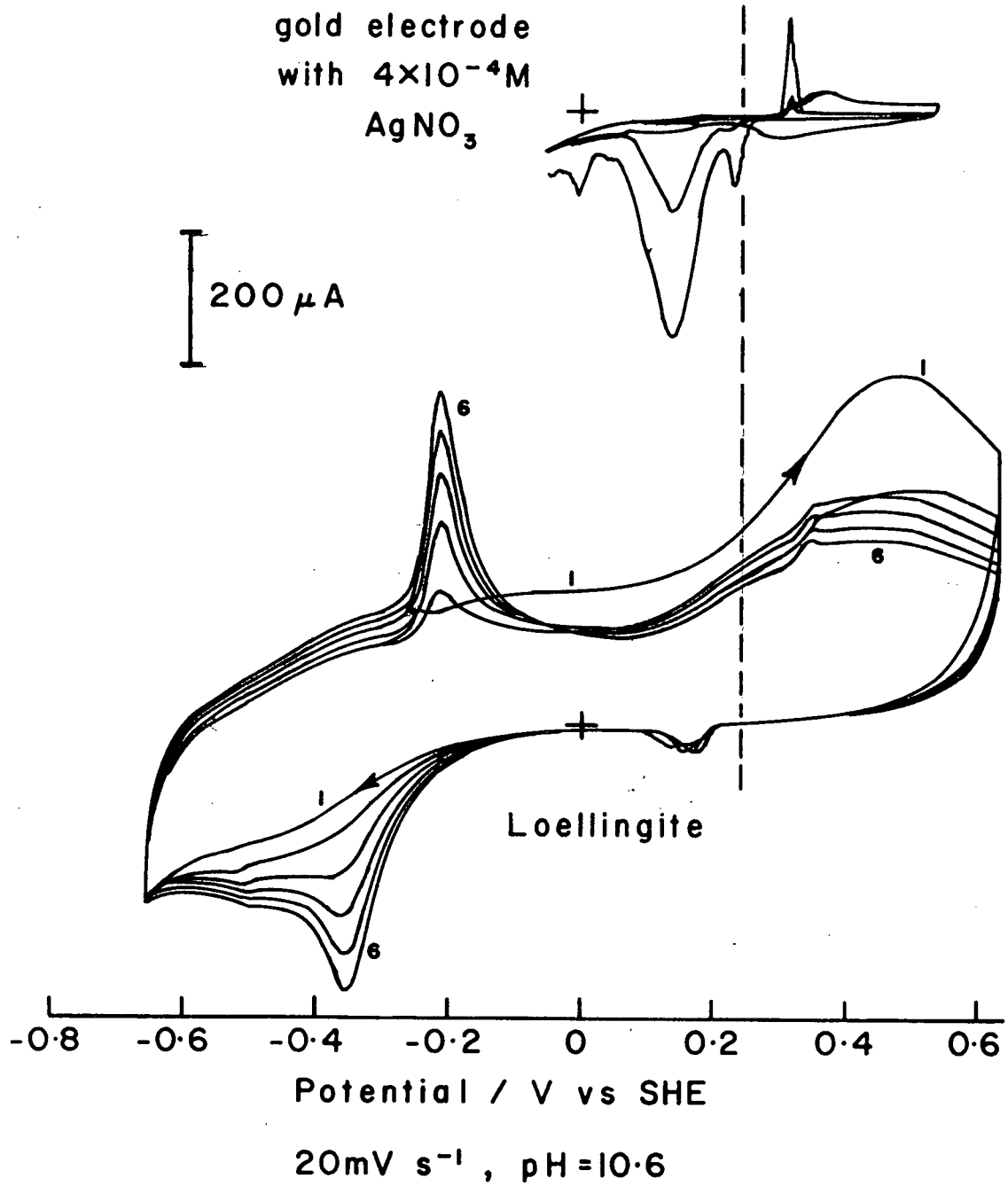

Figure 39

Multiple sweep voltammogram for loellingite at pH = 10.6

Figure 40 shows a voltammogram for iron. This experiment was carried out without KCl in solution since excessive currents and formation of surface hydroxide species were encountered in its presence. The $Fe(OH)_2/Fe(OH)_3$ peaks are apparent although the voltammogram is more complex than those for minerals. This increased complexity is assumed to result from the different physical nature of iron hydroxide films formed on iron compared to those formed on minerals.

Based on this series of experiments, some possibilities regarding the variable floatability of these minerals can be considered. The oxidation behaviour of loellingite is very similar to that of arsenopyrite and similar flotation characteristics would be anticipated. Marcasite shows behaviour more comparable to that of pyrite with the exception that more soluble iron - hydroxy species are formed. It is expected that this unstable behaviour of marcasite would make it more difficult to float with xanthate and would make it more difficult to depress with cyanide than in the case of pyrite.

None of the minerals considered show behaviour similar to that of iron. Although iron hydroxide deposits of some form are developed in each case, each mineral shows anodic decomposition currents in the region where iron is passivated.

I. Ring Disc Study

The rotating arsenopyrite electrode was equipped with a gold ring to detect electroactive oxidation products. The purpose of these experiments was to determine whether any

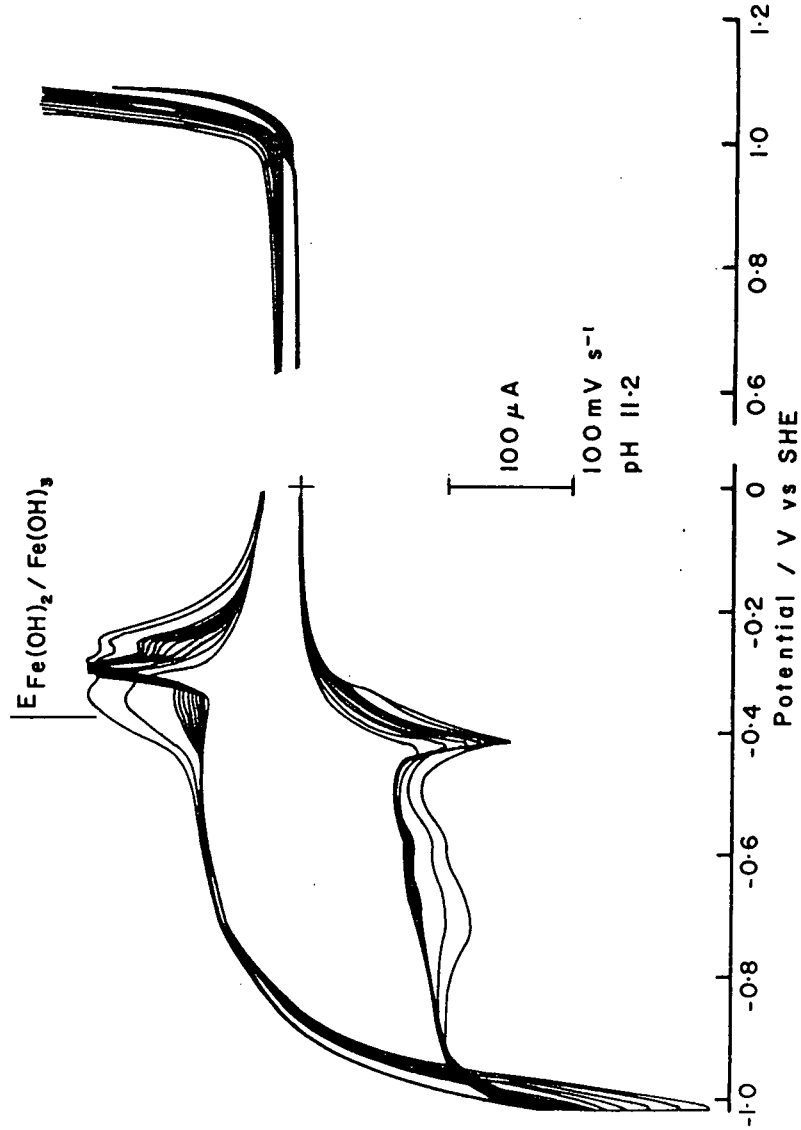

Figure 40

Voltammogram for iron electrode

oxidation products which had previously not been considered were escaping into solution. Experiments were carried out only at pH = 10.6 so that the possible formation of elemental sulphur at lower pH values was not investigated.

Figure 41 shows the solution flow from the disc to the ring and the transport pattern of soluble species formed at the disc (71). Such ring - disc electrodes have been used to study the anodic decomposition of galena (72) as well as the corrosion of dental alloys (73).

The efficiency with which the ring collects species released at the disc is dependent on electrode geometry according to

$$N = ir/id = \left[\frac{r_3^3 - r_2^3}{r_1^3} \right]^{2/3} \qquad (29)$$

where

r_1 = radius of disc

r_2 = inner radius of ring

r_3 = outer radius of ring

ir = ring current

id = disc current

The geometry of the arsenopyrite electrode gives a value for the collection efficiency of 0.77. This value is very high due to the fact that the gold ring is very wide. Such a wide ring is subject to excessive noise pick-up. An attempt was made to determine the actual collection efficiency of the electrode. The arsenopyrite was found to give high background currents

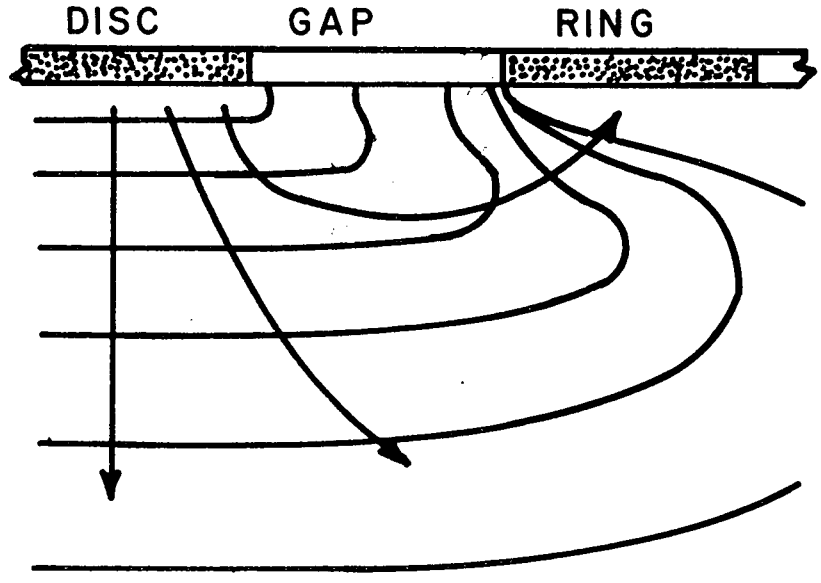

Figure 41

Transport pattern of soluble species at a ring - disc electrode

however and a meaningful result could not be achieved.

Two experiments were carried out with this electrode at pH = 10.6. One experiment involved holding the arsenopyrite disc at the anodic peak potential while scanning the gold ring. The second experiment involved carrying out a triangular potential sweep of the arsenopyrite while holding the ring first at an anodic and second at a cathodic potential.

In neither experiment were any ring currents detected. This result is consistent with the formation of sulphate and arsenate, both of which are electroinactive, at the arsenopyrite disc. The formation of solid oxidation products such as elemental sulphur or As_2S_2 would be consistent with the results of these experiments. The voltammetry experiments which previously have been discussed show no evidence of these species and they are not believed to be present. While more elaborate experiments could have been carried out, it seemed unlikely that these would contribute significantly to the present study and this area therefore was not pursued further.

J. Influence of Hydroxide Formation on Xanthate Oxidation.

It is generally accepted that dixanthogen is the active collector species in pyrite flotation (27). The nature of adsorbed xanthate species on arsenopyrite has not been investigated but it is expected that dixanthogen will be the active collector species.

Since the oxidation of arsenopyrite has been shown to result in a rapid build-up of ferric hydroxide on the surface, it is of interest to determine the influence of this hydroxide

build-up on the oxidation of xanthate to dixanthogen.

(i) Experimental.

Anodic oxidation scans were carried out at a scan rate of 5 mV per second.

Xanthate used for these experiments consisted of Hoechst potassium ethyl xanthate which was purified by dissolving in acetone and recrystallizing by addition of ether.

(ii) Results and Discussion

Figure 42 shows the results of experiments carried out at pH = 5.9. An anodic scan is shown for an arsenopyrite electrode which had been freshly polished. A scan is also shown for the same electrode after it had been held for 5 minutes at a potential of + 460 mV. This potential is part way up the anodic curve for arsenopyrite and represents the potential region achieved in the presence of permanganate at this pH. The anodic treatment is observed to result in only a minor passivation.

Two scans are shown in the presence of 2.6×10^{-3} M potassium ethyl xanthate. One scan is for a fresh electrode while the other is for an electrode as described above. At this pH the oxidation of arsenopyrite has a negligible effect on the oxidation of xanthate to dixanthogen. This is consistent with the view that hydroxide films are not formed by the oxidation of arsenopyrite at this pH.

Figure 43 shows the results for a similar set of experiments carried out at pH = 11.8. At this pH, visible films of ferric hydroxide are formed.

Several differences with the results obtained at pH = 5.9 are apparent. While at pH = 5.9 the oxidation of xanthate occurs

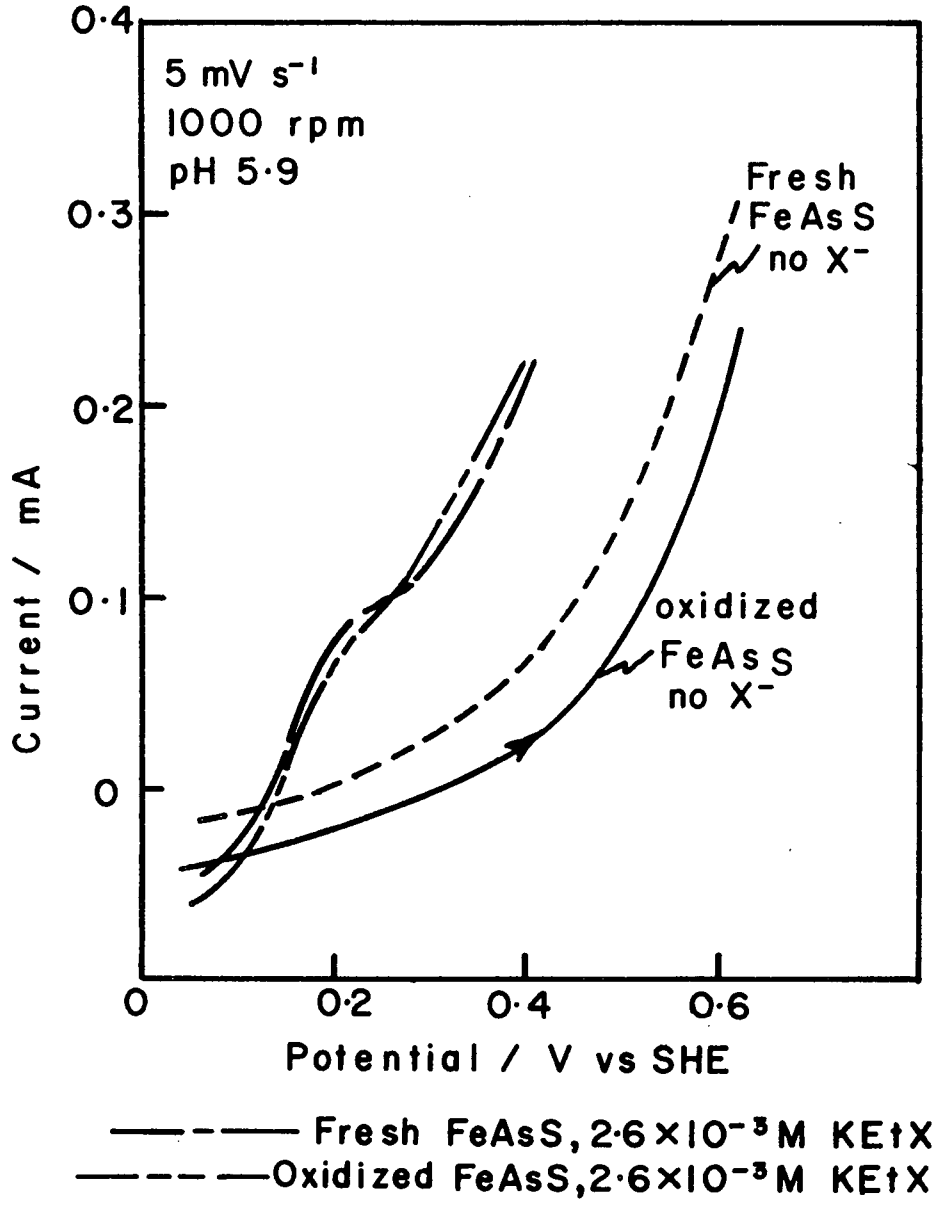

Figure 42

Influence of arsenopyrite oxidation at pH = 5.9 on xanthate oxidation

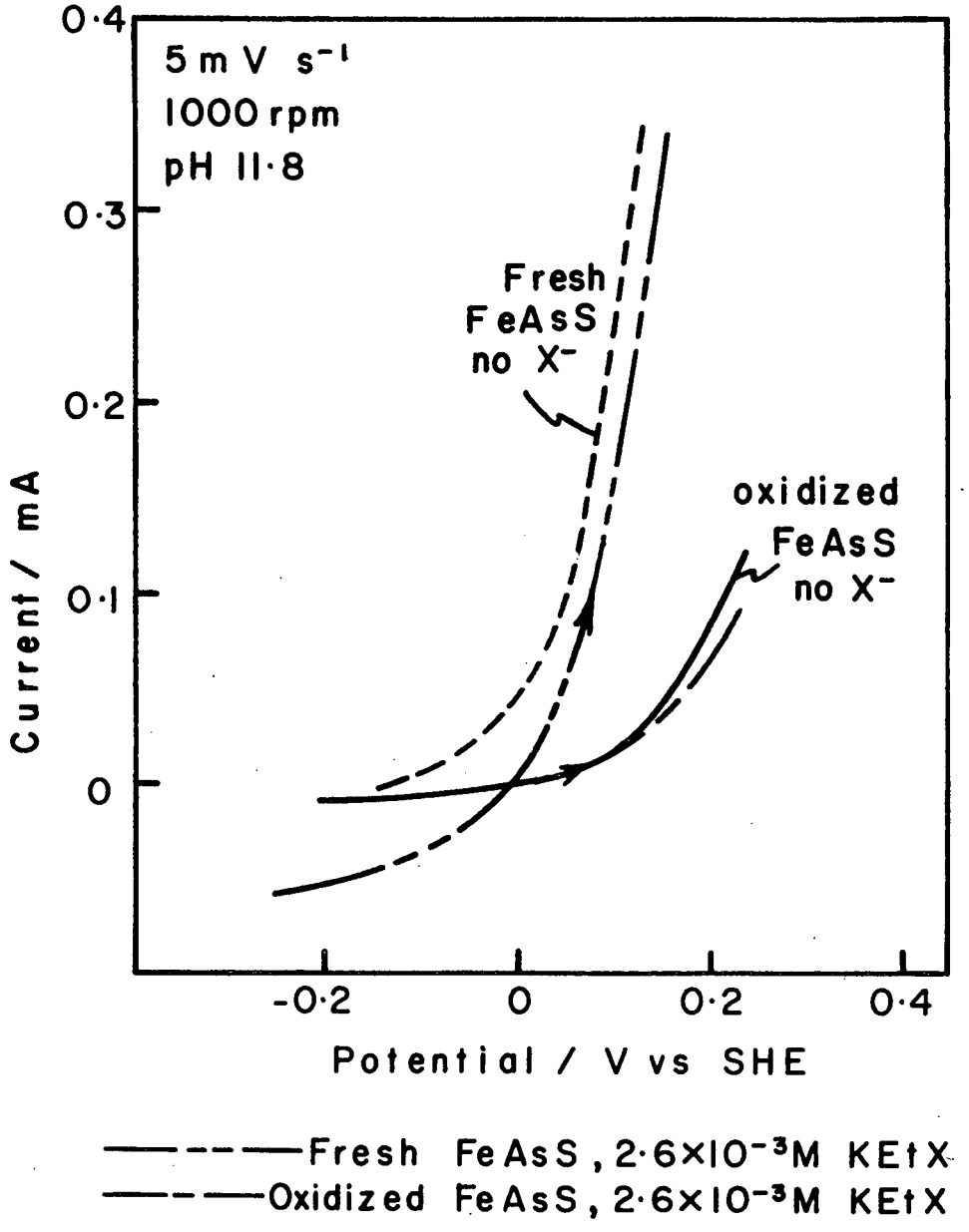

Figure 43

Influence of arsenopyrite oxidation at pH = 11.8 on xanthate oxidation

at potentials which are cathodic to arsenopyrite oxidation, at pH = 11.8 these two curves are reversed. This indicates that oxidation of arsenopyrite will be favored over xanthate oxidation at this pH.

A further difference is that while at pH = 5.9 the electrode was hardly affected by holding at an oxidizing potential, at pH = 11.8 the electrode is passivated to a significant degree. The oxidation of xanthate is greatly inhibited by the presence of this passivating hydroxide layer.

While these experiments clearly show that the presence of thick ferric hydroxide layers such as could be formed under flotation conditions (i.e. 5 minutes conditioning with $KMnO_4$) will prevent the formation of dixanthogen at the surface, the adsorption of xanthate ions at the hydroxide layer has not been ruled out.

4.4 Discussion

The oxidation of arsenopyrite under moderately oxidizing conditions has been shown to result in the formation of relatively thick surface layers of ferric hydroxide. At the same time the arsenic and sulphur are oxidized to arsenate and sulphate respectively. At the lower end of the pH range studied elemental sulphur can be expected to be a product of oxidation.

The influence of oxidation on the floatability of arsenopyrite is exerted through the build-up of the hydroxide layer on the surface of the mineral. The presence of this hydroxide layer inhibits the oxidation of xanthate to dixanthogen. The mineral is therefore not rendered hydrophobic.

At the same time the hydroxide layer itself can be expected to be strongly hydrophilic and the mineral is therefore strongly depressed.

The oxidation potentials required to bring about the oxidation of arsenopyrite have been shown to be achieved in the presence of several common oxidizing agents.

In addition, the oxidizing potentials required for arsenopyrite depression are encountered in some plants even in the absence of oxidizing agents. Figure 44 shows various Eh - pH conditions which were measured in plants (70) as well as the rest potential and oxidation peak potential for arsenopyrite. It is apparent that in some cases the conditions required for the oxidation and thus the depression of arsenopyrite are being achieved.

Current peaks associated with arsenopyrite oxidation increase with increasing pH. The build-up of hydroxide is therefore expected to be greater with increasing pH and flotation should be more difficult. Maximum flotation of arsenopyrite with xanthate is expected at pH less than 7, where ferric hydroxide does not form and where the formation of surface deposits of elemental sulphur would further contribute to the hydrophobicity of the mineral.

The influence of temperature on the oxidation of arsenopyrite showed a complex variation. Over the range of 15°C to 30°C, increasing temperature resulted in increasing development of surface hydroxide. Over the temperature range 30°C to 40°C temperature has no apparent influence on hydroxide build-up while at temperature greater than 40°C, increasing

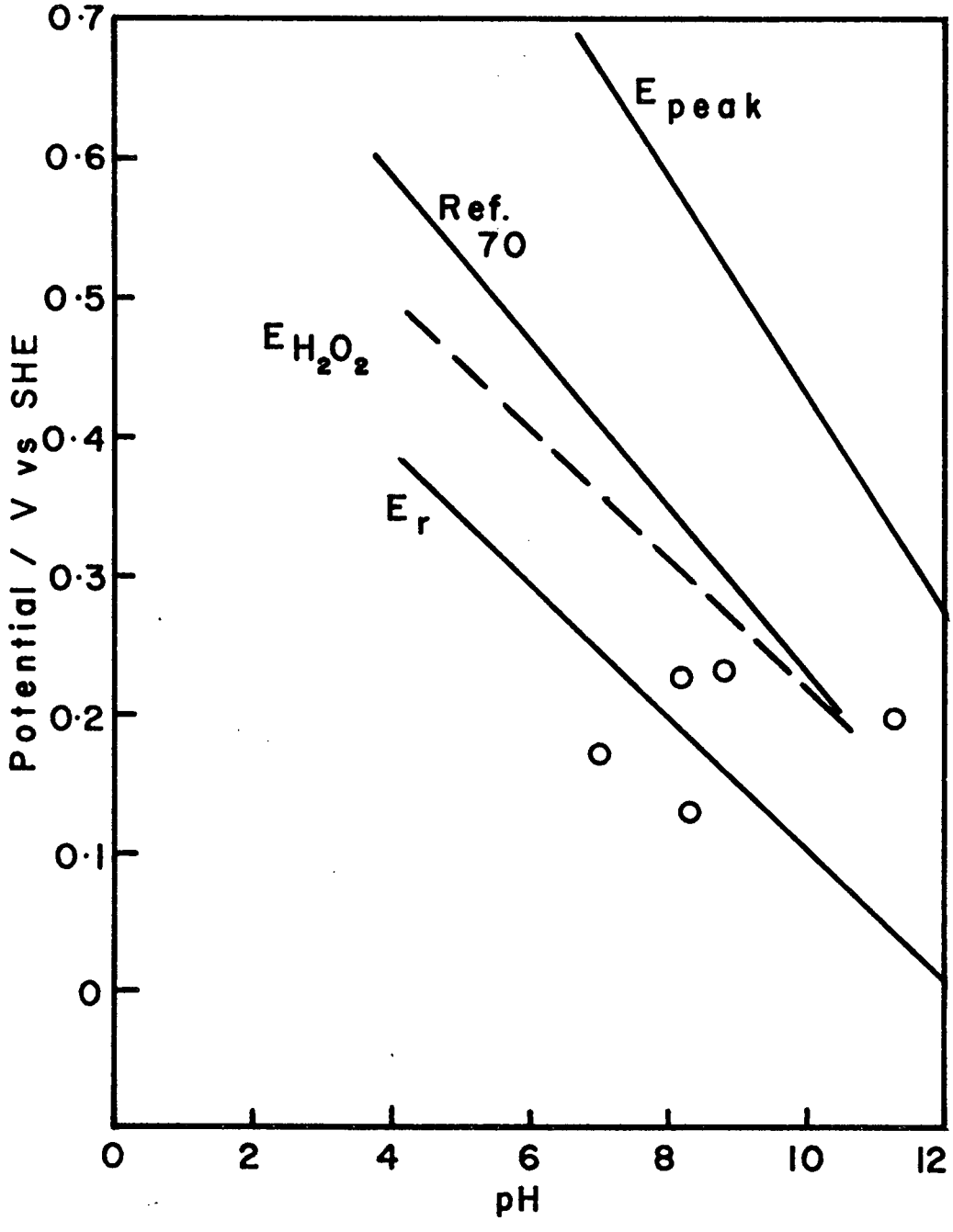

O - Conditions observed in plant measurements (70)

Figure 44

Comparison of arsenopyrite rest potential and oxidation peak potential with operating plant conditions (70)

temperature results in a rapid increase in the quantity of ferric hydroxide. The influence of temperature on the depression of arsenopyrite by oxidation is therefore expected to be minimal until a temperature of 40°C is exceeded. Above this temperature, thick, hydrophilic layers of ferric hydroxide are formed.

Differential flotation of arsenopyrite and pyrite through the use of oxidizing agents should be possible in the temperature region near 20°C. At this temperature, arsenopyrite oxidizes at significantly lower oxidation potentials than does pyrite. Increasing temperature can be expected to diminish the efficiency of the differential flotation of these minerals. At elevated temperature (60°C) the potentials at which the two minerals oxidize at a significant rate are closer together than at low temperatures.

The addition of cyanide to solution resulted in a dissolution of the hydroxide surface deposits previously formed on arsenopyrite. It is expected that cyanide additions would result in increased arsenopyrite floatability by diminishing the effects of oxidation.

Chapter 5

ESCA STUDIES

X-ray photoelectron spectroscopy (XPS) or more commonly known as ESCA, is an experimental technique which permits the analysis of a surface layer on a solid sample. The thickness of the surface layer which will be analyzed may vary from a few angstroms to 50 angstroms.

The method consists of bombarding the sample to be studied with nearly monoenergetic photons and measuring the kinetic energy distribution of the ejected electrons (74). Each element will have a characteristic set of photoelectron peaks due to the different electronic levels. The photon energies used to eject electrons are in the range of 1 KeV or more.

The binding energy of electrons in a given electronic level can be measured with sufficient precision to detect shifts resulting from differences in the chemical state of the atom. For instance, the energy for electrons in a given energy state for a metal will be different than for the metal oxide. Similarly, variations in oxidation state will result in variation of the binding energy of core electrons.

ESCA studies have been carried out on pyrite to determine the nature of suface compounds formed during flotation (75). It was determined that iron hydroxide formed on pyrite during grinding and at high pH during flotation. For values of pH less than 7, surface hydroxide films are dissolved leaving a clean pyrite suface. Only limited quantities of elemental sulphur were

detected even at pH = 3.0.

This observation that limited sulphur was detected suggests that the method may be insensitive to surface concentrations of elemental sulphur since sulphur is known to form during the acid oxidation of pyrite (76). While no explanation has previously been offered in the literature it is proposed that any elemental sulphur present on the surface of particles is volatilized at the high vaccuum (10^{-7} torr) encountered during analysis, before it can be detected.

In the present study, the results of electrochemical experiments on arsenopyrite have been interpreted as indicating the formation of ferric hydroxide with concurrent oxidation of arsenic and sulphur to arsenate and sulphate respectively. The result of ESCA experiments will be used to confirm the existence of iron hydroxide surface films and to show the extent to which arsenate and sulphate are incorporated in these films.

5.1 Experimental

Samples of arsenopyrite, pyrite and loellingite were of the same origin as those used for electrochemical studies. Other mineral samples were obtained from Ward's Scientific and were visually judged to be free of other mineral impurities.

All samples were pulverized with a porcelain mortar and pestle to minus 74 microns and stored in sealed vials prior to use.

The arsenopyrite which is shown in figures 45 to 47 and in Table VI to have been treated at pH = 11.5 was prepared by stirring 2 grams of sample in 100 ml. of water adjusted to

pH = 11.5 with sodium hydroxide. Following 15 minutes of conditioning the sample was filtered and dried under argon at 35°C.

Samples to be analyzed were dusted onto double sided cellulose tape which could be fastened to the sample holder for insertion into the spectrometer.

XPS measurements were carried out using a Varian IEE-15 spectrometer equipped with a magnesium anode. Spectra were recorded at approximately 10^{-7} torr.

From ten to forty scans were made of each mineral. The data points were collected in digital form and a Gaussian fit was applied to the data normalized to overcome the variable number of scans.

5.2 Results and Discussion

The iron, arsenic and sulphur peaks for the various minerals included in the study are shown in Figures 45,46 and 47. The binding energies and intensity data associated with the peaks are summarized in Table 6. Intensities are based on the counts per second at the peak. Binding energies relate to the iron 2p, arsenic 3d and sulphur 2p orbital electrons.

The purpose of including the various minerals other than arsenopyrite in the study is to provide a basis for comparison of peak positions and relative intensity of oxidized and reduced species for each mineral. Intensities for the same element in different minerals can be expected to vary independently of the compositional ratio for that element. Factors such as real surface area and volume per unit cell, taking into account the

number of formula units per unit cell, will influence intensity ratios between minerals. Since XPS analyzes a thickness of the

Table 6
Electron binding energies and intensities for elements in various minerals.

Mineral	Element	Binding Energy eV	Counts/sec.
FeOOH	Fe	713.6	21137
As_2S_3	S	163.4	7406
	As	44.1	4403
FeS_2 (pyrite)	Fe	712.3	758
		709.4	5758
	S	169.7	1352
		163.7	5395
FeS_2 (marc.)	Fe	713.7	1879
		709.5	5949
	S	170.9	1692
		164.9	4187
$FeAs_2$	Fe	713.9	1707
		709.5	2347
	As	46.9	1546
		43.8	2289
FeAsS (dry)	Fe	712.9	5646
		708.6	2761
	As	47.2	1167
		44.1	525
	S	170.6	549
		165.0	1234
FeAsS (pH 11.5)	Fe	712.8	11921
		708.5	1322
	As	47.1	2067
		43.4	281
	S	171.1	837.8
		165.5	831.4

order of 50 angstroms the result for surface product layers thinner than this will represent a composite of the surface product and the substrate.

Intensity ratios of oxidized to total surface species for pyrite, marcasite and arsenopyrite are summarized in Table 7.

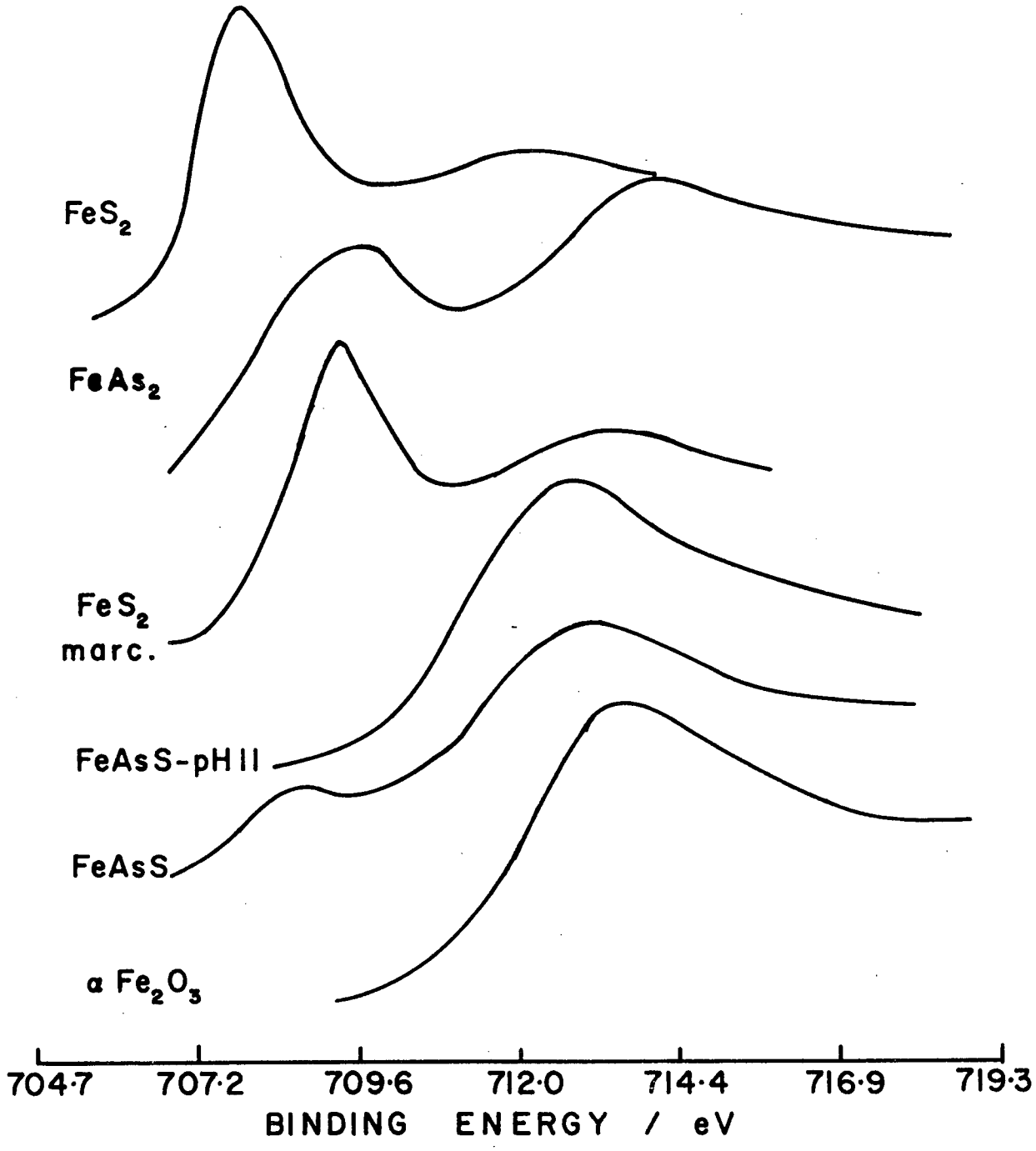

Figure 45

XPS peaks associated with the iron 2p electrons of the various minerals

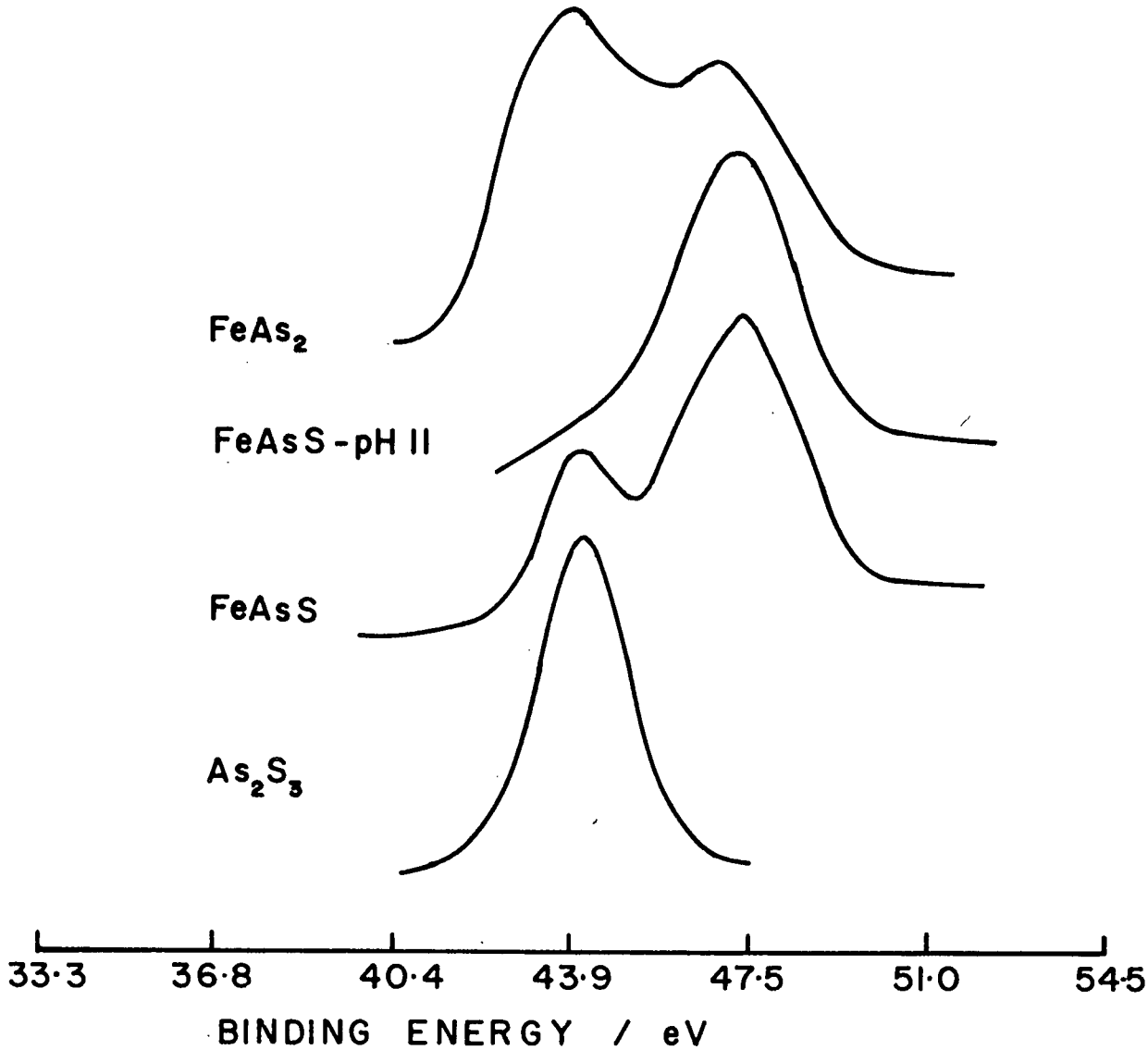

Figure 46

XPS peaks associated with the arsenic 3d electrons of the various minerals

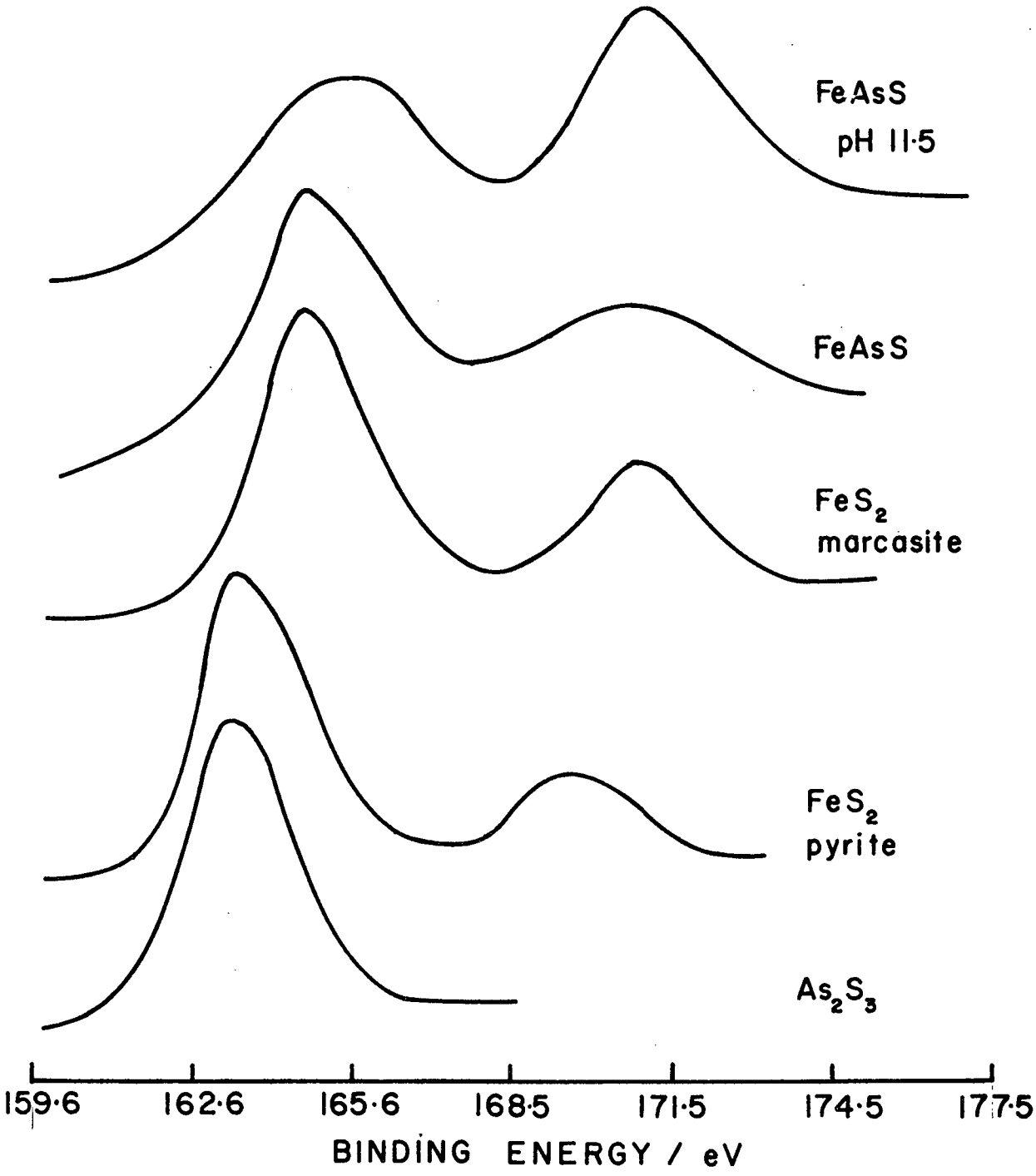

Figure 47

XPS peaks associated with the sulphur 2d electrons of the various minerals

Several trends in these data are consistent with previously cited characteristics for marcasite compared to pyrite and with the electrochemical results for arsenopyrite which are presented in this study.

Marcasite shows a greater proportion of oxidized species than does pyrite. This is consistent with marcasite showing greater oxidation rates than pyrite (37) and with previously published XPS results for these minerals (77).

Arsenopyrite shows an even greater proportion of oxidized surface species than either pyrite or marcasite. It is apparent that although the arsenopyrite was crushed in a dry form, a surface oxide layer was formed. This helps to explain the results of some of the electrochemical experiments. The voltammetry results indicated that iron hydroxide was not formed below a pH of approximately 7.0. At the same time the rest potentials measured at pH less than 7.0 obeyed the same relation as those at higher pH, indicating a consistent surface layer to be present. These results can now be reconciled on the basis

Table 7
XPS Intensity ratios

Mineral	ox Fe/Fe	ox S/S	ox As/As	Fe/As	Fe/S
Pyrite	0.12	0.20	-	-	0.97
Marcasite	0.24	0.29	-	-	1.33
Arseno. - DRY	0.67	0.31	0.69	5.0	4.71
Arseno - pH = 11.5	0.90	0.50	0.88	5.6	7.93

that in each case a surface layer of iron hydroxide was formed

during the electrode preparation. This hydroxide controlled the electrode potential measurements but was of insufficient thickness to affect the voltammetry experiments.

As expected, based on results of electrode potential measurements, subjecting arsenopyrite to pH = 11.5 results in rapid decomposition of the mineral lattice. For each of the three elements Table 7 shows the ratio of oxidized to reduced atoms to increase after oxidation due to dissolved oxygen at pH = 11.5. While the ratio of iron to sulphur increases significantly after treatment, the ratio of iron to arsenic increases only a small amount.

These results indicate that at the same time as the surface layer of ferric hydroxide is formed, much of the sulphur goes into solution presumably as sulphate, while the arsenic remains at the surface in a oxidized state. It is proposed that this arsenic is adsorbed on the ferric hydroxide since it is known that arsenic can be removed from solution in this way (78). The existence of such a surface oxidation product is also consistent with the existence of such secondary arsenic minerals as pitticite ($Fe_2(AsO_4)(SO_4)OH \bullet 2H_2O$) and pharmacosiderite ($6FeAsO_4 \bullet 2Fe(OH)_3 \cdot 12H_2O$).

The results of this spectroscopic study confirm the conclusions drawn from electrochemical experiments. At high pH values, arsenopyrite decomposes to form iron hydroxide surface deposits. Arsenic in the form of arsenate and some sulphur in the form of sulphate are incorporated in this hydroxide layer. Such hydroxide layers can be expected to result in the depression of arsenopyrite during flotation with xanthate.

Chapter 6

FLOTATION STUDIES

Flotation studies were carried out with real ore samples to verify the interpretations made of electrochemical experiments as they relate to the flotation response of arsenopyrite.

Three types of experiments were carried out. In the first type, conditions were controlled to observe the flotation operation.

In the second type, a rougher arsenopyrite concentrate was prepared and its subsequent depression through the use of oxidizing agents was studied.

In the third type, bulk pyrite - arsenopyrite concentrates were prepared. The extent to which arsenopyrite could be selectively depressed from this concentrate through the use of oxidizing agents was explored.

6.0.1 Rougher Flotation

6.0.1.1 Experimental.

Rougher flotation tests were carried out on selected high grade samples from the property of G.M. Resources Ltd. at Hedley, B.C. The sample contained 51.2 percent by weight arsenopyrite in a siliceous gangue. A microscopic examination of the material indicated only minor pyrite to be present. The

arsenopyrite was assayed to contain 270 to 340 grams per tonne Au in the form shown in Figure 2. Minor concentration of other metals are also indicated in Figure 2 as determined by SEM - EDX analysis.

For each test, 1000 grams of ore was ground in a laboratory rod mill to approximately 92% minus 200 mesh. Vancouver tapwater having a pH of 5.5 was used for all tests.

For tests carried out at varying pH the temperature was 24±1°C. The pH was observed to increase from the water value of pH=5.5 to a natural value of pH=8.0 during grinding. Such an increase in pH results from the presence of slightly alkaline rock forming constituents in the ore. The pH was adjusted from the natural value of 8.0 to the desired value using sodium hydroxide or sulphuric acid. Following pH adjustments the slurry was conditioned for 15 minutes with an air flow of 2.4 litres per minute in an Agitair flotation cell at 1000 RPM.

Following this conditioning period with air, an addition of 250 grams per tonne of isopropyl xanthate was made and allowed to condition for 2 minutes.

Rougher flotation was carried out for 15 minutes with an addition of 20 grams per tonne of Dowfroth 250 frother.

Tests carried out at varying temperature were at the natural pH of 8.0. Some tests were also carried out with the pH adjusted to 9.0 using sodium hydroxide. Temperature tests were carried out in a jacketed stainless steel cell with the temperature controlled by means of a Colora Type - K thermostat.

Once the temperature had been stabilized the cell air was turned on and conditioning was carried out as for the tests at

varying pH.

6.0.2 Results and Discussion

The results of tests carried out at varying pH are shown in Figure 48. The recovery of arsenopyrite is 90% or greater until approximately pH=7.5 at which point it starts to decrease steadly until approximately pH=10.5. Above pH=10.5 the recovery continues to decrease but at a lower rate than below this pH.

Results are also shown for two tests carried out in the absence of oxidation. The results of these tests, particularly at pH = 10 indicate that the decrease in recovery observed with increasing pH is not the result of pH alone. The oxidation resulting from aeration during conditioning is necessary to bring about arsenopyrite depression.

The flotation test results agree with the results obtained with voltammetry. The voltammograms shown in Figures 14 and 15 indicate the anodic peak associated with arsenopyrite oxidation to ferric hydroxide to appear in the vicinity of approximately pH = 7. The oxidation peak heights increase with increasing pH. In the present flotation tests the result of the increasing amount of ferric hydroxide associated with these increasing peak heights is observed to lead to decreasing floatability of the mineral. For maximum recovery of arsenopyrite a pH of less than 7.0 should be used while for maximum depression a pH approaching 12.0 would be appropriate. The pH used for depression in most cases would be dictated by the pH dependance of the floatability of other minerals being recovered.

The result of tests carried out at increasing temperature

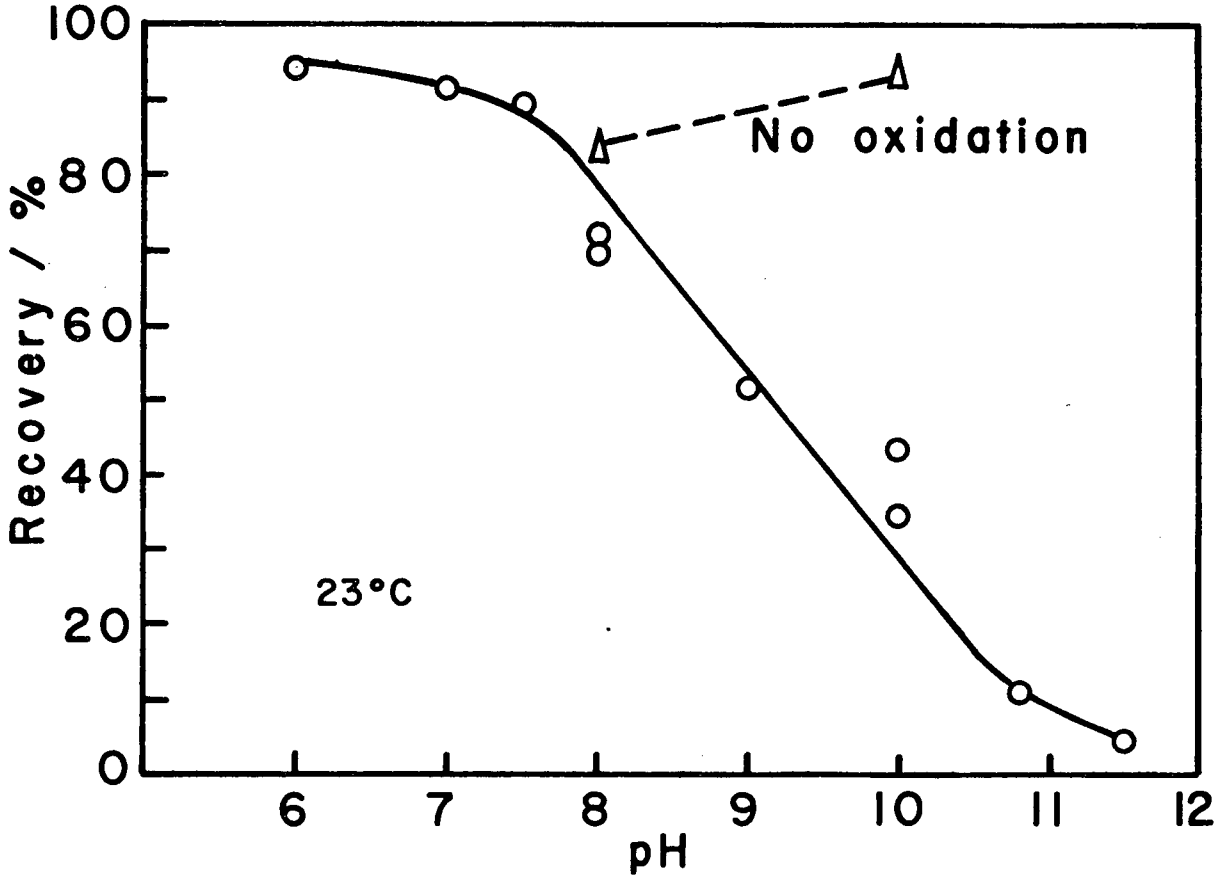

Figure 48

Floatability of arsenopyrite at increasing pH in the presence and absence of oxidation

are shown in Figure 49. The recovery increases somewhat over the temperature range from 7°C to 40°C. Above 40°C the recovery decreases with increasing temperature. The recovery at 60°C in the absence of oxidation was higher than at the lower temperatures with oxidation. If arsenopyrite depression was desired there would be no benefit derived from heating the slurry since plant temperatures can normally be expected to be in the range of 10°C to 20°C.

The results achieved at pH = 9.0 show similar behaviour to those achieved at pH = 8.0 with increasing temperature. In each case the concentrate grade was insensitive to temperature.

6.0.3 Depression of Previously Activated Arsenopyrite

6.0.3.1 Experimental

Tests were carried out using ore samples described in the previous section. Two series of tests were carried out, one using hydrogen peroxide as the oxidant and the other using sodium hypochlorite.

In each case a two kilogram sample was ground in a laboratory rod mill to 74 percent passing 200 mesh. A cleaned arsenopyrite concentrate was prepared according to the flotation conditions shown in Table 8. The rougher flotation was carried out at the natural pH of 8.0. The cleaned concentrate was filtered and split into portions of 120 grams for the individual tests. These tests were carried out in a 500 gram Agitair cell at 800 RPM, a temperature of 20° and pH = 8.0.

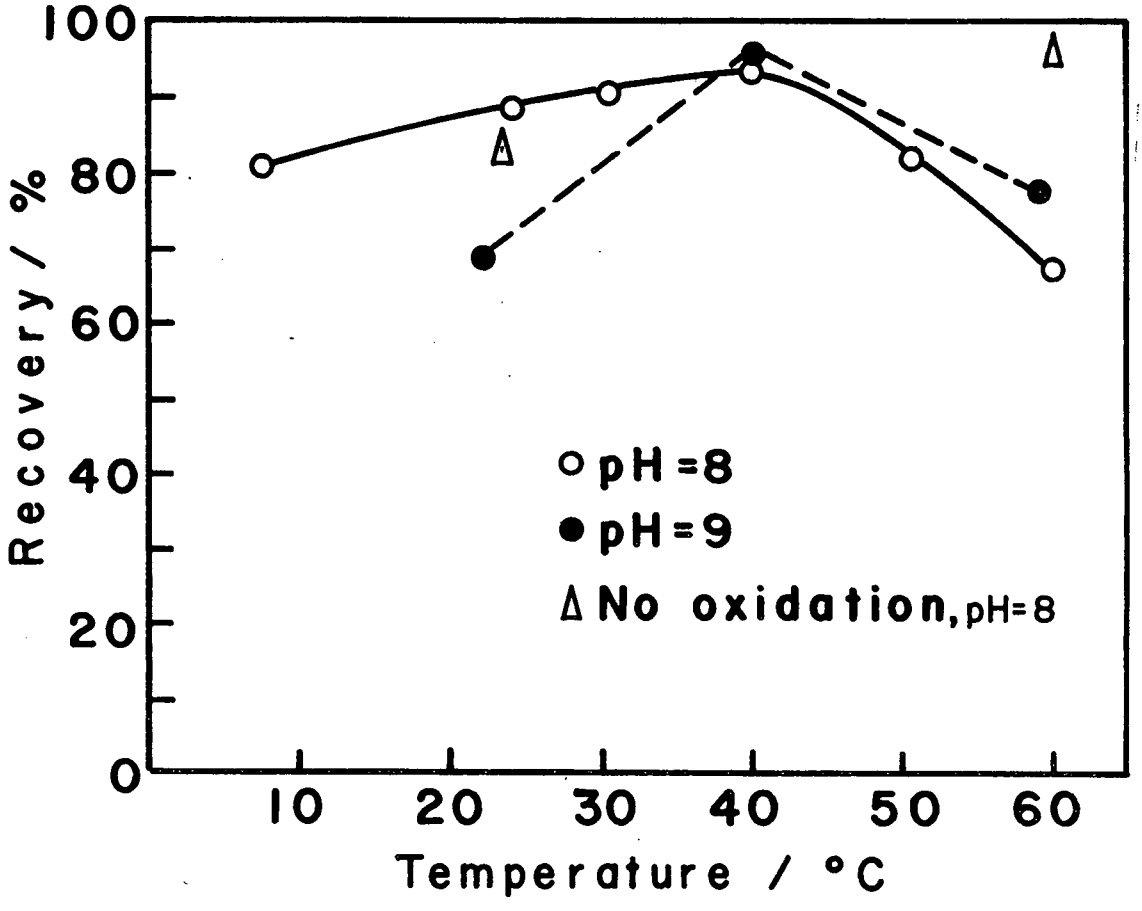

Figure 49

Influence of temperature on arsenopyrite floatability

Table 8
Flotation Conditions

Stage	Isopropyl Xanthate g/tonne	Amyl/ Xanthate g/tonne	Dowfroth 250 g/tonne	Time minutes
Conditioning	150	50	5	2
Rougher	37.5	10	17.5	15
1st. Cleaner	20	10	2.5	10
2nd. Cleaner	10	-	2.5	8

Oxidation was carried out at pH = 8.0 for the time shown in the results. Flotation was allowed to proceed for 5 minutes.

A freshly polished arsenopyrite electrode was immersed into the flotation cell for each test and the electrode potential was monitored relative to a calomel electrode.

The arsenopyrite recovery shown for each test is that which was achieved with no addition of xanthate following oxidation.

6.0.3.2 Results and Discussion

The results of flotation tests using hydrogen peroxide as an oxidant are shown in Table 9. The addition of 357 mg/litre of hydrogen peroxide resulted in a significant decrease in arsenopyrite floatability. Increasing the conditioning time from 5 to 15 minutes gave a further decrease in floatability.

Comparison of the potentials achieved by the arsenopyrite electrode in these tests with the voltammogram at pH = 8.2 in Figure 14 reveals that the potentials lie partway up the arsenopyrite oxidation peak.

For the test shown in Table 9, an addition of up to 900 grams per tonne of ethyl xanthate gave no further increase in recovery with 357 mg/litre H_2O_2 and an increase of 3.1% with 214

mg/litre H_2O_2.

Table 9
Flotation results using hydrogen peroxide as an oxidant

Test No.	Conditions	Arsenopyrite Eh,mV	As Recovery %
1	No oxidation	213 to 233	97.1
2	357 mg/litre H_2O_2 cond. 5 min.	363	11.6
3	357 mg/litre H_2O_2 cond. 15 min.	368	3.3
4	214 mg/litre H_2O_2 cond. 15 min.	323 to 353	6.0

The results using sodium hypochlorite as an oxidant are shown in Table 10. The recovery in the absence of oxidation is lower in this test series than in the series shown in Table 9. While the concentrate was produced from the same ore in each case, slight variations in the rougher flotation procedure caused the variation in floatability. As for the peroxide, a significant decrease in arsenopyrite floatability was achieved through the use of hypochlorite. The addition of hypochlorite required for depression to be achieved is much lower than the required peroxide addition. The reason for this lower hypochlorite requirement is not apparent from the electrochemical investigations which have been carried out. It is believed that the two reagents resulted in different degrees of oxidation not reflected by the potentials. The potential of the arsenopyrite electrode with hypochlorite jumped to approximately +343 mV and then decreased during the conditioning period. While at 389 mg/litre NaClO the addition of a large addition of xanthate failed to result in arsenopyrite flotation,

Table 10
Flotation results using sodium hypochlorite as an oxidant

Test No.	Conditions	Arsenopyrite Eh,mV	As Recovery %
1	No oxidation	203 to 223	83.1
2	389 mg/litre NaClO cond. 5 min.	343 to 283	0.0
3	77.6 mg/litre NaClO cond. 5 min.	343 to 283	0.0
4	19.4 mg/litre NaClO cond. 5 min.	343 to 193	28.7
5	19.4 mg/litre NaClO cond. 15 min.	343 to 203	22.5

at the lower NaClO additions xanthate additions resulted in 20 percent to 30 percent additional arsenopyrite recovery.

6.0.4 Selective Flotation of Pyrite From Arsenopyrite

Selective flotation tests were carried out on bulk pyrite - arsenopyrite concentrates from Giant Yellowknife Mines and from Equity Silver Mines Limited.

6.0.4.1 Experimental and Results.

(i) Equity Concentrate

Tests were carried out on a bulk concentrate supplied by Equity Mines. The concentrate had been produced at the site by flotation of the silver circuit (tetrahedrite and chalcopyrite) tailing. The concentrate contained approximately five times as much pyrite as arsenopyrite. Some oxidation was observed on the concentrate and it was therefore reground, filtered and refloated with 85 grams per tonne isopropyl xanthate. This

refloated concentrate was then filtered and split into portions for the individual tests.

The tests were carried out in an Agitair flotation cell using 150 grams concentrate in a 500 gram (1.4 litre) cell. The repulped concentrate was found to have a pH of 5.7 and this was adjusted to pH = 9.2 using NaOH. After the pH was adjusted the oxidizing agent was added and conditioned. Flotation was carried out for 3 minutes with an addition of 5 grams per tonne Downfroth 250. The oxidant used was H_2O_2. All tests were at 20°C. The test results are shown in Table 11.

Table 11
Flotation Test Results with Equity Concentrate

H_2O_2 mg/litre	Conditioning Time minutes	Arsenopyrite Recovery %	Pyrite Recovery %
0	-	92.3	92.4
357	5	17.5	61.4
178	5	18.5	55.2
178	0	35.1	63.2
71	5	23.6	53.2
71	15	26.3	49.2

(ii) Giant Yellowknife Concentrate

Several series of tests were carried out on a bulk concentrate produced at the minesite. This concentrate had been produced with additions of copper sulphate as well as xanthate. Microscopy of this material revealed numerous middlings and it was therefore reground to 94% minus 200 mesh prior to being used. The reground concentrate was refloated with an addition of 25 grams per tonne isopropyl xanthate and cleaned twice more with no further additions. The cleaned concentrate was filtered

and split into 90 gram portions for individual tests.

The pH for each test was adjusted using H_2SO_4 or NaOH as required. The conditioning period for each test was 15 minutes and the temperature was 20°C.

The results of tests using both air and hypochlorite as the oxidant are shown in Figure 50. While with air the arsenopyrite recovery is somewhat lower than for pyrite, with hypochlorite the two minerals show essentially the same behaviour. The result of these tests when compared with those shown in Table 11 as well as with those for the arsenopyrite tested individually make it apparent that each ore occurrence can be expected to show some variation in response to depression by oxidation. Such factors as the ratio of pyrite to arsenopyrite and the previous flotation history of the samples can be expected to influence the results.

Additional tests were carried out on a bulk concentrate prepared in the laboratory from Giant Yellowknife ore.

The concentrate was prepared by grinding 2 kilograms of ore in a laboratory rod mill to 80% passing 200 mesh. Flotation was carried out with 65 grams per tonne isopropyl xanthate 25 grams per tonne amyl xanthate and 10 grams per tonne Dowfroth 250 at pH = 6.0. The concentrate was cleaned twice without further additions and was then filtered and split into three portions for testing.

Two test series were carried out, one with constant potassium permanganate addition and the second with increasing permanganate addition and constant xanthate addition. In each case a five minute conditioning period was used following the

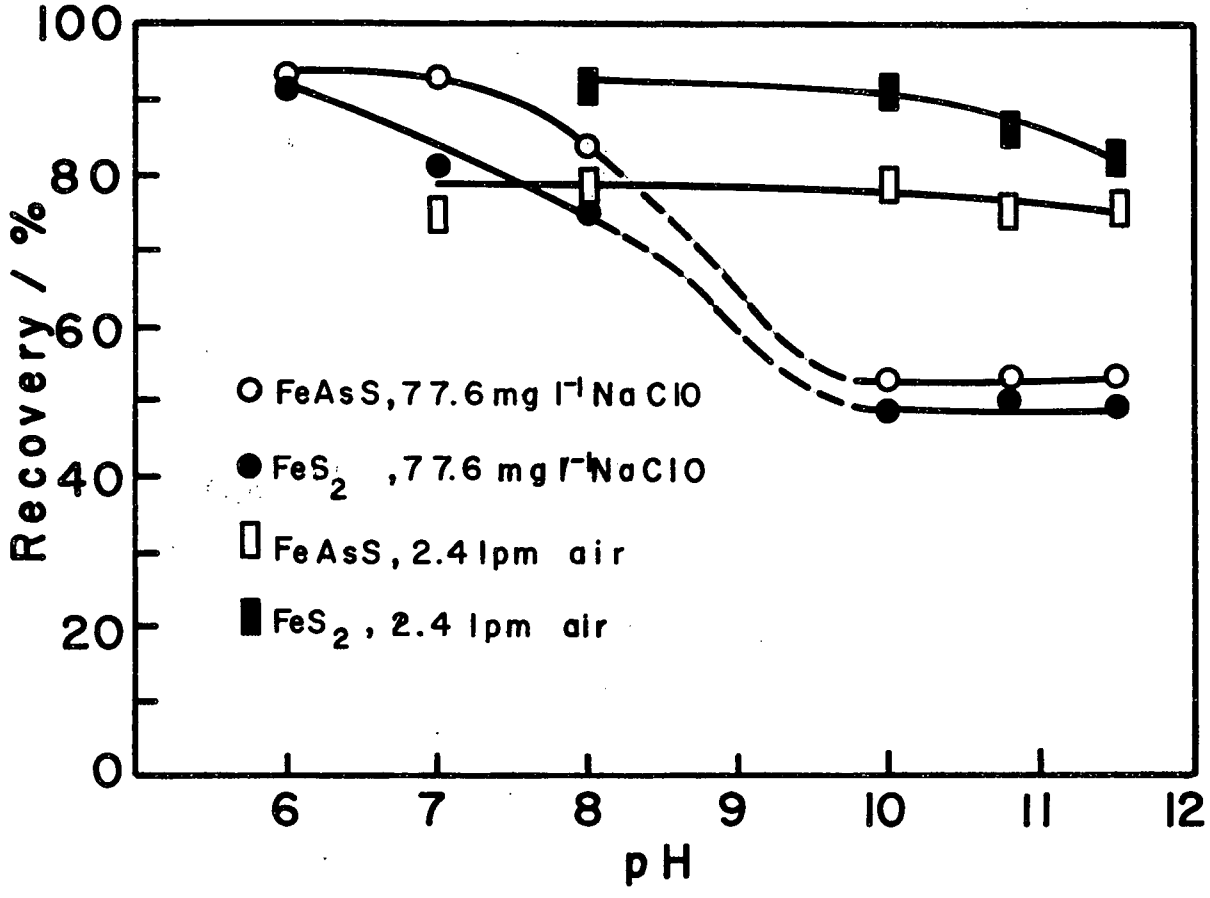

Figure 50

Influence of oxidation on pyrite and arsenopyrite floatability at increasing pH

permanganate addition. At the end of this period neither pyrite nor arsenopyrite were found to float. The xanthate and 12 mg. per litre Dowfroth 250 were added and flotation was then carried out. The addition of frother alone failed to result in any flotation.

6.0.4.2 Discussion

The result of tests on the Equity concentrate, using hydrogen peroxide show greater depression of arsenopyrite than pyrite. Maximum depression of arsenopyrite is achieved with a high peroxide addition (357 mg./litre). Much lower peroxide additions can be used but with increasing arsenopyrite floatability resulting. Pyrite appears to be less floatable in the presence of low peroxide additions than with high peroxide additions. Increasing conditioning time does not improve the separation of pyrite from arsenopyrite.

The results of tests with Giant Yellowknife concentrate show both pyrite and arsenopyrite to be equally depressed by hypochlorite while air oxidation results in preferential depression of arsenopyrite.

While the addition of potassium permanganate, depressed both pyrite and arsenopyrite, a subsequent addition of xanthate resulted in preferential pyrite flotation.

The complete depression of both minerals followed by preferrential activation of the pyrite with xanthate has not been attempted with oxidants other than permanganate.

The selective flotation of pyrite from a bulk pyrite-arsenopyrite concentrate appears to be feasible although

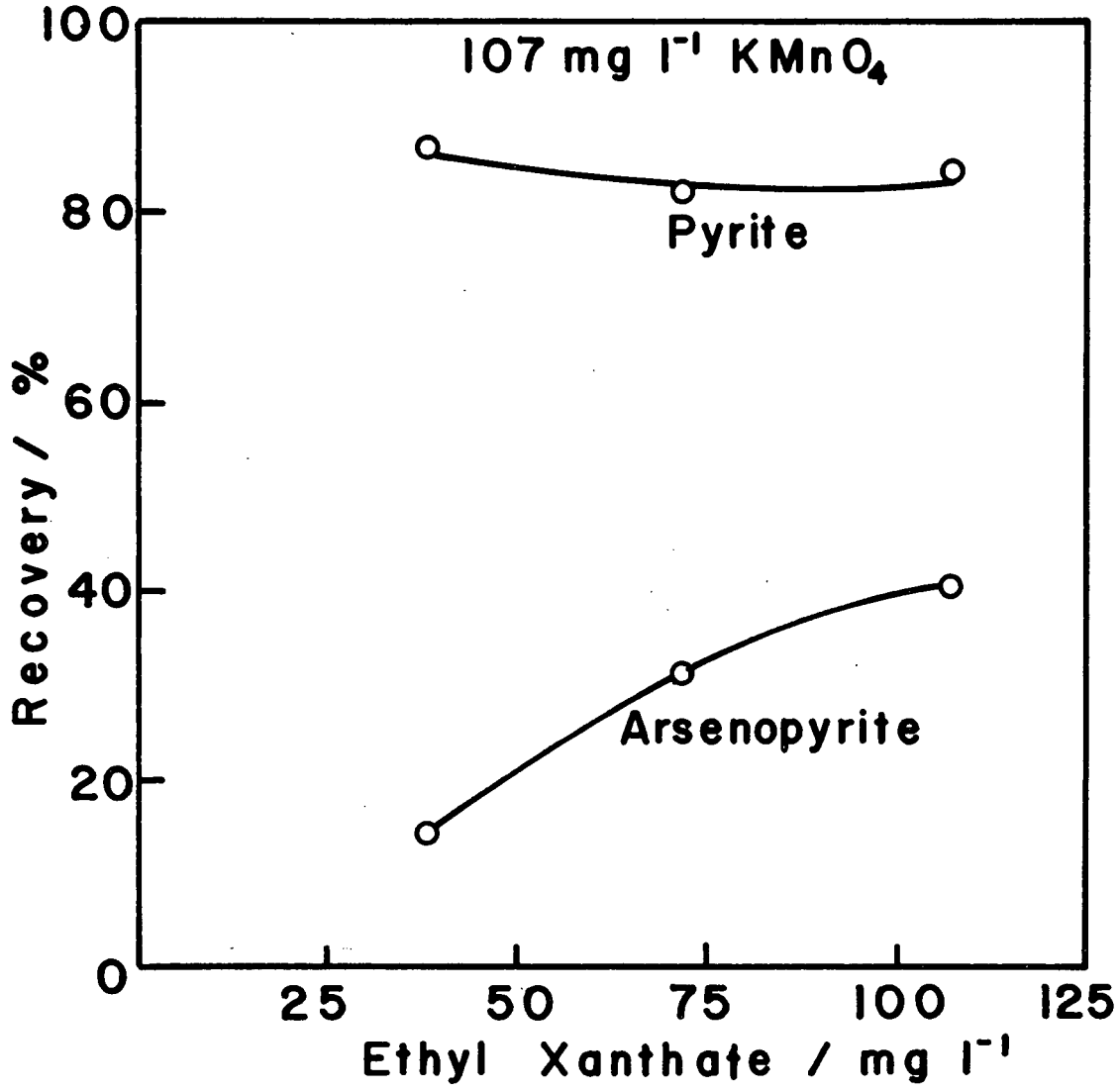

Figure 51

Depression of arsenopyrite from bulk concentrate with increasing xanthate addition

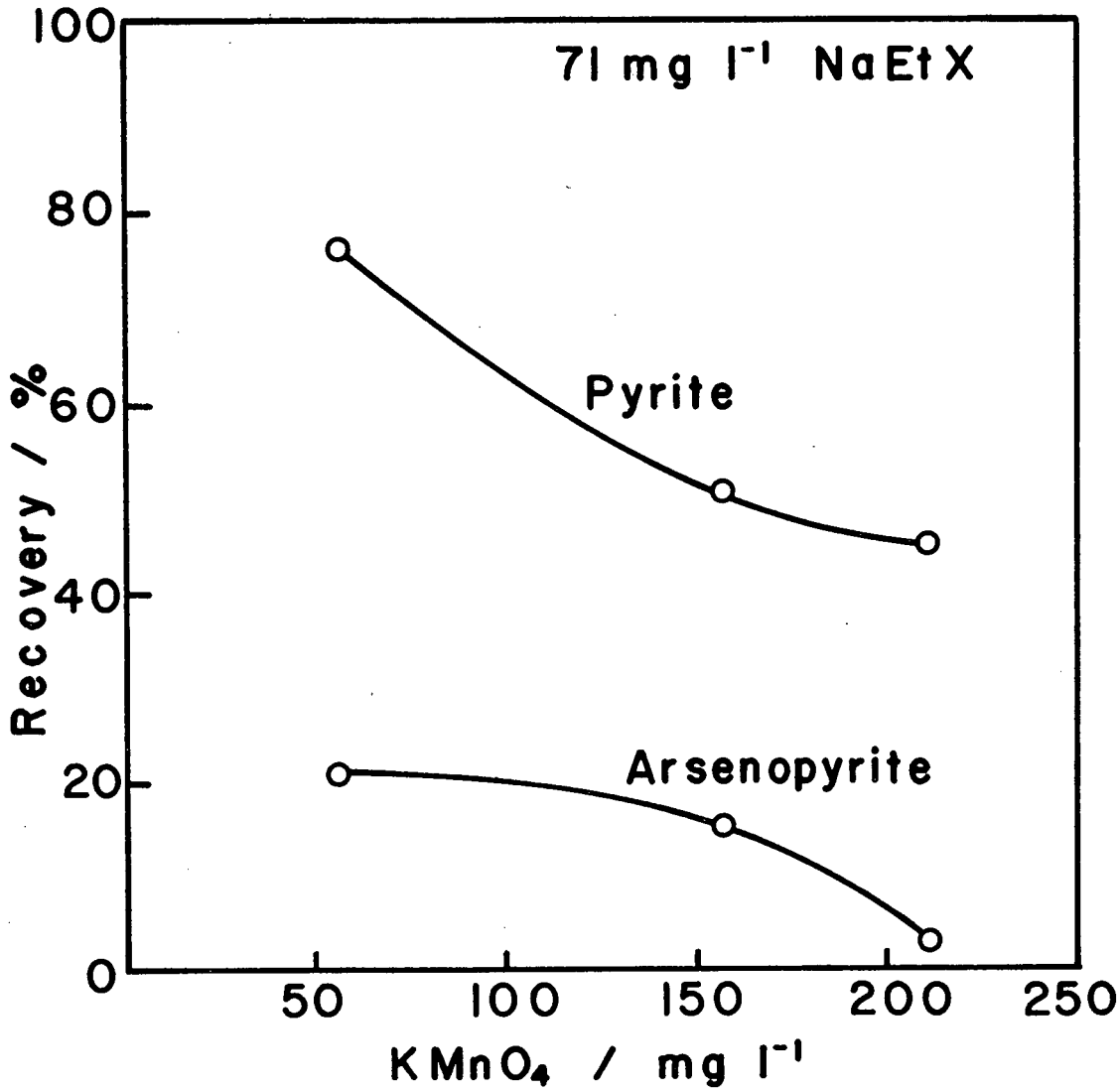

Figure 52

Depression of arsenopyrite from bulk concentrate with increasing permanganate addition

considerable effort would be required to optimize the conditions for separation. These optimum conditions can be expected to vary depending on the pyrite to arsenopyrite ratio and on the history of the concentrate.

The results of the various tests in which previously floated arsenopyrite has been depressed though the use of oxidizing agents reveal that a greater influence on floatability is exerted by the ferric hydroxide surface deposits than by the adsorbed collector layer.

Chapter 7

CONCLUSIONS

1. Cyclic voltammetric studies have revealed the oxidation of arsenopyrite across the pH range from 7 - 12 to result in the formation of ferric hydroxide surface deposits with the concurrent oxidation of arsenic to the arsenate state and sulphur to the sulphate state. Across the pH range studied, the hydroxide film thickness increases with increasing pH.

At temperatures below 30°C, increasing temperature results in increasing hydroxide film thickness. Across the temperature range from 30°C to 45°C, film development appears to be independent of temperature. At temperatures greater than 45°C, film thickness increases rapidly with increasing temperature.

Below pH = 7, ferric hydroxide deposits are not formed but the formation of elemental sulphur at the electrode surface is indicated.

2. ESCA studies have revealed that most of the arsenate and some of the sulphate is incorporated in the ferric hydroxide deposits.

3. Electrode potential measurements in the presence of several oxidizing agents indicate that the potentials required for ferric hydroxide formation (as indicated by cyclic voltammetry) will be achieved with these agents.

4. The presence of ferric hydroxide deposits on the surface of arsenopyrite inhibits the oxidation of xanthate to dixanthogen. Dixanthogen is believed to be the active collector species on

arsenopyrite.

5. Flotation studies show arsenopyrite to be increasingly depressed with increasing pH when the ore slurry has been conditioned in the presence of aeration prior to xanthate addition. This influence of pH holds true over the pH range from 7 to 12. At pH less than 7, arsenopyrite shows high floatability due to the absence of hydroxide films and the presence of elemental sulphur.

Temperatures greater than 40°C result in increased depression of arsenopyrite.

The influence of both pH and temperature on the floatability of arsenopyrite correlate well with the interpretations of electrochemical experiments. It is concluded that the floatability of arsenopyrite is controlled by the formation of ferric hydroxide surface deposits.

The depression of arsenopyrite which has previously been floated with xanthate and the selective depression of arsenopyrite from bulk concentrates through the use of oxidizing agents has been demonstrated. It is therefore concluded that the floatability of the mineral is influenced to a greater degree by the ferric hydroxide deposits formed by oxidation of the mineral than by adsorbed collector layers.

6. Voltammetric studies in the presence of cyanide indicate that cyanide does not contribute to the development of depressant films on arsenopyrite and may in fact result in some degree of activation.

7. Electrochemical studies of other minerals in the Fe-As-S system reveal significant differences in the nature of surface

hydroxide deposits which correlate well with observed differences in mineral solubility and may explain variations in their floatabilty with xanthate.

Chapter 8

RECOMMENDATIONS FOR FUTURE WORK

Additional work to be carried out on the flotation of arsenopyrite can be divided into fundamental and applied categories.

Fundamental research should be directed at further study of the growth and morphology of hydroxide films on arsenopyrite. The influence of various depressants and activating agents on the structure of the hydroxide layers should also be investigated. While additional electrochemical studies could contribute much to the understanding of these surface deposits, the use of spectroscopic techniques will be required to give a complete appreciation of their nature.

Applied research should be directed at optimizing the utilization of surface oxidation for the depression of arsenopyrite from other minerals, particularly pyrite. While to some extent the optimum conditions can be expected to be specific for each mineral occurrence, a significant common base is anticipated. The influence of other dissolved species such as calcium ion or soluble silicates on arsenopyrite depression should also be evaluated.

Appendix I

Potential/pH diagrams for the Iron - Arsenic - Sulphur - Water System

---

Potential/pH diagrams have been prepared for the iron - arsenic - sulphur - water system at 25°C. The assumptions made for each diagram are as follows:

Figure 53. Arsenopyrite stability diagram assuming iron, arsenic and sulphur activities of 10^{-6} M. As_2S_2 and As_2S_3 are shown as stable species. Soluble arsenic species are not shown.

Figure 54. Arsenopyrite stability diagram assuming iron, arsenic and sulphur activities of 10^{-3} M. As_2S_2 and As_2S_3 are shown as stable species.

Figure 55. Arsenopyrite stability diagram assuming iron, arsenic and sulphur activities of 1 M. As_2S_2 and As_2S_3 are shown as stable species. Soluble arsenic species are not shown.

Figure 56. Loellingite stability diagram assuming iron and arsenic activities of 10^{-3} M.

Figure 57. Arsenopyrite stability diagram considering FeS_2, FeS and $FeAs_2$ as possible stable species. Stability domains of As_2S_2 are indicated. Soluble arsenic and sulphur species are not shown. Activity of each dissolved species = 10^{-6} M.

Ferric arsenate is not shown in Figures 53 through 57. At low iron and arsenic activity it has only a narrow stability region near the ferric ion - ferric hydroxide boundary. The stability region for ferric arsenate at 1 molar activity of iron and arsenic is shown in Figure 58.

Table 12
Thermodynamic Data at 25°C

Species	State	G°f Kcol/mole	298°K
HS^-	aq	2.88	80
S^{2-}	aq	20.5	80
HSO_4^-	aq	-180.69	80
SO_4^{2-}	aq	-177.97	80
H_2S	aq	-6.66	80
S	s	0	80
H_3AsO_4	aq	-184.0	82
$H_2AsO_4^-$	aq	-181.0	82
$HAsO_4^{2-}$	aq	-171.5	82
AsO_4^{3-}	aq	-155.8	82
H_3AsO_3	aq	-154.4	82
$H_2AsO_3^-$	aq	-141.8	82
$HAsO_3^{2-}$	aq	-125.3	82
AsH_3	aq	23.8	82
AS	s	0	82
As_2S_2	s	-17.0	81
As_2S_3	s	-23.0	81
FeAsS	s	-26.2	81
$FeAs_2$	s	-12.5	81
$FeAsO_4$	s	-185.18	83
Fe^{3+}	aq	-1.1	80
Fe^{2+}	aq	-18.85	80
$HFeO_2^-$	aq	-90.6	80
FeS	s	-24	80
FeS_2	s	-38.3	80
$Fe(OH)_2$	s	-116.3	80
$Fe(OH)_3$	s	-116.5	80

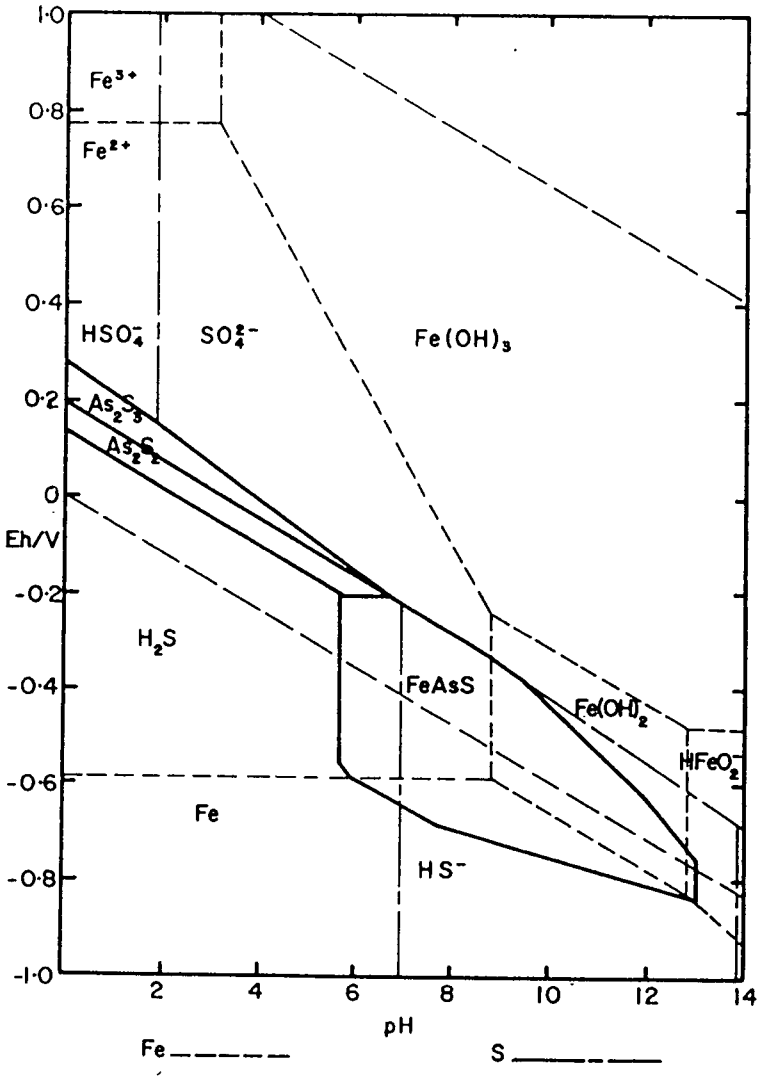

Figure 53

Arsenopyrite stability diagram at 10^{-6} M activity of dissolved species

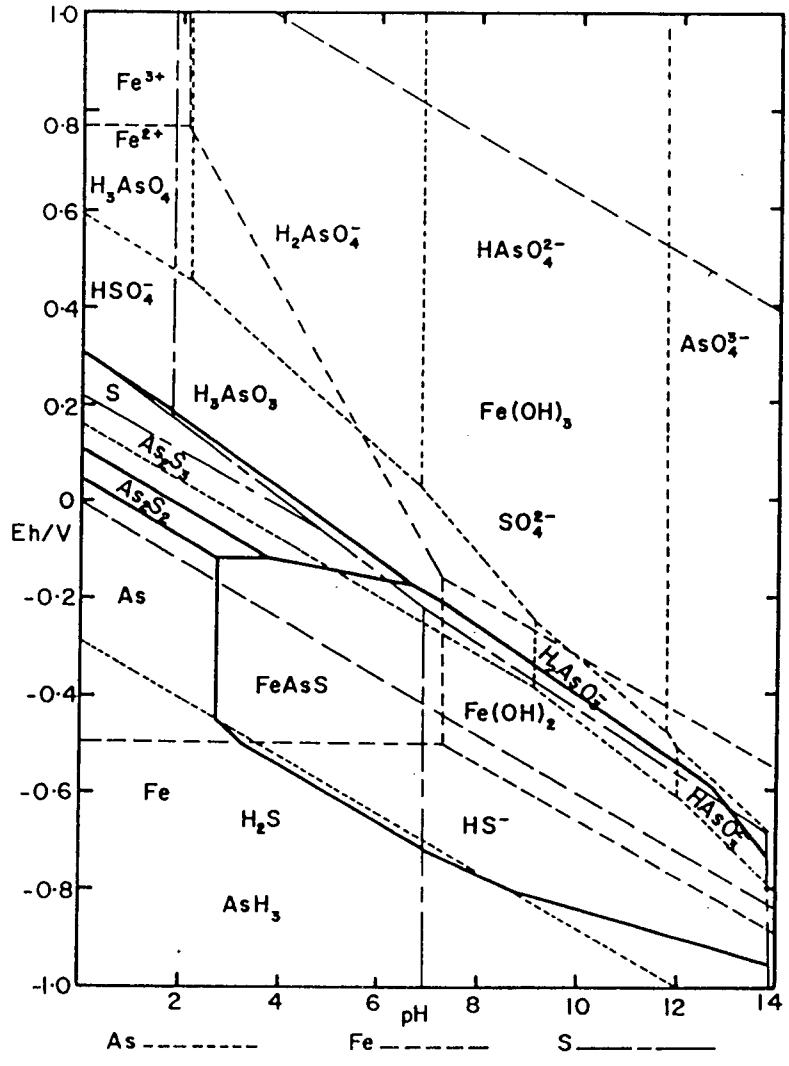

Figure 54

Arsenopyrite stability diagram at 10^{-3} M activity of dissolved species

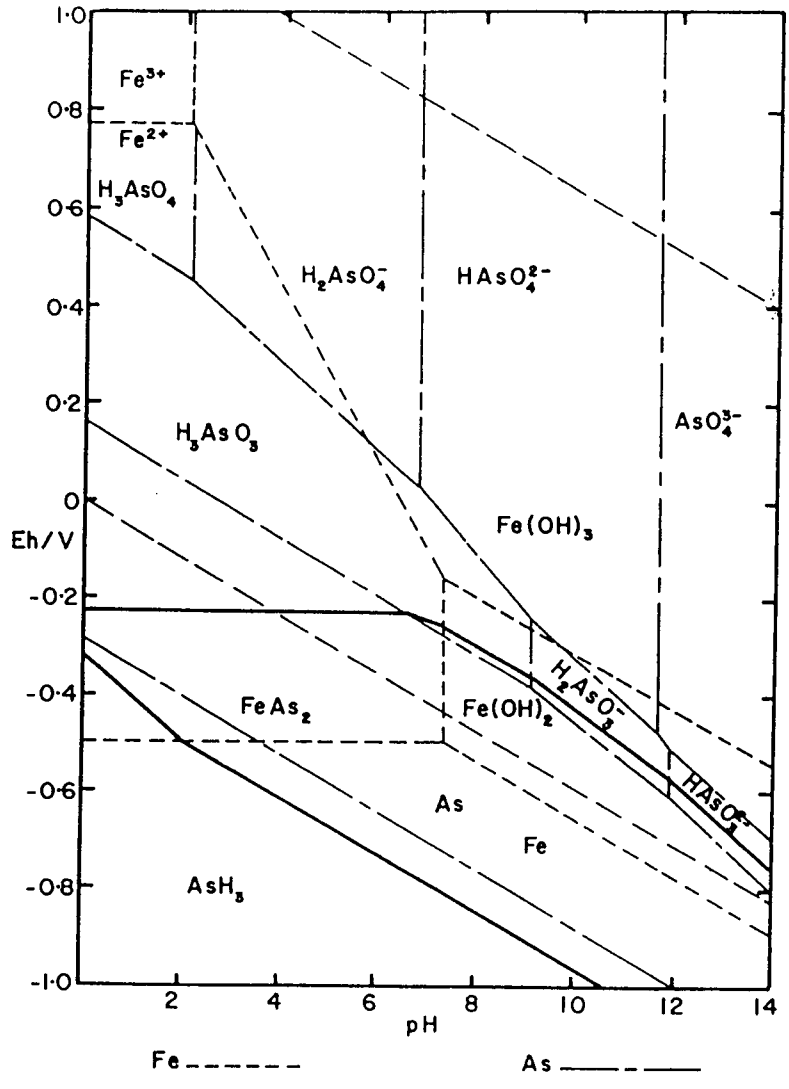

Figure 55

Loellingite stability diagram at 10^{-3} M activity of dissolved species

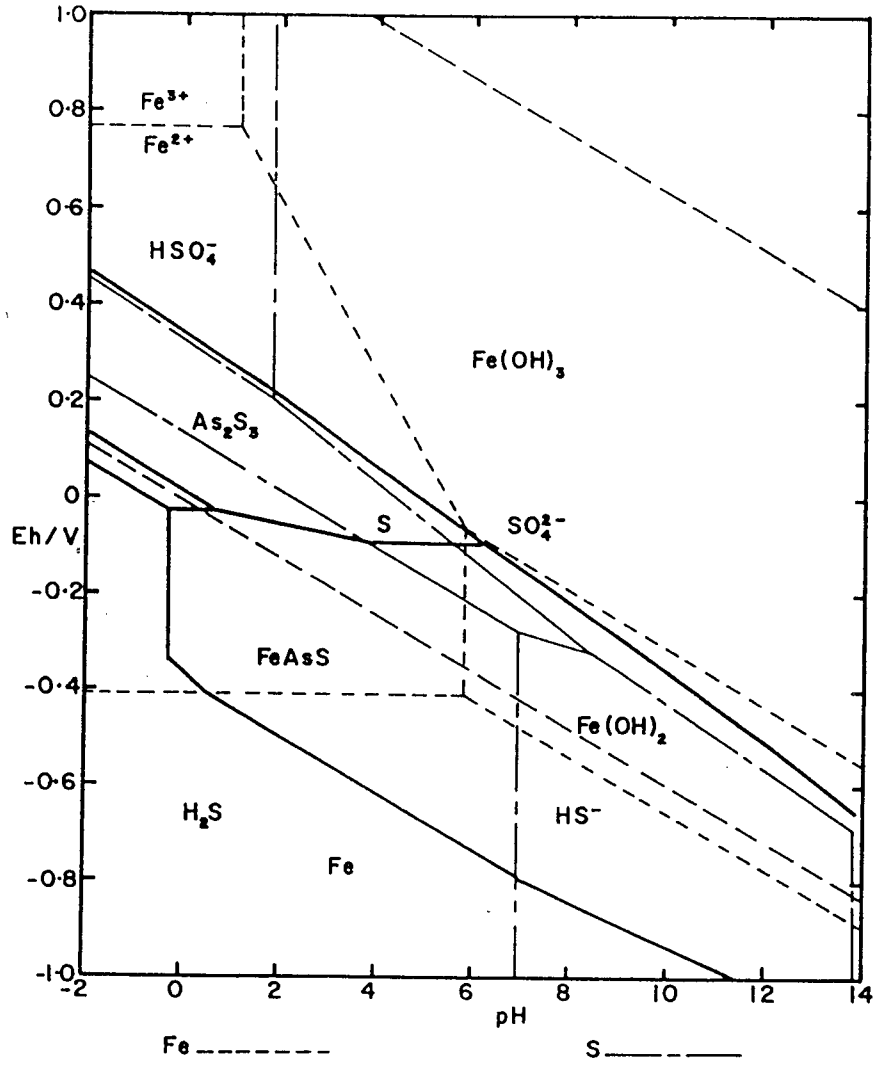

Figure 56

Arsenopyrite stability diagram at 1 M activity of dissolved species

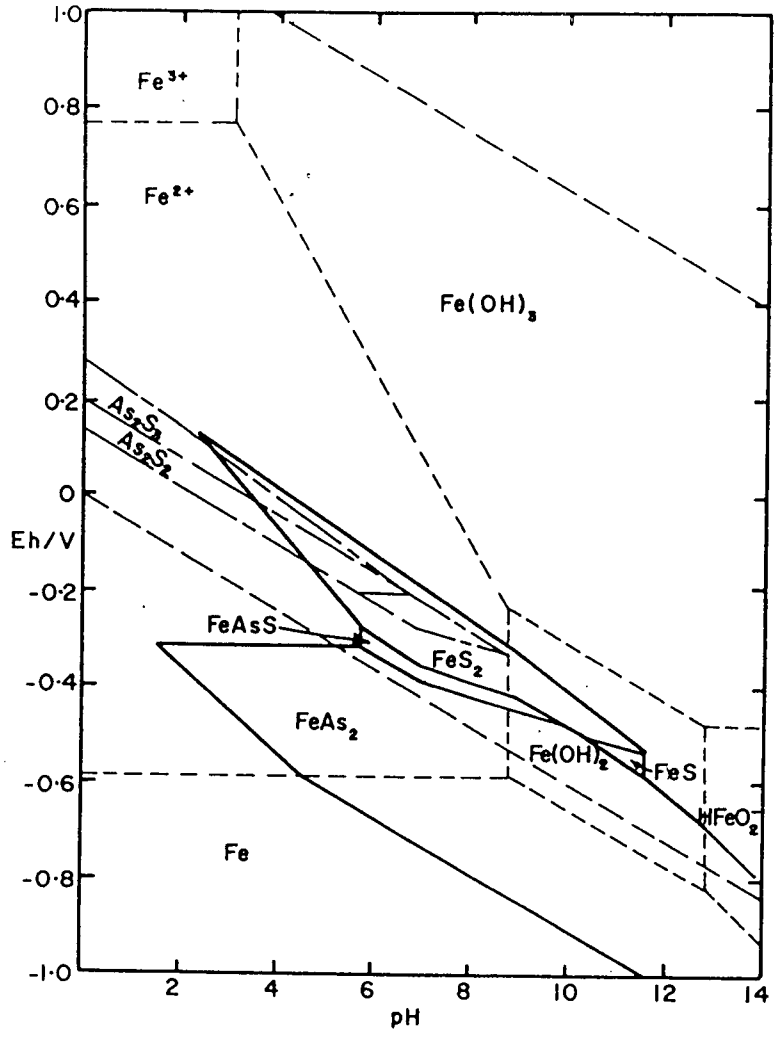

Figure 57

Arsenopyrite stability diagram considering FeS, FeS_2 and $FeAs_2$ as stable products

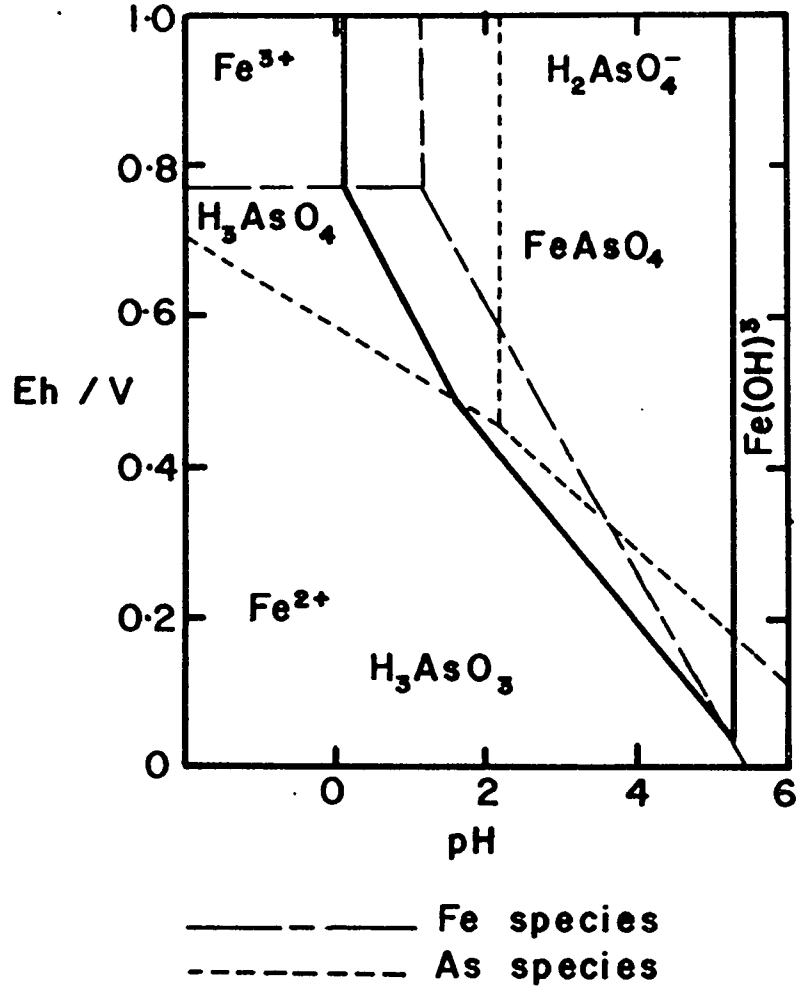

Figure 58

Stability region of ferric arsenate at 1 M activity

Appendix II

Equations Used For The Construction Of The Diagrams

---

1. $FeAsS + 2H^+ = Fe^{++} + H_2S + As.$

   $-0.030 = 0.0591 \log(Fe^{++})(H_2S) + 0.118\ pH$

2. $Fe^{2+} + H_3AsO_3 + H_2S + H^+ + 3e^- = FeAsS + 3H_2O$

   $E = 0.236 - 0.0197 \log(Fe^{2+})(H_3AsO_3)(H_2S) - 0.0197\ pH$

3. $Fe(OH)_2 + H_3AsO_3 + SO_4^{--} + 13H^+ + 11e^- = FeAsS + 9H_2O$

   $E = 0.396 + 0.005 \log(H_2AsO_3)(SO_4^{--}) - 0.070\ pH$

4. $Fe(OH)_2 + H_2AsO_3^- + SO_4^{--} + 14H^+ + 11e^- = FeAsS + 9H_2O$

   $E = 0.396 + 0.005 \log(H_2AsO_3^-)(SO_4^{--}) - 0.075\ pH$

5. $Fe(OH)_2 + HAsO_3^{2-} + SO_4^{--} + 15H^+ + 11e^- = FeAsS + 9H_2O$

   $E = 0.461 + 0.005 \log(HAsO_3^{2-})(SO_4^{--}) - 0.080\ pH$

6. $Fe(OH)_2 + HAsO_3^{2-} + HS^- + 6H^+ + 3e^- = FeAsS + 5H_2O$

   $E = 1.025 + 0.0197 \log(HAsO_3^{2-})(HS^-) - 0.118\ pH$

7. $FeAsS + 5H^+ + 3e^- = AsH_3 + Fe^{++} + H_2S$

   $E = -0.354 - 0.0197 \log(AsH_3)(Fe^{++})(H_2S) - 0.0985\ pH$

8. $FeAsS + 5H^+ + 5e^- = AsH_3 + H_2S + Fe$

   $E = -0.376 - 0.0118 \log(AsH_3)(H_2S) - 0.0591\ pH$

9. $FeAsS + 4H^+ + 5e^- = AsH_3 + HS^- + Fe$

$E = - 0.459 - 0.0118 \log(AsH_3)(HS^-) - 0.0473\ pH$

10. $FeAsS + H^+ + 2e^- = AsH_3 + HS^- + Fe$

$E = - 0.631 - 0.0295 \log(HS^-) - 0.0295\ pH$

11. $2\ H_3AsO_3 + 3HSO_4^- + 27H^+ + 24e^- = As_2S_3 + 18H_2O$

$E = 0.348 + 0.0025 \log(H_3AsO_3)^2(HSO_4^-)^3 - 0.066\ pH$

12. $2H_3AsO_3 + SO_4^{--} + 30H^+ + 24e^- = As_2S_3 + 18H_2O$

$E = 0.363 + 0.0025 \log(H_3AsO_3)^2(SO_4^{--})^3 - 0.074\ pH$

13. $As_2S_2 + 4H^+ + 4e^- = 2As + 2H_2S$

$E = - 0.040 - 0.0148 \log (H_2S)^2 - 0.0591\ pH$

14. $As_2S_2 + 2H^+ + 4e^- = 2As + 2HS^-$

$E = -0.0247 - 0.0148 \log(HS^-)^2 - 0.0295\ pH$

15. $2H_3AsO_3 + 2SO_4^{--} + 22H^+ + 18e^- = As_2S_2 + 14H_2O$

$E = 0.352 + 0.0033 \log(H_3AsO_3)^2(SO_4^{--})^2 - 0.0722\ pH$

16. $2H_2AsO_3^- + 2SO_4^{--} + 24H^+ + 18e^- = As_2S_2 + 14\ H_2O$

$E = 0.412 + 0.0033 \log(H_2AsO_3^-)^2(SO_4^{--})^2 - 0.0788\ pH$

17. $H_2AsO_3^- + 2HS^- + 6H^+ + 2e^- = As_2S_2 + 6H_2O$

$E = 1.719 + 0.0295 \log(H_2AsO_3)^2(HS^-)^2 - 0.1773\ pH$

18. $As_2S_3 + 2H^+ + 2e^- = As_2S_2 + H_2S$

$$E = 0.0143 - 0.0148 \log(H_2S)^2 - 0.0591\ pH$$

19. $As_2S_3 + H^+ + 2e^- = As_2S_2 + HS^-$

$$E = -0.193 - 0.0295 \log(HS^-) - 0.0295\ pH$$

20. $As_2S_2 + SO_4^{--} + 3H^+ + 6e^- = As_2S_3 + 4H_2O$

$$E = 0.395 + 0.0098 \log(SO_4^{--}) - 0.0788\ pH$$

21. $1/2\ As_2S_3 + Fe^{++} + H^+ + 3e^- = FeAsS + 1/2\ H_2S$

$$E = -0.012 - 0.0295 \log\frac{(H_2S)^{1/2}}{(Fe^{++})} - 0.0197\ pH$$

22. $1/2\ As_2S_2 + Fe^{++} + 2e^- = FeAsS$

$$E = -0.025 + 0.0295 \log(Fe^{++})$$

23. $2H_3AsO_3 + Fe(OH)_2 + 8H^+ + 8e^- = FeAs_2 + 8H_2O$

$$E = 0.220 + 0.007 \log(H_3AsO_3)^2 - 0.059\ pH$$

24. $Fe^{++} + 2As + 2e^- = FeAs_2$

$$E = -0.138 + 0.0295 \log(Fe^{++})$$

25. $2H_3AsO_3 + Fe^{++} + 6H^+ + 8e^- = FeAs_2 + 6H_2O$

$$E = 0.135 + 0.007 \log(H_3AsO_3)^2\ (Fe^{++}) - 0.044\ pH$$

26. $FeAs_2 + 6H^+ + 6e^- = Fe + 2AsH_3$

$$E = -0.434 - 0.010 \log(AsH_3)^2 - 0.059\ pH$$

27. $FeAs_2 + 6H^+ + 4e^- = Fe^{++} + 2AsH_3$

$$E = - 0.447 - 0.015 \log(AsH_3)^2 (Fe^{++}) - 0.089 pH$$

28. $2H_2AsO_3^- + Fe(OH)_2 + 10H^+ + 18e^- = FeAs_2 + H_2O$

$$E = 0.358 + 0.007 \log (H_2AsO_3^-)^2 - 0.074 pH$$

29. $2HAsO_3^{2-} + Fe(OH)_2 + 12H^+ + 8e^- = FeAs_2 + 8H_2O$

$$E = 0.537 + 0.007 \log(HAsO_3^{2-})^2 - 0.089 pH$$

30. $1/2\ As_2S_3 + Fe^{++} + 2e^- = FeAsS + 1/2\ S$

$$E = - 0.090 + 0.0295 \log(Fe^{++})$$

31. $Fe^{2+} + 2SO_4^{2-} + 14e^- = FeS_2 + 8H_2O$

$$E = 0.362 + 0.0042 \log(Fe^{2+}) (SO_4^{2-})^2 - 0.068 pH$$

32. $FeS_2 + 4H^+ + 2e^- = Fe^{2+} + 2H_2S$

$$E = - 0.133 - 0.0296 \log(Fe^{2+}) (H_2S)^2 - 0.118 pH$$

33. $FeS_2 + 2H^+ + 2e^- + As = FeAsS + H_2S$

$$E = -0.118 - 0.0295 \log(H_2S) - 0.059 pH$$

34. $FeS_2 + As + H^+ + 2e^- = FeAsS + HS^-$

$$E = -0.325 - 0.0295 \log(HS^-) - 0.0295 pH$$

35. $Fe(OH)_2 + 2SO_4^{--} + 18H^+ + 14e^- = FeS_2 + 10H_2O$

$$E = 0.412 + 0.0042 \log(SO_4^{--})^2 - 0.076 pH$$

36. $FeS_2 + H_2AsO_3^- + 5H^+ + 5e^- = FeAsS + HS^- + 3H_2O$

$$E = 0.115 - 0.012 \log \frac{(HS^-)}{} - 0.059 pH$$

$(H_2AsO_3^-)$

37. $FeS_2 + H^+ + 2e^- = FeS + HS^-$

$E = - 0.372 - 0.0295\ pH - 0.0296 \log HS^-$

38. $Fe(OH)_2 + HS^- + H^+ = FeS + 2H_2O$

$1.039 = 0.059 \log(HS^-) - 0.059\ pH$

39. $FeAsS + As + 2H^+ + 2e^- = FeAs_2 + H_2S$

$E = - 0.153 - 0.0295 \log(H_2S) - 0.059\ pH$

40. $FeAsS + As + H^+ + 2e^- = FeAs_2 + HS^-$

$E = -0.359 - 0.0295 \log(HS^-) - 0.0295\ pH$

41. $FeS + 2H_2AsO_3^- + 9H^+ + 8e^- = FeAs_2 + HS^- + 6H_2O$

$$E = 0.229 - 0.007 \log \frac{(HS^-)}{(H_2AsO_3^-)^2} - 0.066\ pH$$

42. $HFeO_2^- + 2HAsO_3^{2-} + 13H^+ + 8e^- = FeAs_2 + 8H_2O$

$E = 0.677 + 0.007 \log(HAsO_3^{2-})^2(HFeO_2^-) - 0.096\ pH$

43. $FeAsO_4 + 3H^+ = H_3AsO_4 + Fe^{3+}$

$pH = 0.12 - 1/3 \log(H_3AsO_4)(Fe^{3+})$

44. $FeAsO_4 + 3H_2O = Fe(OH)_3 + H_2AsO_4^- + H^+$

$pH = 5.30 + \log(H_2AsO_4^-)$

45. $FeAsO_4 + 3H^+ + e^- = Fe^{2+} + H_3AsO_4$

$$E = 0.766 - 0.059 \log(Fe^{2+})(H_3AsO_4) - 0.177\ pH$$

46. $FeAsO_4 + 5H^+ + 3e^- = H_3AsO_3 + Fe^{2+} + H_2O$

$$E = 0.647 - 0.020 \log(H_3AsO_3)(Fe^{2+}) - 0.098\ pH$$

Figure 1.

Voltammograms for platinum in presence and absence of xanthate (49).

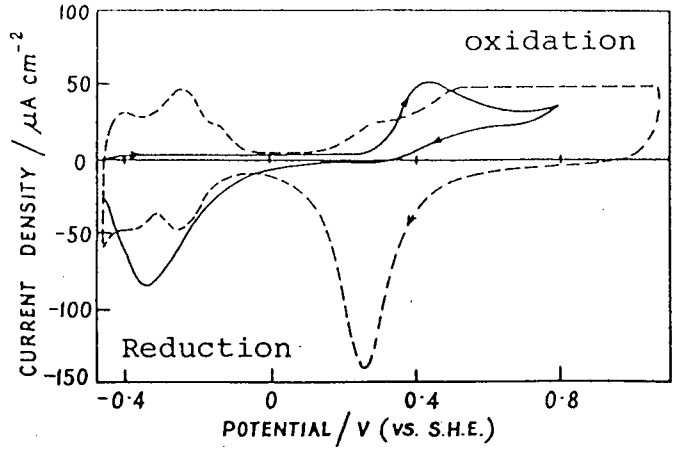

Figure 2.

Voltammogram for arsenopyrite at pH = 8.2 showing potentials achieved with oxidizing agents.

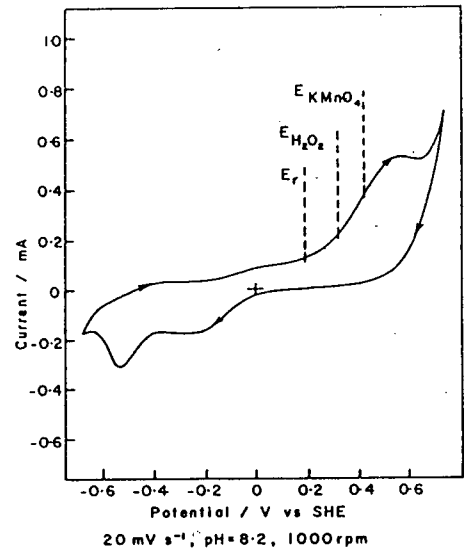

Figure 3.

Multiple sweep voltammogram for rotating electrode at pH = 11.7

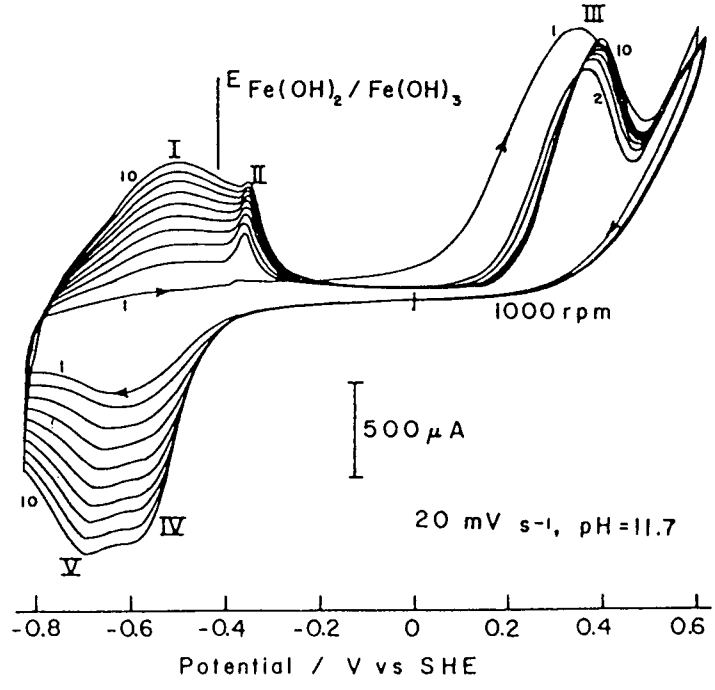

REFERENCES

1. Heinen, H.J., McClelland, G.E. and Lindstrom, R.E. " Recovery of gold from arsenopyrite concentrates by cyanidation - carbon adsorption " USBM, RI 8458, (1980).
2. Clark, L.A., " The Fe - As - S system: phase relations and applications ", Econ. Geol. Vol.55, pp. 1631 - 1652, (1960).
3. Addison, R. " Gold and Silver extraction from sulphide ores ", Min. Cong. J., Oct., pp. 47 - 54, (1980).
4. Tait, R.J.C., " The Milling of Canadian Ores ", CIMM Special Vol., Western Miner Press, Toronto, (1957).
5. More, M.A. and Pawson, H.E., " Milling Practice in Canada ", CIMM Special Volume 16, D. Pickett (ed), (1971).
6. " Effects of Arsenic in the Canadian Environment ", NRC publications No. NRCC 15391, (1978).
7. Hurst, M.E., " Arsenic - Bearing Deposits in Canada ", Can. Geol. Survey, Econ. Geol. Series No. 4, Ottawa (1927).
8. Landsburg, A., Mauser, J.E. and Henry, J.L. " Behavior of arsenic in a static bed during roasting of copper smelter feed ", USBM, RI 8493, (1980).
9. Loebenstein, J.R., " Arsenic " from " Mineral Facts and Problems " USBM Bulletin 671, (1980).
10. Hall, E.H., " Arsenic poisoning at Bralorne Pioneer Mines Ltd. " Proc. 1st Ann. Meeting of Can. Gold Met., Ottawa, pp. 79 - 84, (1964).
11. Habashi, F. and Ismail, M.I., " Health hazards and pollution in the metallurgical industry due to phosphine

and arsine. ", CIM Bull., Aug. pp. 99 - 104, (1975).

12. Sutherland, K.L. and Wark, I.W. " Principles of Flotation ", Aust. Inst. of Min. and Met., Melbourne, (1955).
13. Mitrofanov, S.I. etal, " Flotation of arsenic and bismuth sulphide ores ", USSR pat. 180,537 (1966), CA. 65:11843.
14. Plaksin, I., " Interaction of minerals with gases and reagents in flotation ", Min. Eng. March, pp. 319 - 324, (1959).
15. Glembotskii, V.A., Klassen, V.I. and Plaksin, I.N. " Flotation " pp. 539 - 541, Primary Sources, New York, (1963).
16. Nekrasov, B.D. " Flotation separation of pyrite and arsenopyrite ", Tsvetnye Metally, N. 2, pp. 23 - 26, (1956).
17. Machovic, V., " Flotation separation of pyrite and arsenopyrite from a bulk concentrate ", RUDY, Vol. 10, pp. 199 - 202, 1962, CA 62:8718
18. Herkenhoff, E.C., " Separation of pyrite, arsenopyrite and pyrrhotite by flotation ", U.S. pat. 2,342,277, (1944).
19. Rand, D.A.J., " Oxygen reduction on sulphide minerals " Part III. Comparison of activities of various copper iron lead and nickel mineral electrodes ", J. Electroanal. Chem., Vol. 83 pp. 19 - 32, (1977).
20. Biegler, T., Rand, D.A.J. and Woods, R. " Oxygen reduction on sulphide minerals ", in " Trends in Electrochemistry ", Bockris, Rand and Welch (ed), Plenum, New York, pp. 291 - 302, (1977)

21. Abeidu, A.M. and Almahdy, A.M., " Magnesia mixture as a regulator in the separation of pyrite from chalcopyrite and arsenopyrite ". Int. J. Proc. Vol. 6, pp. 285 - 302, (1980).

22. Allison, S.A., et al, " A determination of the products of reaction between various sulphide minerals and aqueous xanthate solution, and correlation of the products with electrode rest potentials ", Met. Trans., Vol. 3, pp. 2613 - 2618, (1972).

23. Janetski, N.D., Woodburn, S.I. and Woods, R., " An electrochemical investigation of pyrite flotation and depression ", Int. J. Minl. Proc., Vol. 4, pp. 227 - 239, (1977).

24. Critchley, J.K., " Reaction of ethylxanthate at an iron electrode ", Trans. IMM, Vol. C90, pp. 42 - 44, (1980).

25. Haung, H.H. and Miller, J.D., " Kinetics and thermochemistry of amyl xanthate adsorption by pyrite and marcasite ", Int. J. Minl. Process. Vol. 5, pp. 241 - 266, (1978).

26. Harris, P.J. and Finkelstein, N.P., " The interaction of pyrite, oxygen and xanthate " NIM Report NO. 1854, (1977).

27. Fuerstenau, D.W. and Mishra, R.K., " On the mechanism of pyrite flotation with xanthate collectors ", pp. 271 - 278 in " Complex Sulphide Ores ", IMM, London, (1980).

28. Hornsby, D. and Leja. J., " Selective flotation and its surface chemical characteristics ", pp. 217 - 301 in " Surface and Colloid Science ", E. Matijevic (ed), Plenum, New York, (1982).

29. Kostina, G.M. and Chernyak, A.S., " Electrochemical conditions for the oxidation of pyrite in alkaline and acid solutions ", Zhurn. Prikl. Khim., Vol. 49, No. 7 pp. 1534 - 1539, (1976).

30. Kostina, G.M. and Chermyak, A.S., " Kinetics of electrochemical oxidation of arsenopyrite and pyrite in caustic soda solutions ", Zhurn. Prikl. Khim., Vol. 59, No. 4, pp. 766 - 772, (1979).

31. Kostina, G.M. and Chernyak, A.S., " Coulometric study of oxidation of arsenopyrite and pyrite in caustic soda solutions ", Zhurn. Prickl. Khim. Vol. 50, No. 12, pp. 2701 - 2705, (1977).

32. Yakhontova, L.K., and Grudnev, A.P., " Oxidation mechanism of arsenopyrite ", Tr. Mineral. Muz., Akad. Nauk SSSR, No. 22, pp. 172 - 178, 1973, C.A. 80:50359.

33. Buerger, M.J. " The symmetry and crystal structure of the minerals of the arsenopyrite group, " Z. Krist., Vol. 95, pp. 83 - 113 (1963).

34. Buerger, M.J., " Interatomic distances in marcasite and notes on the bonding in crystals of loellingite, arsenopyrite and marcasite types, " Z. Krist., Vol. 97, pp. 504 - 513, (1937). "

35. Buerger, M.J., " The crystal structure of loellingite, $FeAs_2$ ", Z. Krist., Vol. 32, pp. 165 - 187, (1932).

36. Morimoto, N. and Clark, L.A., " Arsenopyrite crystal - chemical realations ", Am. Mineral., Vol. 46, pp. 1448 - 1469, (1961).

37. Hawley, J.R., " A detailed look at the iron sulphides ", in

" The Problem of Acid Mine Drainage in the Province of Ontario ", Ont. Water Res. Commission, Ontario, (1972).

38. Clark, L.A., " The Fe - As - S system: Phase relations and applications ", Econ. Geol., Vol. 55, No. 7 pp. 1345 - 1381, 1631 - 1652, (1960).

39. Kretschmar, U. and Scott,S.D., " Phase realations involving arsenopyrite in the system Fe - As - S and their application ", Can. Minl., Vol. 14, pp. 364 - 386 (1976).

40. Krasnikov, V.I., " Zoning of electrophysical properties of arsenopyrite in the middle Golgotai gold - ore deposit ", Geol. Geokhim. Prognoznaya Otsenka Rudn. Raionov Mestorozhd. Zabaikal'ya, pp. 178 - 180, (1973) CA. 84:76869v

41. Favorov, V.A., Krasnikov, V.I. and Sychugov, V.S, " Factors determining the variability of the semiconduction properties of pyrite and arsenopyrite ", Izv. Akad. Nauk SSSR, Ser. Geol., Vol.11, pp. 72 - 84 (1972) Ca: 78:46116f.

42. Keller, G.V. and Frischknecht, F.C., " Electrical Methods in Geophysical Prospecting ", p.6 Pergamon, (1966).

43. Parkhomenko, E.I., " Electrical Properties of Rocks ", p. 88 Plenum, (1967).

44. Parasnis, D.S., " The electrical resistivity of some sulphide and oxide minerals and their ores ", Geophys. Pros., Vol. 4, pp. 249 - 278, (1956).

45. Shuey, R.T., " Semiconducting Ore Minerals ", p. 205, Elsevier, (1975).

46. Plaksin, I.N. and Shafeev, R.Sh., " The influence of surface properties of sulphide minerals on adsorption of

flotation reagents ", Trans. I.M.M., Vol. 72, pp. 715 - 722 (1963).

47. Tolun, R. and Kitchener, J.A., " Electrochemical study of the galena - xanthate - oxygen flotation system, " Trans. I.M.M., Vol. 73, pp. 313 - 322 (1964).

48. Springer, G., " Observations on the electrochemical reactivity of semiconducting minerals ", Trans. I.M.M., Vol. 79, pp. ch 11 - 14, (1970)

49. Woods, R, " The oxidation of ethyl xanthate on platinum, gold, copper and galena electrodes. Relation to the mechanism of mineral flotation ", J.Phys.Chem., Vol. 75, No. 3, pp. 354 - 362 (1971).

50. Biegler, T., " Oxygen Reduction on sulphide minerals ", Part II. " Relation between activity and semiconducting properties of pyrite electrodes ", J. Electroanal. Chem. Vol. 70, pp. 265 - 275 (1976)

51. Natarjan, K.A. and Iwasaki, I, " Eh - pH response of noble metal and sulphide mineral electrodes ", Trans. AIME, Vol. 252, Dec., pp. 437 - 439 (1972).

52. Johnson, E.W., Fera, W, and Budrea, F. " Pamour Porcupine Mines Limited, Pamour No. 1 " in milling Practice in Canada ", D.E. Pickett (ed) p. 73 (1978).

53. Philips, C.S.G, and Williams, R.J.P., " Inorganic Chemistry " , Oxford Press, pp. 312 - 321, (1965).

54. Haque, K.E. and Ritcey, G.M., " Comparison of oxidants for the leaching of uranium ores in sulphuric acid ", CIM Bulletin, Vol. 75, No. 841, pp. 127 - 133, (1982).

55. Natarajan, K.A. and Iwasaki, I, " Eh measurements in

hydrometallurgical systems ", Minerals SCI. Engng., Vol. 6, no. 1, pp. 35 - 44, (1974).

56. Gileadi, E., Kirowa - Eisner, E. and Penciner, J. " Interfacial Electrochemistry: an Experimental Approach ", Addison - Wesley, pp. 370 - 395, (1975).

57. Woods, R., " The anodic oxidation of ethyl xanthate on metal and galena electrodes ", Aust. J. Chem., Vol. 25, pp. 2329 - 35, (1972).

58. Gardner, J.R. and Woods, R., " A Study of the surface oxidation of galena using cyclic voltammetry " J.Chem., Vol. 100, pp. 447 - 459, (1979).

59. Weisnberg, I.J., Bakshi, P.S. and Vervaert, A.E. " Arsenic distribution and control in copper smelters ", Jour. of Metals, Vol. 31, No. 9, pp. 38 - 44, (1979)

60. Markovac, V. and Cohen, M. " The anodic deposition of iron oxide films on iron ", J. Electrochem. Soc., Vol. 114, NO. 7, pp. 674 - 678, (1967).

61. Guzman, R.S.S, Vilche, J.R. and Ariva, A.J, " The potentiodynamic behavior of iron in alkaline solutions ", Electrochimica Acta, Vol. 24, pp. 395 - 403, (1979).

62. Carbonio, R.E, Macagno, V.A. and Giordano, M.C., " A transition in the kinetics of the $Ni(OH)_2/NiOOH$ electrode reaction ", Soc., Vol. 129, No. 5, pp. 983 - 991, (1982).

63. Hamilton, I.C. and Woods, R., " An investigation of surface oxidation of pyrite and pyrrhotite by linear potential sweep voltammetry ", J. Electroanal Chem. & Interfacial Electrochem., Vol. 118, pp. 327 - 343, (1981).

64. Robins, R.G., " The solubility of metal arsenates ", Met.

Trans. B, Vol. 12B, pp. 103 - 109, (1981).

65. " Determination of arsenic by differential pulse polarography", Princeton Applied Research Application Brief A - 6.

66. Arnold, J.P. and Johnson, R.M., " Polarography of arsenic ", Talanta, Vol. 16, pp. 1191 - 1207, (1969).

67. Forsberg, G., O'Laughlin, J.W. and Megargle, R.G., " Determination of arsenic by anodic stripping voltammetry and differential pulse anodic stripping voltammetry ", Anal. Chem., Vol. 47, No. 9, pp. 1586 - 1592, (1975).

68. Chander, S. and Fuerstenau, D.W., " The effect of potassium diethyldithiophosphate on the electrochemical properties of platinum, copper and copper sulphide in aqueous solutions ", Electroanal. Chem. and Interfac. Electrochem., Vol. 56, pp. 217 - 247, (1974).

69. Elgillani, D.A. and Fuerstenau, M.C., " Mechanisms involved in cyanide depression of pyrite ", Trans AIME, Vol. 241, pp. 437 - 445, (1968).

70. Woodcock, J.T. and Jones M.H.," Oxygen concentrations redox potentials, xanthate residuals, and other parameters in flotation plant pulps ", Min Process and Extr. Met., I.M.M. London, pp. 439 - 468, (1970).

71. Albery, W.J., " Developments and applications of the rotating disk system in " Physicochemical Hydrodynamics ", D.B. Spalding (ed), Advance Publications, pp. 413 - 433, (1977).

72. Paul, R.L., Nicol, M.J., Diggle, J.W. and Saunders, A.P., " The electrochemical behaviour of galena (lead sulphide) -

I.Anodic dissolution ", Electrochimica Acta, Vol. 23, pp. 625 - 633, (1978).

73. Gal - or, L., Bruckenstein,S. and Carter, J.M., " A study of the corrosion of dental amalgam using the ring - disc electrode " , J. Biomed. Mat. Res., Vol. 12, pp. 1 - 12, (1978).

74. Frost, D.C., Wallbank, B. and Leeder, W.R., " X-ray photoelectron spectroscopy of coal and coal related problems ", Ch. 11 in Analytical Methods for Coal and Coal products ", Academic Press, (1978).

75. Brion, D., Hayer, J. and Predali, J.J., " Characterization of fine pyrite surface compounds ", ch. 28 in " Fine Particles Processing ", P. Somasumdaran (ed), AIME (1980).

76. Bailey, L.K. and Peters E.," Decomposition of pyrite in acids by pressure leaching and anodization: the case for an electrochemical mechanism ", Can. Met. Quart., Vol. 15, No. 4, pp. 333 - 344, (1976).

77. Frost, D.C. Leader, W.R., and Tapping, R.L.," X-ray photoelectron spectroscopic investigation of coal ", Fuel, Vol. 53, pp. 206 - 211, (1974).

78. Gulledge, J.H. and O'Connor, J.T., " Removal of arsenic (v) from water by adsorption on aluminum and ferric hydroxides ", J. AWWA, Vol. 65, No. 8, pp. 548 - 552, (1973).

79. Biegler, T. and Swift, D.A., " Anodic electrochemistry of chalcopyrite ", J. Appl. Electrochem., Vol. 9, pp. 545 - 554 (1979).

80. Biernat, R,J, and Robins, R.G., " High temperature

potential/pH diagrams for the iron - water and iron - water - sulphur systems ", Electrochimica Acta, Vol. 17, pp. 1261 - 1283, (1972).

81. Barton, P.B., " Thermochemical study of the system Fe - As - S ", Geochim. Cosmochim. Acta. Vol. 33, pp. 841 -857, (1961).

82. Sergeyeva, E.I. and Khondahovsky, I.L., " Physiochemical conditions of formation of native arsenic in hydrothermal deposits ", Geokhimiya, No. 7, pp. 846 - 459, (1969).

83. Wagman, D.D., Evans, W.H, Parker, V.B., " Selected values of chemical thermodynamic properties ", Natl. Bur. Stand. Tech. Note 270 - 3, (1968).

84. Pine Instrument Co., Grove City, Pennsylvania, 16127.